Slab tear propagation:
Numerical model and implications to Apennines

Taras Gerya
ETH-Zurich

Dave Bercovici
Yale University

Claudio Faccenna
University of Texas at Austin
Università Roma TRE

Plan of the talk

1. Self-excuses why unpublished (30 min)

2. Talk itself (15 min)

1. Self-excuses

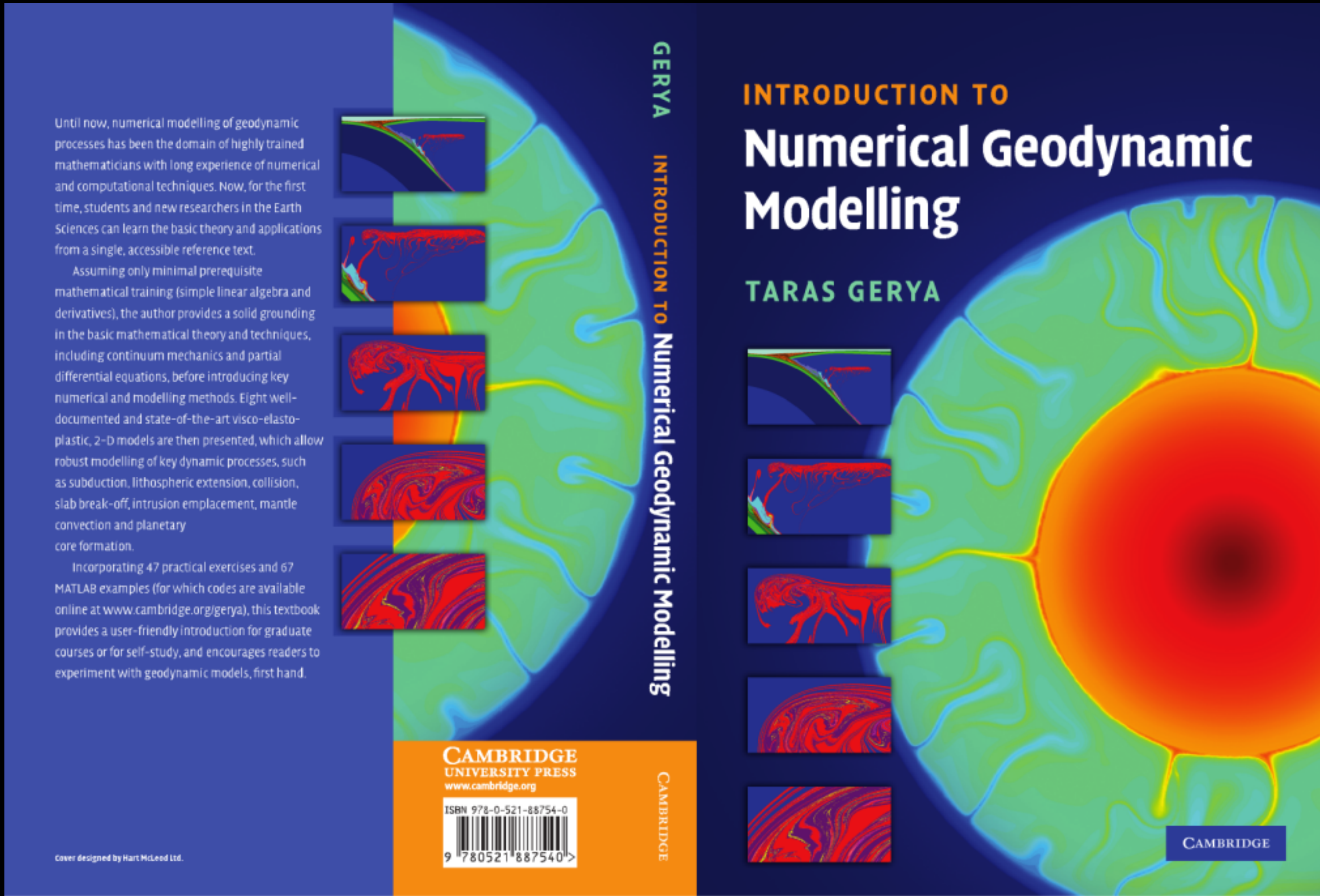

INTRODUCTION TO Numerical Geodynamic Modelling

Taras Gerya

SECOND EDITION

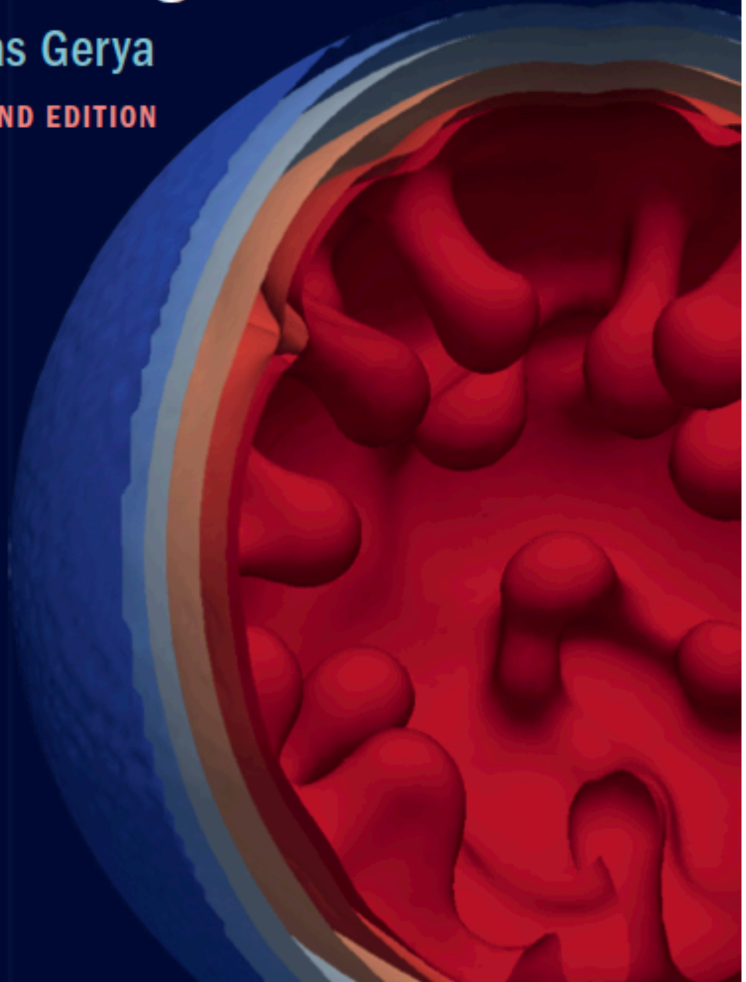

INTRODUCTION TO Numerical Geodynamic Modelling SECOND EDITION

Gerya

CAMBRIDGE

This hands-on introduction to numerical geodynamic modelling provides a solid grounding in the necessary mathematical theory and techniques, including continuum mechanics and partial differential equations, before introducing key numerical modelling methods and applications. Fully updated, this second edition includes four completely new chapters covering the most recent advances in modelling inertial processes, seismic cycles and fluid-solid interactions, and the development of adaptive mesh refinement algorithms. Many well-documented, state-of-the-art visco-elasto-plastic 2-D models are presented, which allow robust modelling of key geodynamic processes. Requiring only minimal prerequisite mathematical training, and featuring over 60 practical exercises and 90 MATLAB examples, this user-friendly resource encourages experimentation with geodynamic models. It is an ideal introduction for advanced courses and can be used as a self-study aid for graduates seeking to master geodynamic modelling for their own research projects.

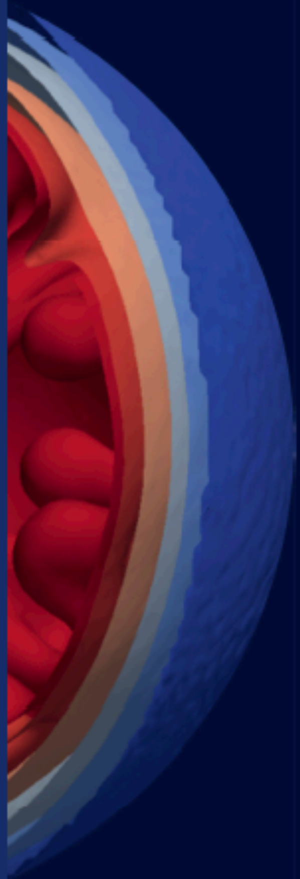

Online Resources
www.cambridge.org/gerya2e

- MATLAB code examples
- Video clips: silly putty deformation and 3D model animation
- PowerPoint slides: animation for two models explaining continuum behaviour

Cover illustration: xxxxxxxxxxxxxxxxxxxxx

COVER DESIGNED BY HART MCLEOD LTD

CAMBRIDGE UNIVERSITY PRESS
www.cambridge.org

ISBN 978-1-107-14314-2

9 781107 143142 >

Introduction to Numerical Geodynamic Modeling II

is out!

What's new?

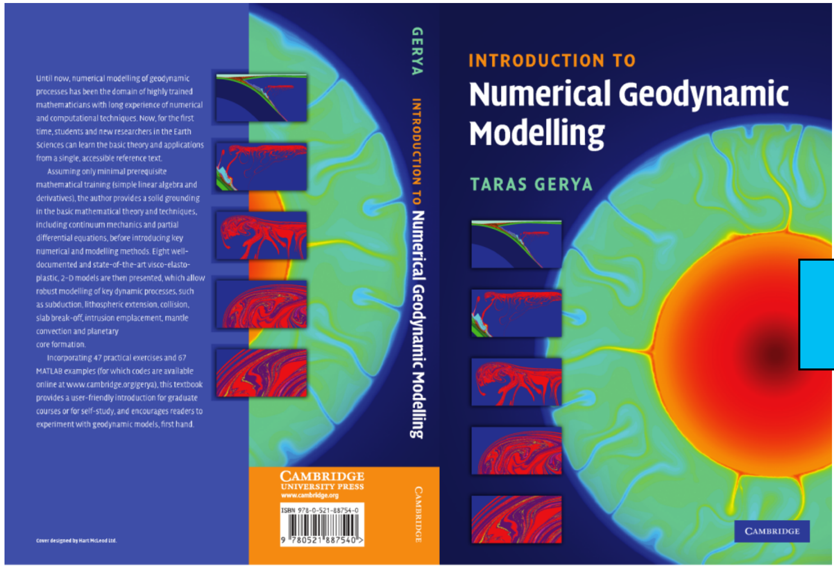

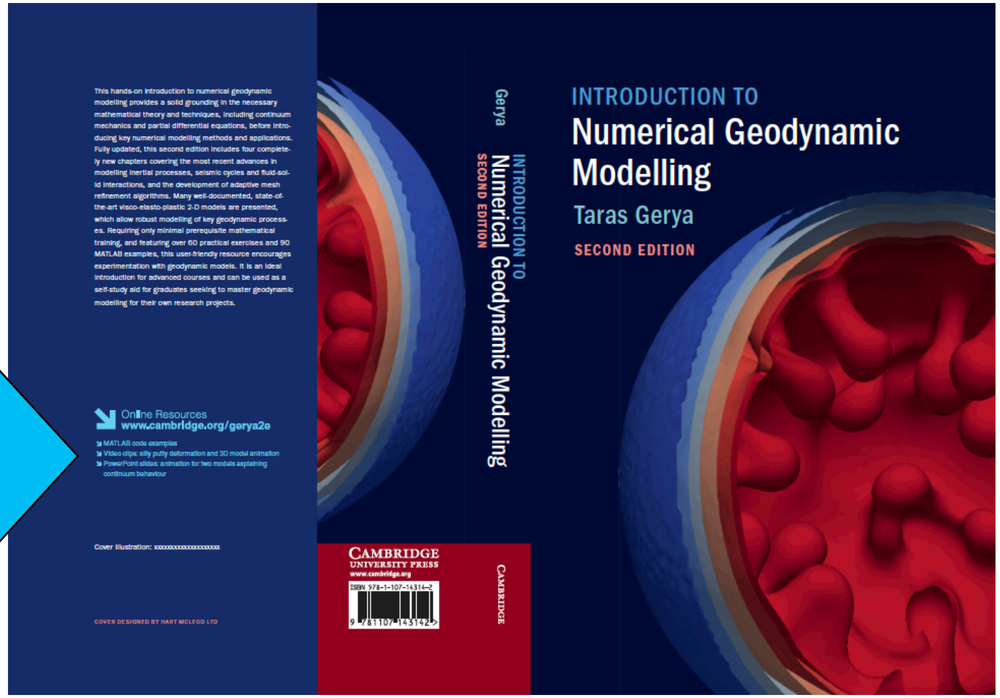

17 chapters
b&w figures
67 MatLab examples

21 chapters
color figures
90 MatLab examples

What’s new?
Free surface stabilization (Chapter 8)

8

The advection equation and marker-in-cell method

Theory: Advection equation. Solution methods for continuous and discontinuous variables. Eulerian schemes: upwind differences, flux corrected transport (FCT). Lagrangian schemes: marker-in-cell method. Runge–Kutta advection schemes. Interpolation between markers and nodes. Continuity-based velocity interpolation. ‘Sticky air’ approach. ‘Drunken sailor’ instability. Stabilization of free surface.
Exercises: Programming of various advection schemes and markers.

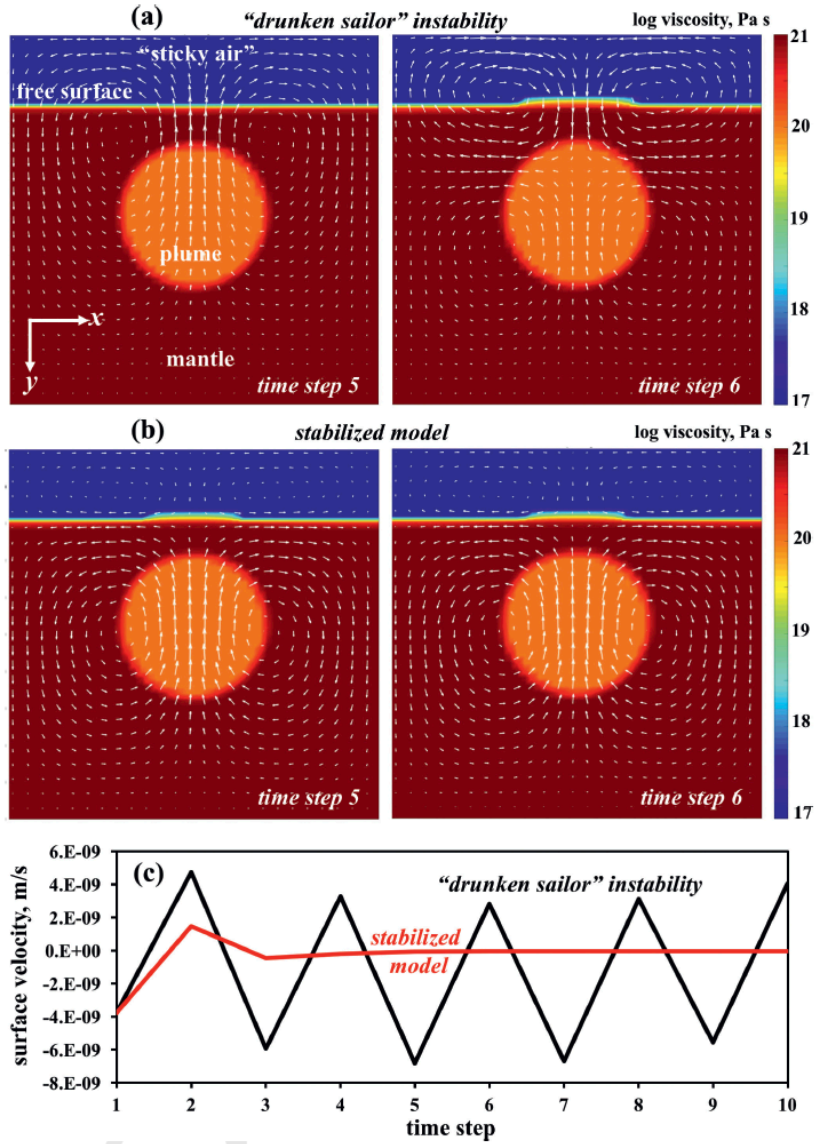

What's new?

Continuity-based marker advection (Chapter 8)

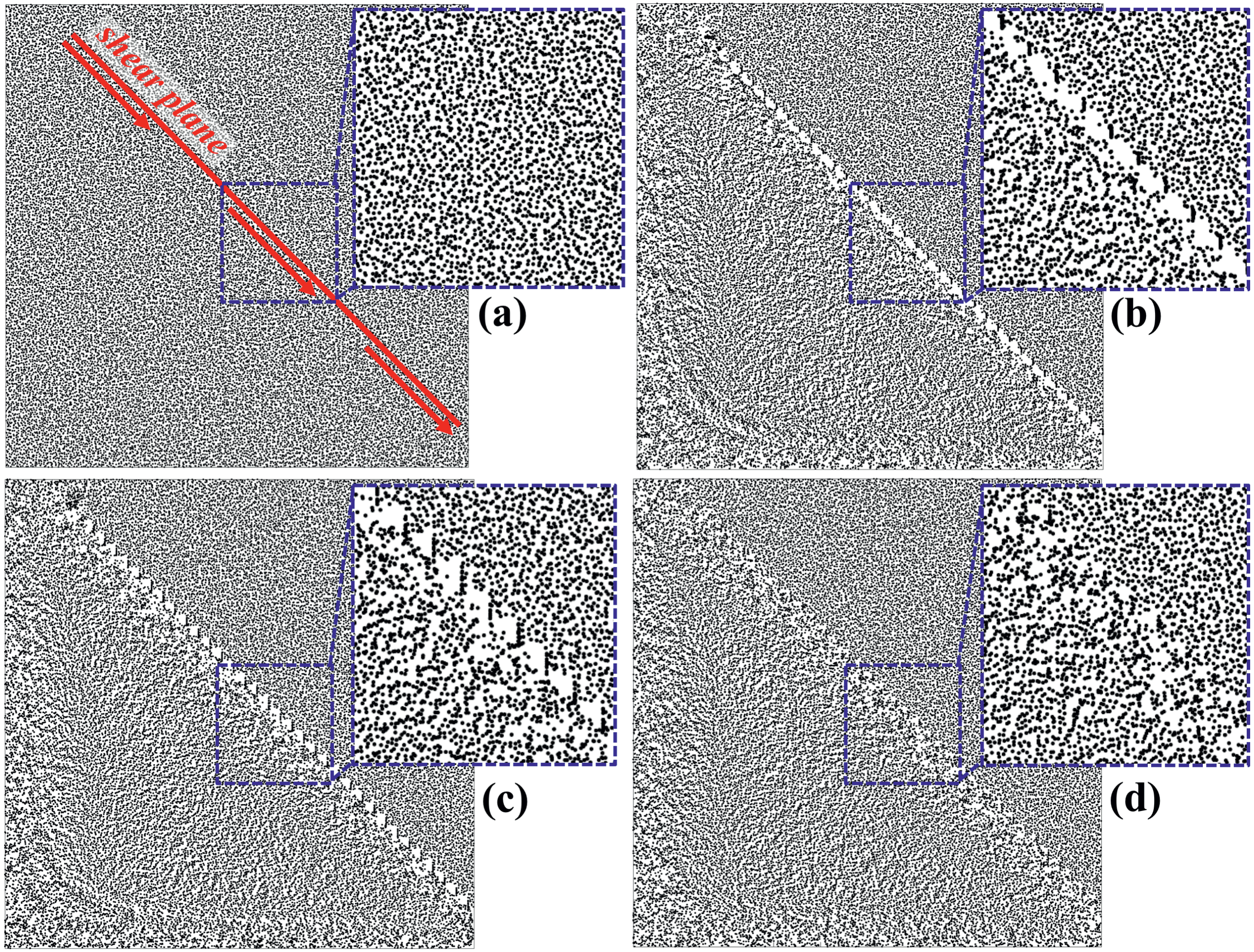

What's new?

New 3D elastic stress rotation algorithms (Chapter 12)

12

Elasticity and plasticity

Theory: Elastic rheology. Rotation of elastic stresses. Maxwell visco-elastic rheology. Plastic rheology. Plastic yielding criterion. Plastic flow potential. Plastic flow rule. Visco-elasto-plastic rheology.
Exercises: Stress buildup/relaxation with a visco-elastic Maxwell rheology, elastic stress rotation programming.

According to this approach, 3D rotation is represented by a vorticity pseudo-vector ($\vec{\omega}$), which has three components:

$$\omega_x = \frac{1}{2}\left(\frac{\partial v_z}{\partial y} - \frac{\partial v_y}{\partial z}\right),\ \omega_y = \frac{1}{2}\left(\frac{\partial v_x}{\partial z} - \frac{\partial v_z}{\partial x}\right),\ \omega_z = \frac{1}{2}\left(\frac{\partial v_y}{\partial x} - \frac{\partial v_x}{\partial y}\right). \tag{12.37}$$

The 3D algorithm can then be summarized as follows (Popov et al., 2014a, personal communication).

(1) Compute the vorticity vector magnitude:

$$\omega_{mag} = \sqrt{\omega_x^2 + \omega_y^2 + \omega_z^2}\,. \tag{12.38}$$

(2) Compute the unit rotation vector $\vec{n}$, which also has three components:

$$n_x = \frac{\omega_x}{\omega_{mag}},\ n_y = \frac{\omega_y}{\omega_{mag}},\ n_z = \frac{\omega_z}{\omega_{mag}}. \tag{12.39}$$

(3) Integrate the incremental rotation angle:

$$\theta = \omega_{mag}\Delta t. \tag{12.40}$$

(4) Evaluate the rotation matrix using the Euler–Rodrigues formula:

$$R_{mat} = \cos(\theta)\begin{pmatrix} 1 & 0 & 0 \\ 0 & 1 & 0 \\ 0 & 0 & 1 \end{pmatrix} + \sin(\theta)\begin{pmatrix} 0 & -n_z & n_y \\ n_z & 0 & -n_x \\ -n_y & n_x & 0 \end{pmatrix} + \left(1 - \cos(\theta)\right)\begin{pmatrix} n_x n_x & n_x n_y & n_x n_z \\ n_y n_x & n_y n_y & n_y n_z \\ n_z n_x & n_z n_y & n_z n_z \end{pmatrix}. \tag{12.41}$$

What's new?

Better visco-elasto-plasticity treatment (Chapter 13)

13

2D implementation of visco-elasto-plasticity

Theory: Numerical implementation of visco-elasto-plastic rheology. Organization of a thermomechanical code in the case of a 2D, visco-elasto-plastic medium. Numerical treatment of plasticity. Visco-elasto-plastic iterations. Visco-plastic rheology.
Exercises: Programming 2D thermomechanical codes with a visco-elasto-plastic rheology.

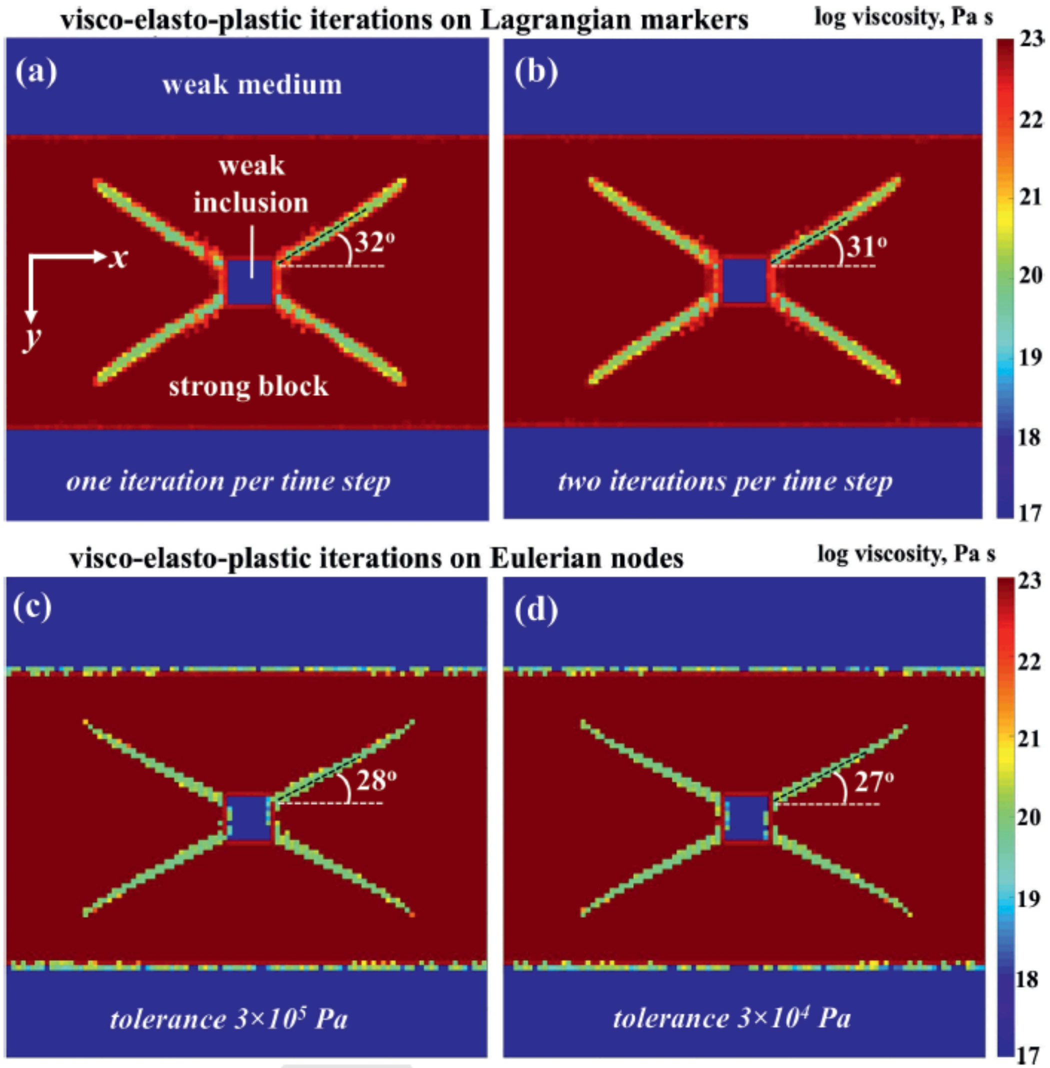

What's new?

Modeling of compressible materials and inertial processes (Chapter 14)

14

2D thermomechanical modelling of inertial processes

Theory: Numerical implementation of inertia and elastic compressibility. Organization of a thermomechanical code in the case of 2D, visco-elasto-plastic deformation with inertia. Thermomechanical iterations.
Exercises: Programming a 2D thermomechanical code with inertia.

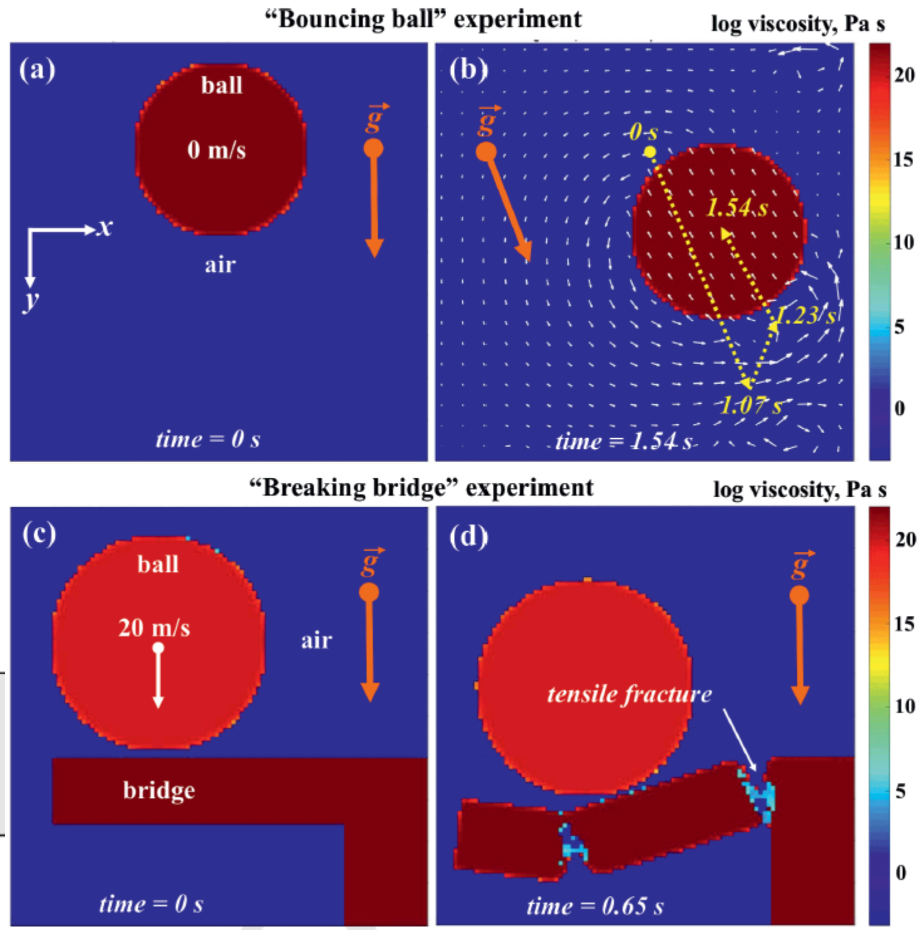

What’s new?
Modeling of earthquakes (Chapter 15)

15

Seismo-thermomechanical modelling

Theory: What is seismo-thermomechanical modelling? Rate-dependent friction. Rate- and state-dependent friction. Regularized rate- and state-dependent friction formulation. Invariant plasticity-like reformulation of rate- and state-dependent friction. Adaptive time stepping. Organization of a seismo-thermomechanical code. Visco-elasto-plastic iterations.
Exercises: Programming a 2D seismo-thermomechanical code.

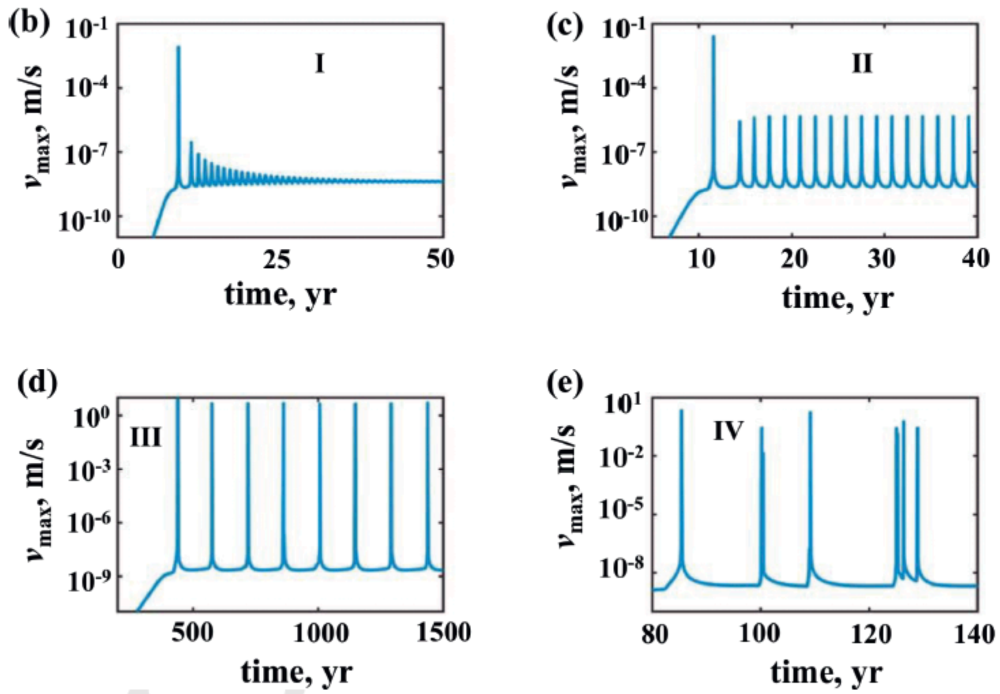

What’s new?

Modeling of two-phase flow processes (Chapter 16)

16

Hydro-thermomechanical modelling

Theory: What is hydro-thermomechanical modelling? Fluid percolation processes. Darcy law and its derivation from simple principles. Permeability and its dependence on porosity. Governing equations for modelling coupled hydro-thermomechanical visco-elasto-plastic systems. Visco-elasto-plastic compaction. Mass transfer. Organization of a hydro-thermomechanical code. Hydro-thermomechanical iterations. Toy melting and dehydration models.
Exercises: Programming of 2D hydro-thermomechanical codes.

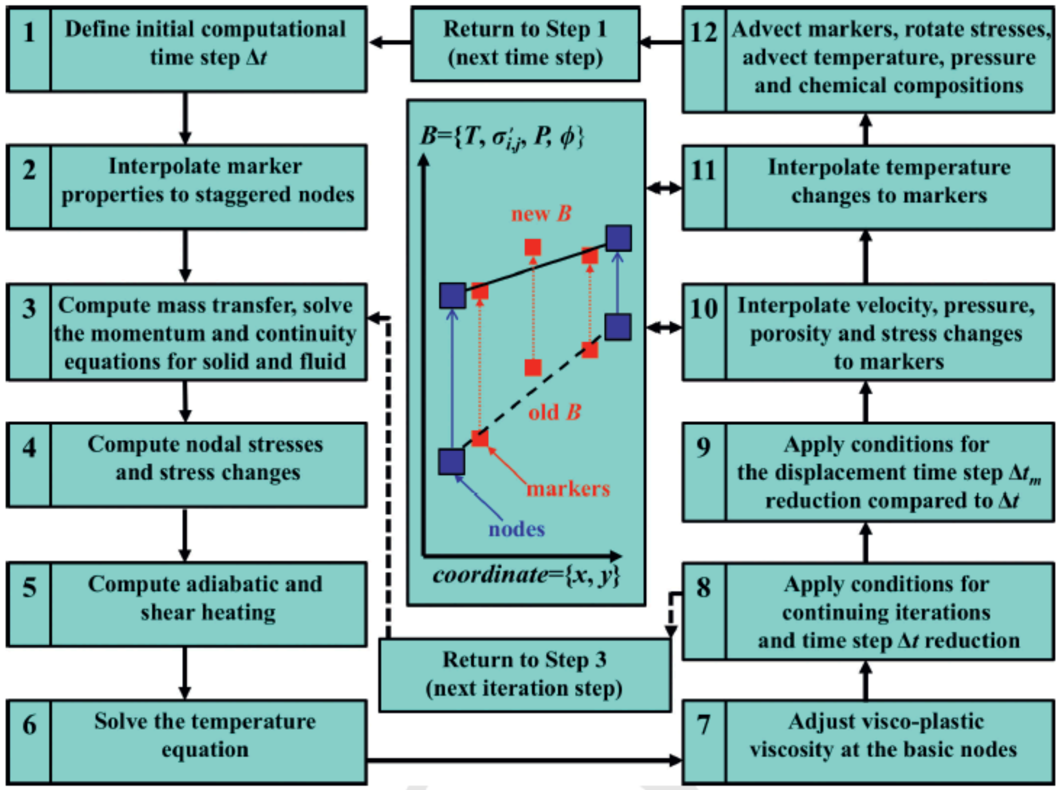

Optimal formulation of conservation laws:

Using formulation by Yarushina and Podladchikov (2015) based on principles of irreversible thermodynamics

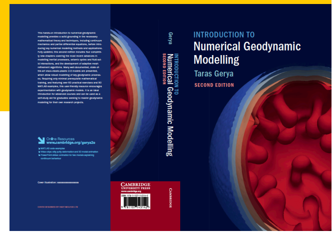

momentum conservation for fluid

inertia

$$q_i^D = -\frac{k^\phi}{\eta^f}\left(\frac{\partial P^f}{\partial x_j} - \rho^f g_i + \rho^f \frac{D^f v_i^f}{Dt} + \frac{v_i^f}{\phi}\Gamma^{mass}\right)$$

mass transfer

mass conservation for fluid

$$\phi\left(\frac{D^f ln\rho^f}{Dt} - \frac{D^s ln\rho^s}{Dt}\right) - \frac{D^s ln(1-\phi)}{Dt} + \mathrm{div}(\vec{q}^D) = \frac{\Gamma^{mass}\rho^t}{\rho^f\rho^s(1-\phi)}$$

momentum conservation for bulk (solid+fluid)

$$\frac{\partial \sigma'^t_{ij}}{\partial x_j} - \frac{\partial P^t}{\partial x_i} + \rho^t g_i = \rho^f \phi \frac{D^f v_i^f}{Dt} + \rho^s(1-\phi)\frac{D^s v_i^s}{Dt} + \left(v_i^f - v_i^s\right)\Gamma_{mass}$$

mass conservation for solid

$$\frac{D^s ln\rho^s}{Dt} + \frac{D^s ln(1-\phi)}{Dt} + \mathrm{div}(\vec{v}^s) = -\frac{\Gamma^{mass}}{\rho^s(1-\phi)}$$

energy conservation for bulk (solid+fluid)

$$(1-\phi)\rho^s C_P^s \frac{D^s T}{Dt} + \phi\rho^f C_P^f \frac{D^f T}{Dt} = -\frac{\partial q_i^t}{\partial x_i} + H_r^t + H_a^t + H_s^t + H_L^t$$

Poro-visco-elasto-plastic rheology:

Using visco-elasto-plastic formulation by Yarushina and Podladchikov (2015) based on Biot's poroelasticity theory (Biot, 1941)

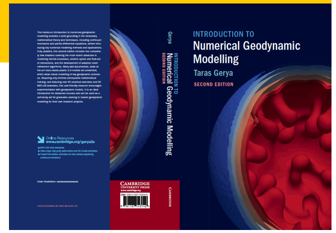

Maxwell visco-elasto-plastic model: $\dot{\varepsilon}'_{ij} = \dot{\varepsilon}'_{ij(viscous)} + \dot{\varepsilon}'_{ij(elastic)} + \dot{\varepsilon}'_{ij(plastic)},$

where

$$\dot{\varepsilon}'_{ij(viscous)} = \frac{1}{2\eta}\sigma'_{ij},$$

$$\dot{\varepsilon}'_{ij(elastic)} = \frac{1}{2\mu}\frac{D\overset{\frown}{\sigma}'_{ij}}{Dt},$$

$$\dot{\varepsilon}'_{ij(plastic)} = 0 \quad \text{for} \quad \sigma_{\text{II}} < \sigma_{\text{yield}},$$

$$\dot{\varepsilon}'_{ij(plastic)} = \chi\frac{\partial G_{plastic}}{\partial \sigma'_{ij}} = \chi\frac{\sigma'_{ij}}{2\sigma_{\text{II}}} \quad \text{for} \quad \sigma_{\text{II}} = \sigma_{yield},$$

$$G_{plastic} = \sigma_{\text{II}},$$

$$\sigma_{\text{II}} = \sqrt{\frac{1}{2}\sigma'^{2}_{ij}},$$

Drucker-Prager plasticity model with fluid pressure: $\sigma_{\text{II}} = \sigma_{yield}$

$$\sigma_{yield} = \sigma_c + \gamma_{int}(P^t - P^f) \quad \text{when} \quad P^t - P^f > \frac{\sigma_c - \sigma_t}{1 - \gamma_{int}} \quad \text{(confined fractures)}$$

critical hydro-mechanical feedback

$$\sigma_{yield} = \sigma_t + (P^t - P^f) \quad \text{when} \quad P^t - P^f < \frac{\sigma_c - \sigma_t}{1 - \gamma_{int}} \quad \text{(tensile fractures)}$$

$$P^t = (1 - \phi)P^s + \phi P^f,$$

Self-consistent formulation of closure relations:

Using visco-elasto-plastic formulation by Yarushina and Podladchikov (2015) based on Biot's poroelasticity theory (Biot, 1941)

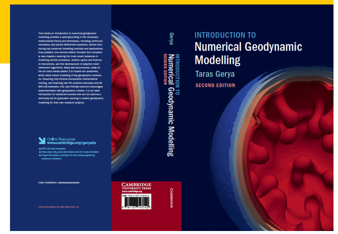

mass transfer

$$\frac{D^s ln(1-\phi)}{Dt} = \frac{\beta^{\phi}}{(1-\phi)}\left(\frac{D^s P^t}{Dt} - \frac{D^f P^f}{Dt}\right) - \frac{\alpha^{\phi}}{(1-\phi)}\frac{D^s T}{Dt} + \frac{P^t - P^f}{(1-\phi)\eta^{\phi}} - \Gamma^{mass} A^{\phi},$$

$$\frac{D^s ln\rho^s}{Dt} = \frac{\beta^s}{1-\phi}\left(\frac{D^s P^t}{Dt} - \phi\frac{D^f P^f}{Dt}\right) - \alpha^s\frac{D^s T}{Dt} + \Gamma^{mass} A^s,$$

$$\frac{D^f ln\rho^f}{Dt} = \beta^f\frac{D^f P^f}{Dt} - \alpha^f\frac{D^f T}{Dt} + \Gamma^{mass} A^f,$$

How to formulate mass transfer related terms?

C-component approach
(C-component = Chemical trash can)

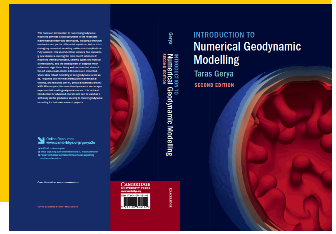

1. We characterize complex reactive mass transfer by considering a net mass transfer **$\Delta M=\Sigma\ \Delta Mi$**, where **$\Delta Mi$** is the mass of i-th chemical component transferred from the solid to the fluid during a time increment **Δt**: positive **ΔMi** values corresponds to the mass transfer from the solid to the fluid (dehydration, melting, dissolution, etc.), whereas negative **ΔMi** values imply the mass transfer from the fluid to the solid (hydration, solidification, precipitation, etc.).
2. The transferred mass **ΔM** is formally described as a single chemically complex **pseudo-component C** of the solid and fluid. Stoichiometry of C-component is given by **$C=\Sigma\Delta Mi/\Delta M*Ci$**, where **$Ci$** is chemical formula of i-th chemical component.
3. C-component has different density in its solid ($\rho^s{}_C$) and fluid ($\rho^f{}_C$) state, which can also differ from the bulk density of the solid (ρ^s) and fluid (ρ^f).

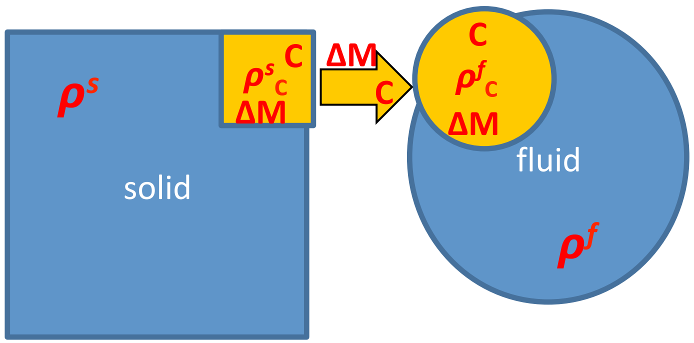

How to formulate mass transfer related terms with C-component approach?

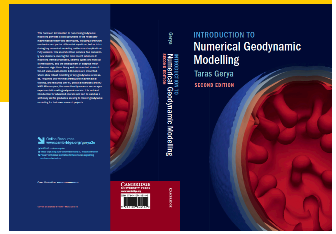

mass conservation for solid (porous matrix divergence depends on mass transfer)

$$\operatorname{div}(\vec{v}^s) + \beta_d\left(\frac{D^sP^t}{Dt} - K_{BW}\frac{D^fP^f}{Dt}\right) + \frac{P^t - P^f}{(1-\phi)\eta^\phi} = \left(\alpha^s + \frac{\alpha^\phi}{(1-\phi)}\right)\frac{D^sT}{Dt} + \Gamma_{mass}\left(\frac{1}{\rho^f_C} - \frac{1}{\rho^s_C}\right)$$

mass conservation for fluid (Darcy flux divergence is independent of mass transfer)

$$\operatorname{div}(\vec{q}^D) - K_{BW}\beta_d\left(\frac{D^sP^t}{Dt} - \frac{1}{K_{Sk}}\frac{D^fP^f}{Dt}\right) - \frac{P^t - P^f}{(1-\phi)\eta^\phi} = \phi\left[\alpha^f\frac{D^fT}{Dt} - \left(\alpha^s + \frac{\alpha^\phi}{(1-\phi)\phi}\right)\frac{D^sT}{Dt}\right]$$

The advantage of C-component approach is that the form of the discretized conservation equations becomes independent of the actual chemistry, thermodynamics and kinetics of mass transfer, which can be computed separately during SHTMC-iteration.

How to formulate mass transfer related terms with C-component approach

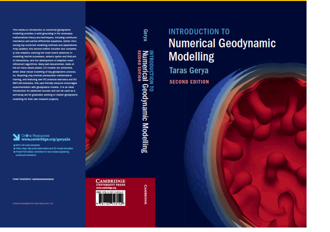

mass conservation for solid (porous matrix divergence depends on mass transfer)

$$\mathrm{div}(\vec{v}^s) + \beta_d\left(\frac{D^s P^t}{Dt} - K_{BW}\frac{D^f P^f}{Dt}\right) + \frac{P^t - P^f}{(1-\phi)\eta^\phi} = \left(\alpha^s + \frac{\alpha^\phi}{(1-\phi)}\right)\frac{D^s T}{Dt} + \Gamma_{mass}\left(\frac{1}{\rho_C^f} - \frac{1}{\rho_C^s}\right)$$

Γ_{mass}, A^ϕ, A^s and A^f can be formulated locally as a function of *six independent quantities*: porosity and density of the solid and fluid before (i.e., for the beginning of the time step, $\phi^o, \rho^{so}, \rho^{fo}$) and after (i.e., for the end of the time step, ϕ, ρ^s, ρ^f) chemical reactions.

$$\Gamma_{mass}\left(\frac{1}{\rho_C^f} - \frac{1}{\rho_C^s}\right) = \frac{1-R_V}{\Delta t}$$

INITIAL/FINAL volume ratio

$$R_V = \frac{V^o}{V} = \frac{\rho^s(1-\phi) + \rho^f\phi}{\rho^{so}(1-\phi^o) + \rho^{fo}\phi^o}$$

FINAL/INITIAL density ratio

How to formulate mass transfer related terms with C-component approach

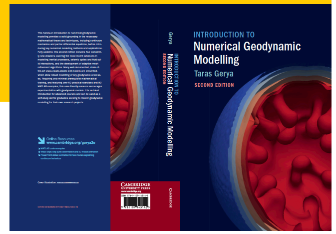

INITIAL/FINAL volume ratio

$$R_V = \frac{V^o}{V} = \frac{\rho^s(1-\phi) + \rho^f\phi}{\rho^{so}(1-\phi^o) + \rho^{fo}\phi^o}$$

FINAL/INITIAL density ratio

$$\Gamma^{mass} = \frac{1}{V}\frac{\Delta M}{\Delta t} = \frac{R_V\rho^{so}(1-\phi^o) - \rho^s(1-\phi)}{\Delta t} = \frac{\rho^f\phi - R_V\rho^{fo}\phi^o}{\Delta t},$$

$$\Gamma^{mass}A^\phi = \frac{R_V(\phi-\phi^o)}{\Delta t(1-\phi)}$$

$$\Gamma^{mass}A^s = \frac{R_V}{\Delta t}\left(\frac{1-\phi^o}{1-\phi}\right)\left(1-\frac{\rho^{so}}{\rho^s}\right)$$

$$\Gamma^{mass}A^f = \frac{R_V\phi^o}{\Delta t\phi}\left(1-\frac{\rho^{fo}}{\rho^f}\right)$$

How to implement coupled SHTMC equations?

Global iteration

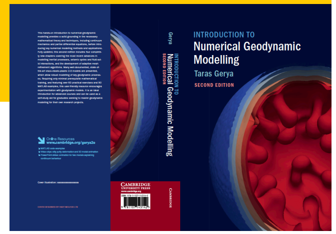

thermodynamic box to compute

$\phi^o, \rho^{so}, \rho^{fo}$ ϕ, ρ^s, ρ^f

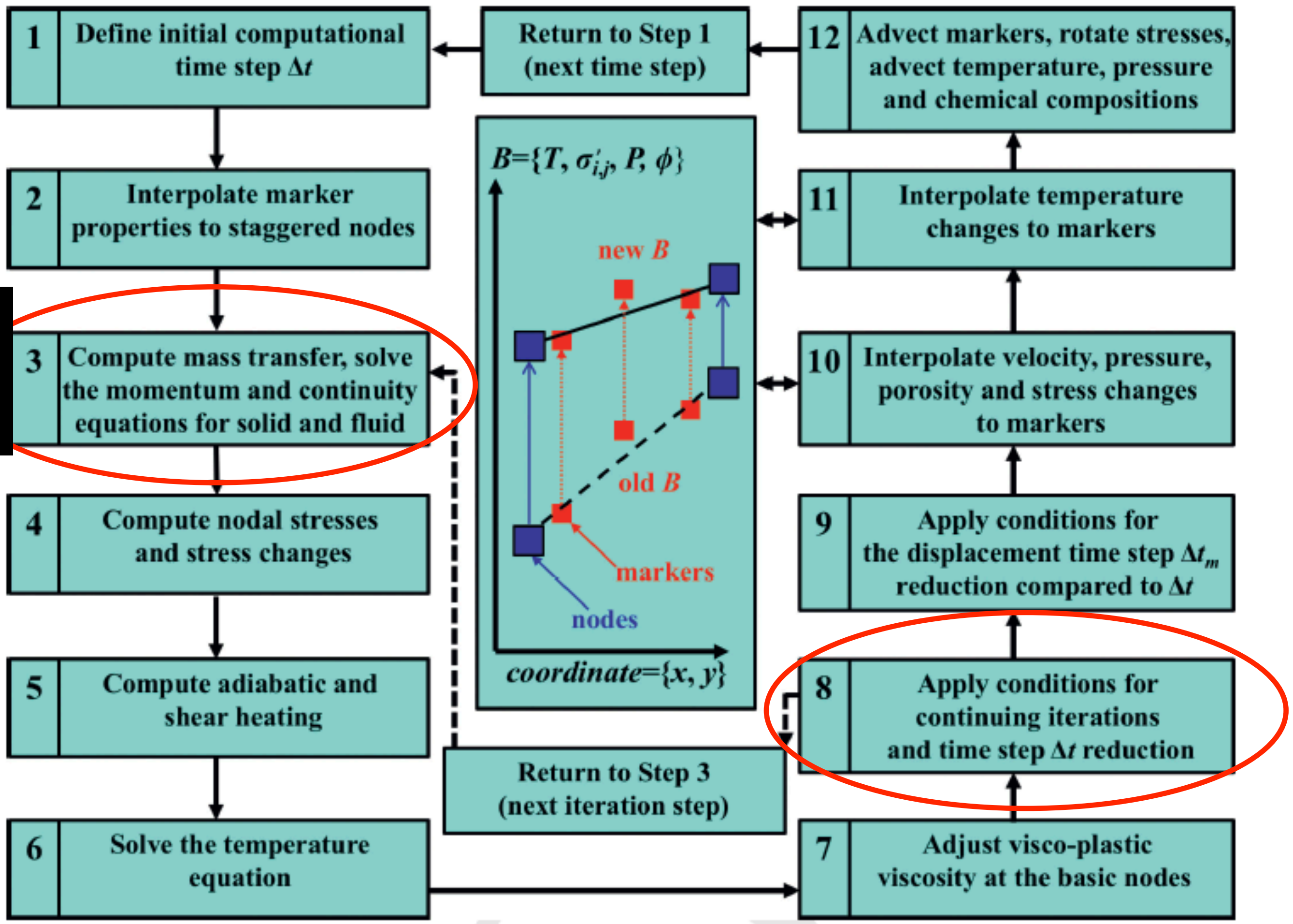

Examples

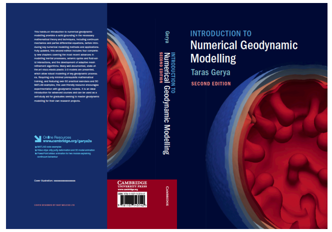

16.10 Toy thermodynamic model of mantle melting

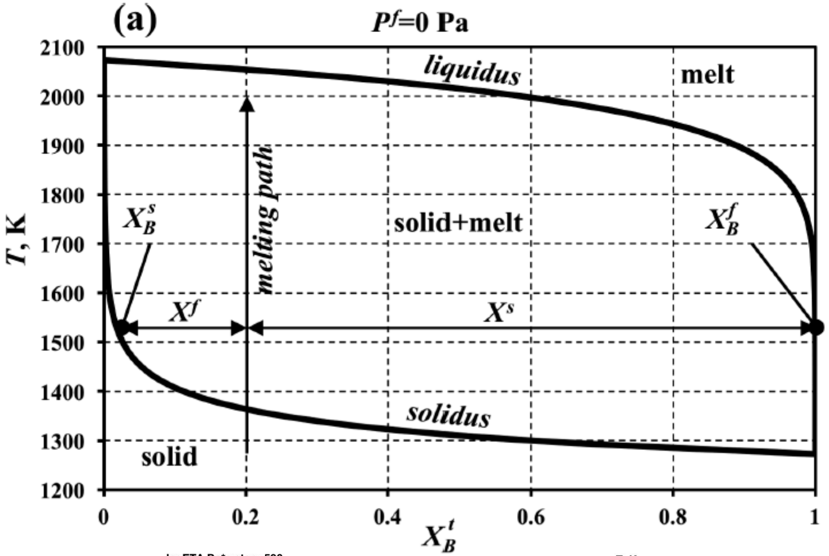

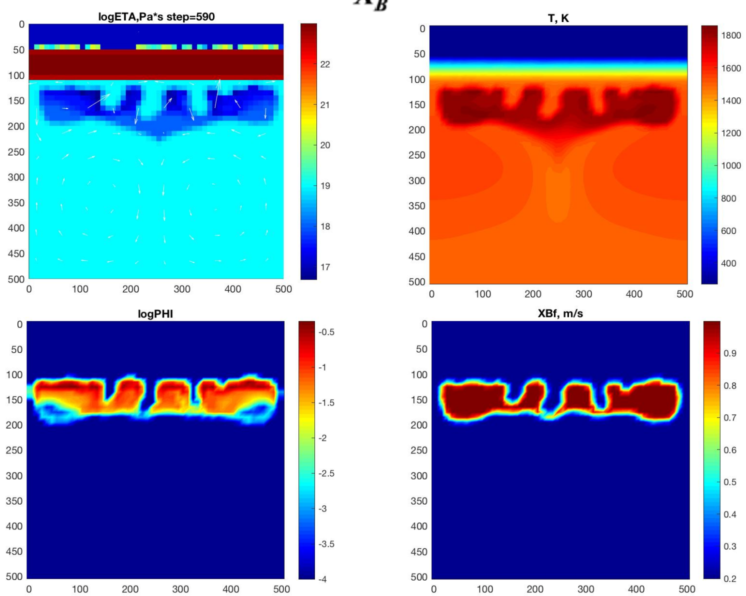

16.11 Toy thermodynamic model of rocks hydration/dehydration

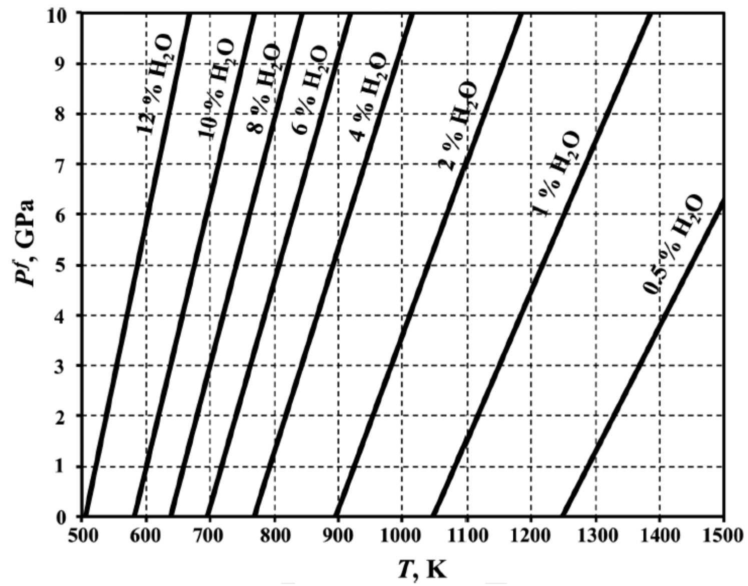

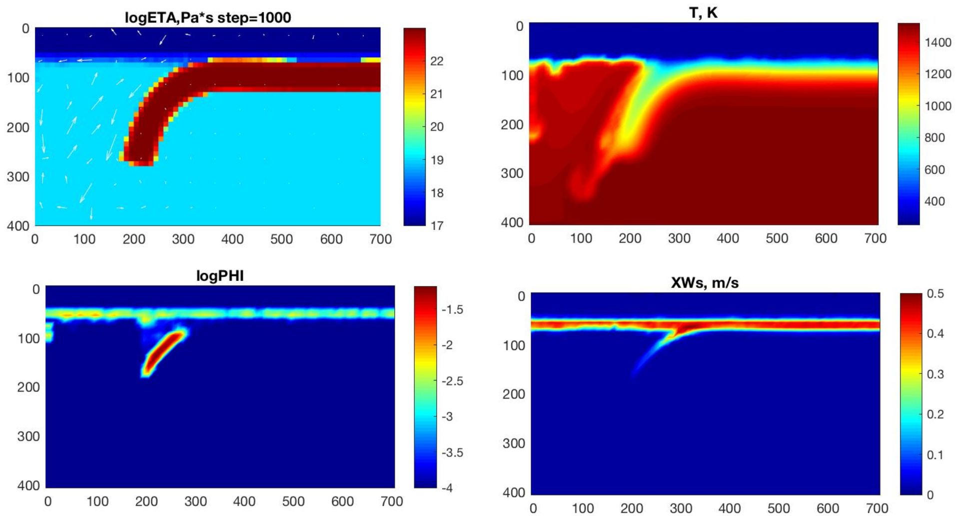

What's new?

Adaptive mesh refinement (Chapter 17)

17

Adaptive mesh refinement

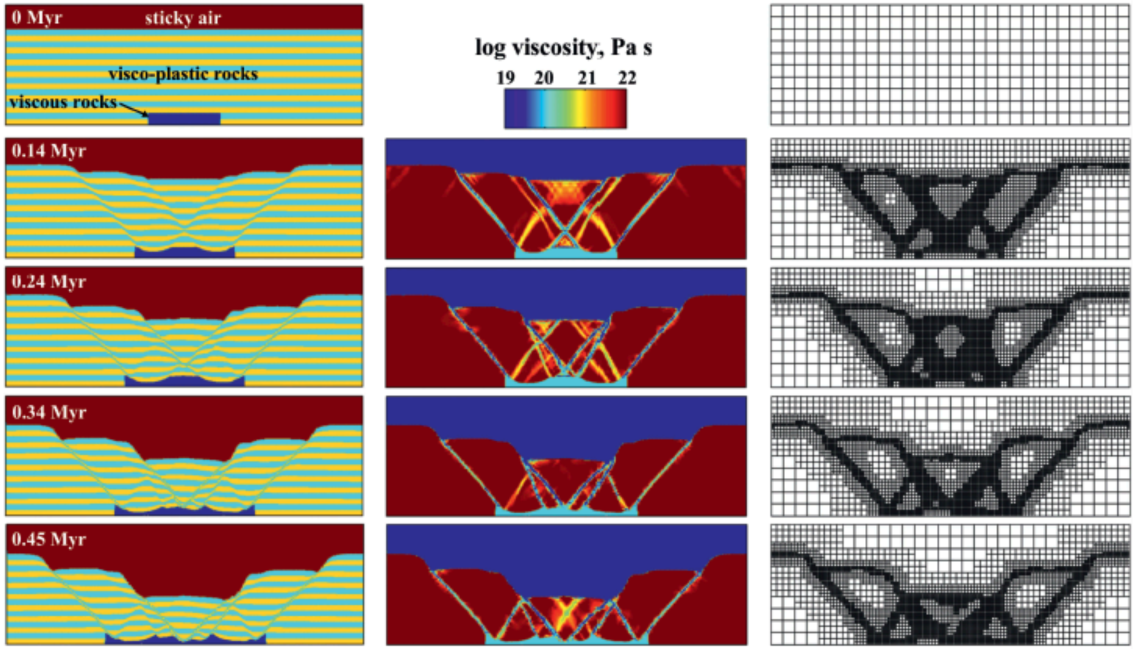

Theory: What is AMR? Mesh refinement with staggered finite differences. 'Swiss cross' approach. Block-structured AMR approach. Conditions for 'hanging nodes'. Refinement criteria. Convergence of the numerical solution. AMR for different conservation equations.
Exercises: Programming of AMR code.

What's new?

Color figures, 90 MatLab examples.

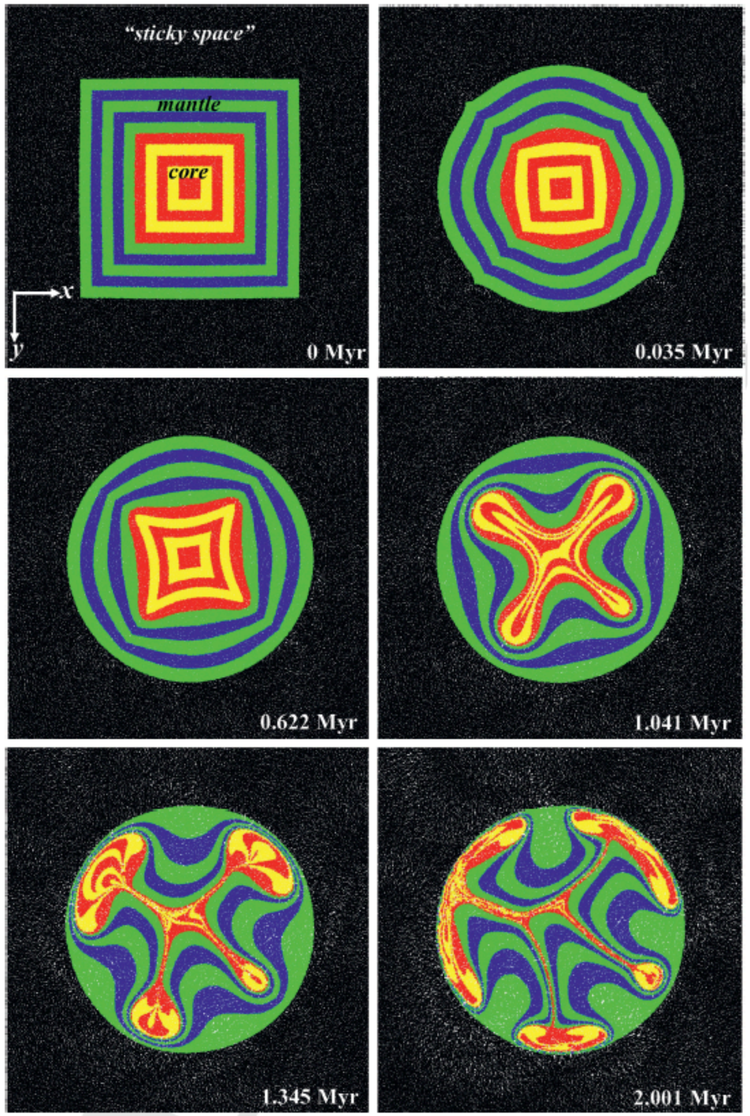

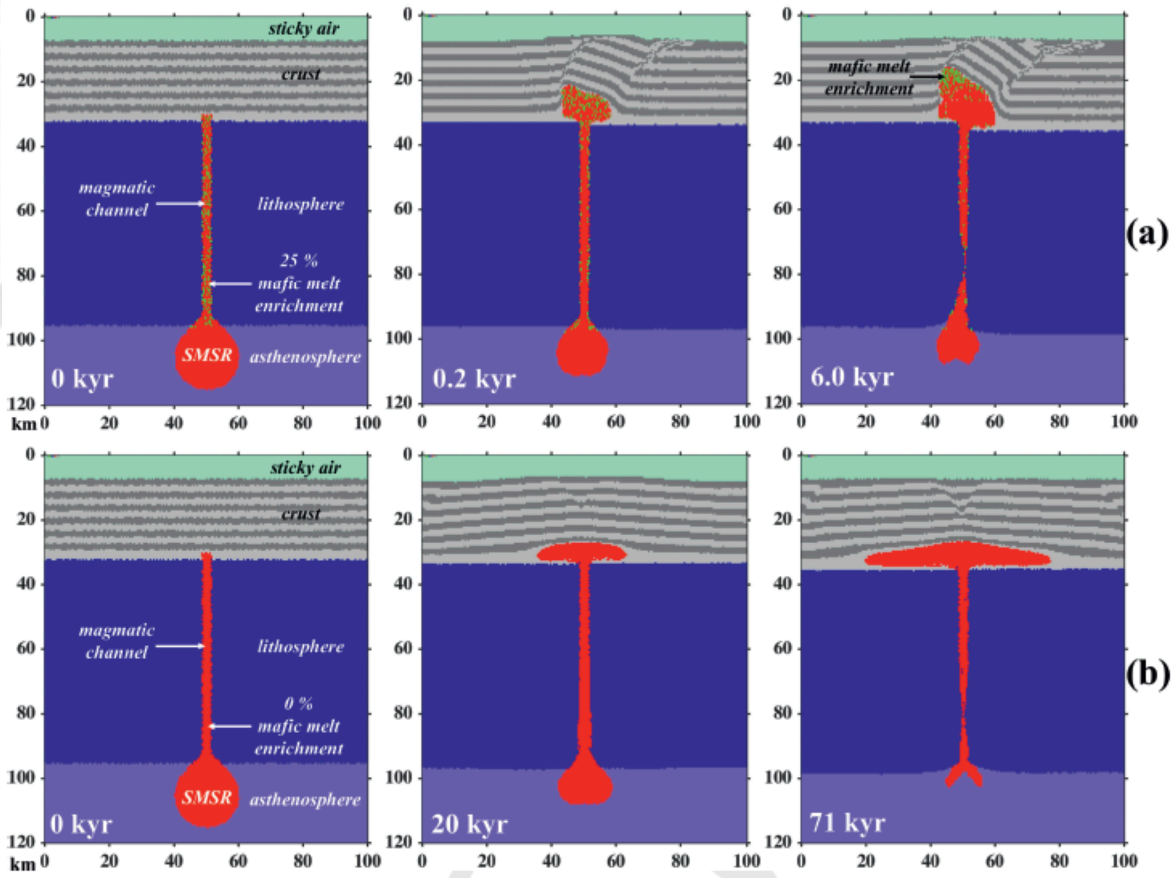

CAMBRIDGE

For more information, and to order, visit:

www.cambridge.org/9781107143142

and enter the code GERYA19 at the checkout

20% Discount *on this title*

Expires 4 March 2020

Introduction to Numerical Geodynamic Modelling

2nd edition

Taras Gerya

Swiss Federal University (ETH), Zürich

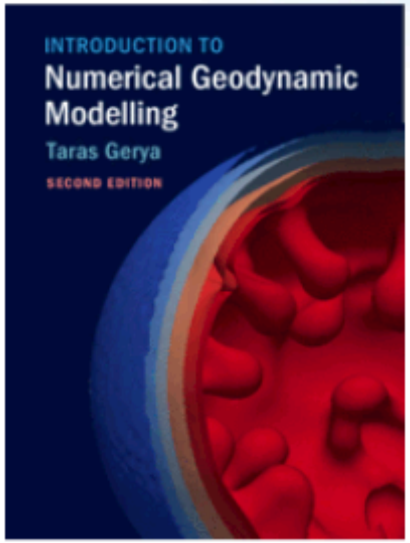

This hands-on introduction to numerical geodynamic modelling provides a solid grounding in the necessary mathematical theory and techniques, including continuum mechanics and partial differential equations, before introducing key numerical modelling methods and applications. Fully updated, this second edition includes four completely new chapters covering the most recent advances in modelling inertial processes, seismic cycles and fluid-solid interactions, and the development of adaptive mesh refinement algorithms. Many well-documented, state-of-the-art visco-elasto-plastic 2D models are presented, which allow robust modelling of key geodynamic processes. Requiring only minimal prerequisite mathematical training, and featuring over sixty practical exercises and ninety MATLAB examples, this user-friendly resource encourages experimentation with geodynamic models. It is an ideal introduction for advanced courses and can be used as a self-study aid for graduates seeking to master geodynamic modelling for their own research projects.

May 2019

247 x 174 mm 454pp 66 b/w illus. 96 colour illus.

Hardback 978-1-107-14314-2

Original price	*Discount price*
£59.99	£47.99
$79.99	$63.99

Slab tear propagation:
Numerical model and implications to Apennines

Taras Gerya
ETH-Zurich

Dave Bercovici
Yale University

Claudio Faccenna
University of Texas at Austin
Università Roma TRE

Modeler's classification of geodynamical processes

Easy to imagine and Easy to model

Difficult to imagine but Easy to model

Difficult to imagine and Difficult to model

Easy to imagine but Difficult to model

Wortel and Spakman (2000)

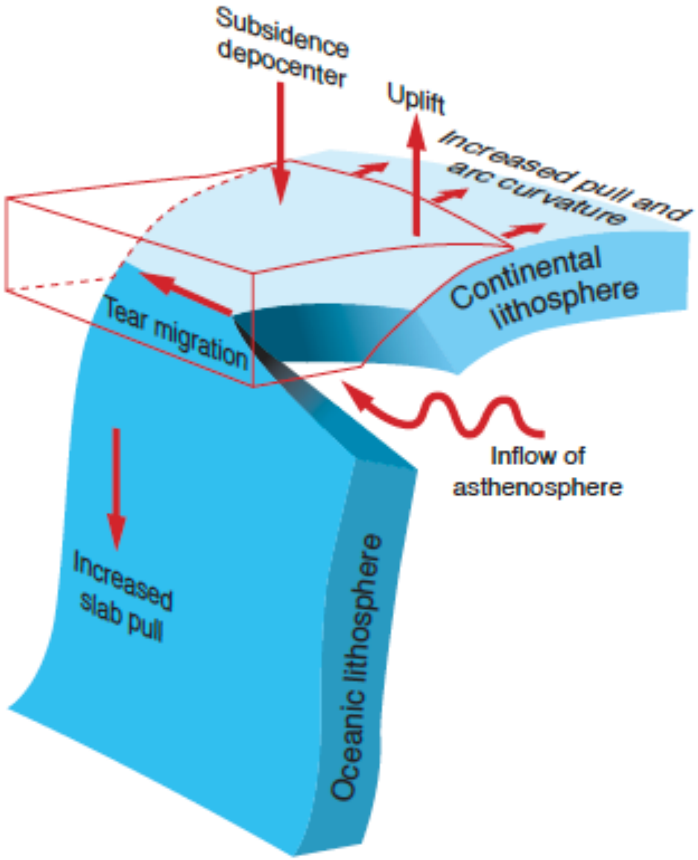

Fig. 4. Plate boundary processes predicted to accompany lateral migration of slab detachment. The concentration of slab pull forces causes a pattern of subsidence (depocenter development) and uplift migrating along strike. It also enhances arc migration (roll-back). Asthenospheric material flows into the gap resulting from slab detachment and causes a specific type of variable composition magmatism, of finite duration, and possibly mineralization.

Gerya et al. (2004)

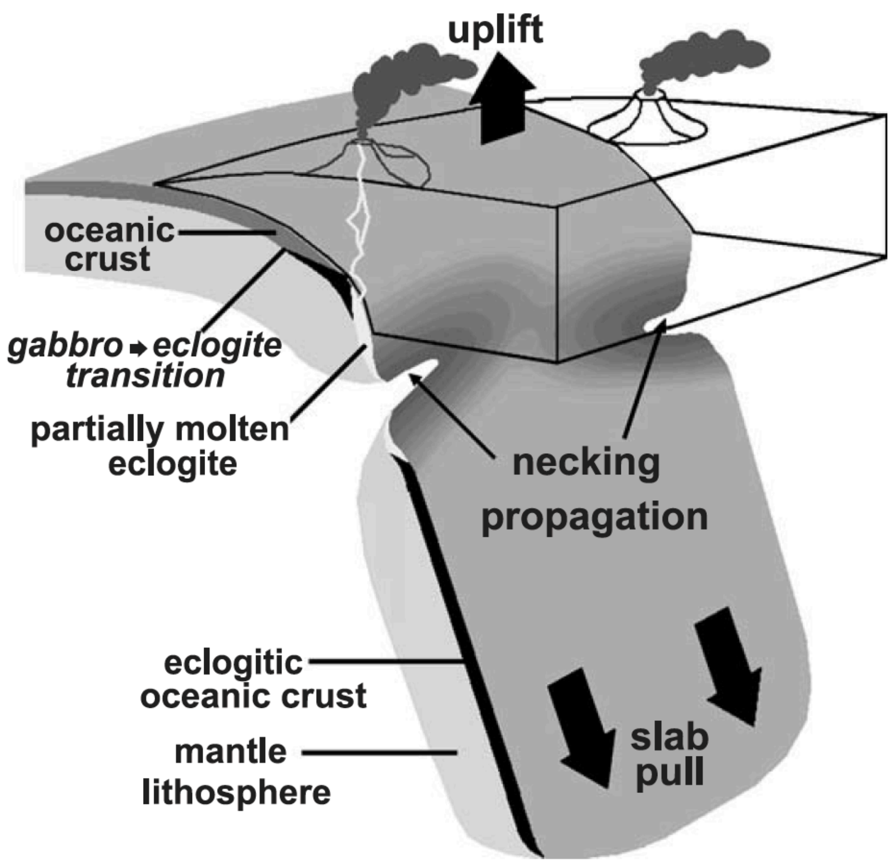

Fig. 8. Conceptual 3-D model of the slab breakoff geometry inferred from our 2-D numerical experiments. See the text for discussion.

Easy to imagine but Difficult to model

Motivation

3D slab tearing under Appenines

C. Faccenna et al. / Earth and Planetary Science Letters 407 (2014) 163–174

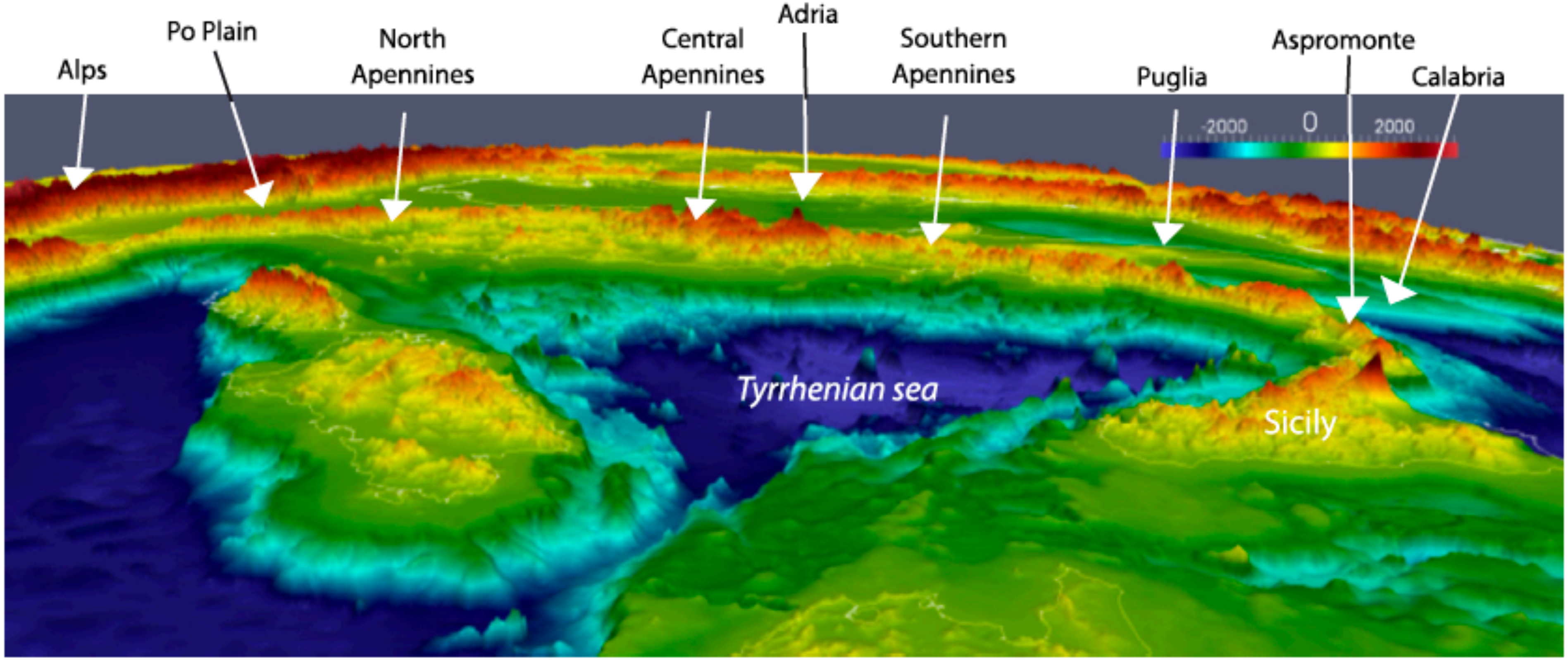

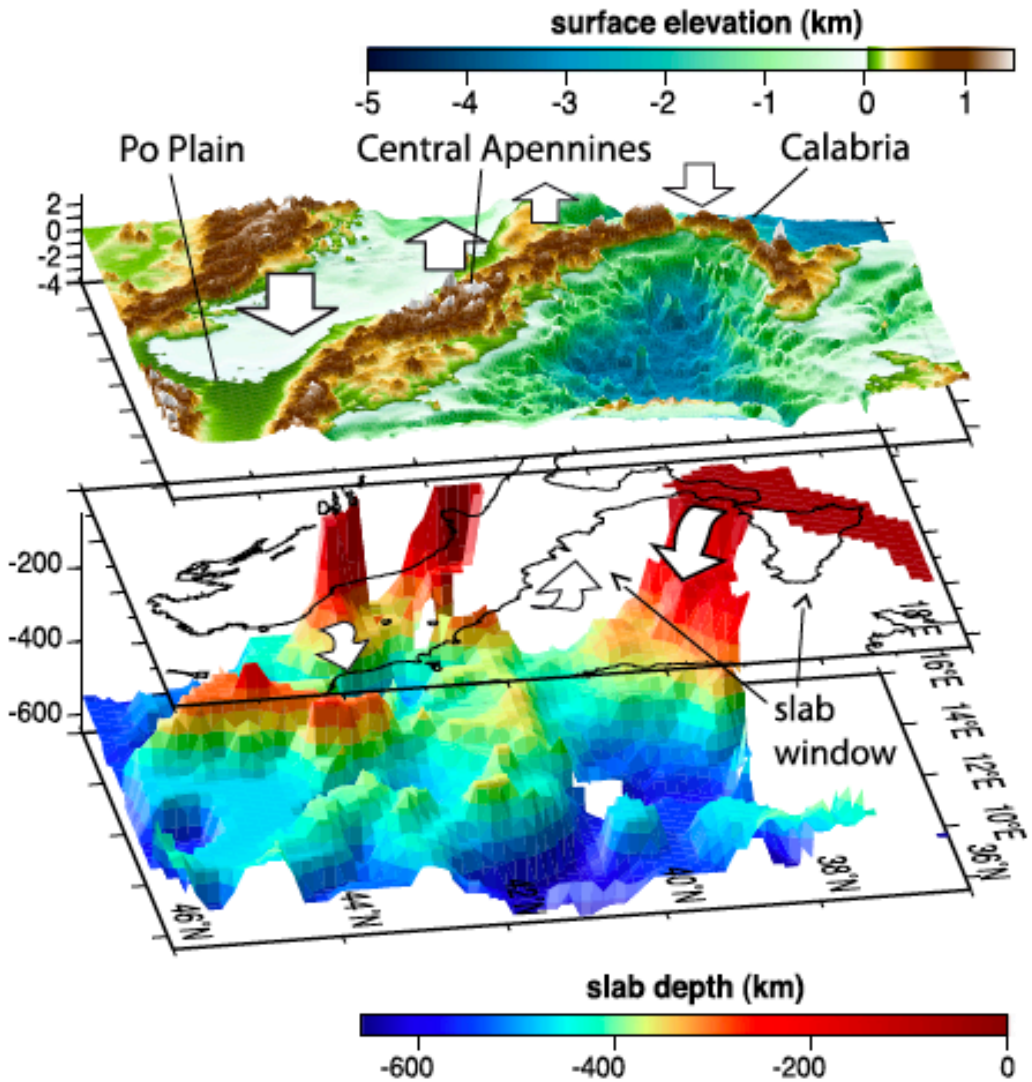

Fig. 5. 3D view of the topography on top of the isosurface enclosing the >0.8% anomaly volume from *P* wave M01 tomography model (Piromallo and Morelli, 2003), where the colors indicate depth in km. Notice the correspondence between low topography and locations of active subduction with attached slab segments and the slab window beneath the Central-Southern Apennines. Modified from Faccenna et al. (2011).

Faccenna et al. (2014)

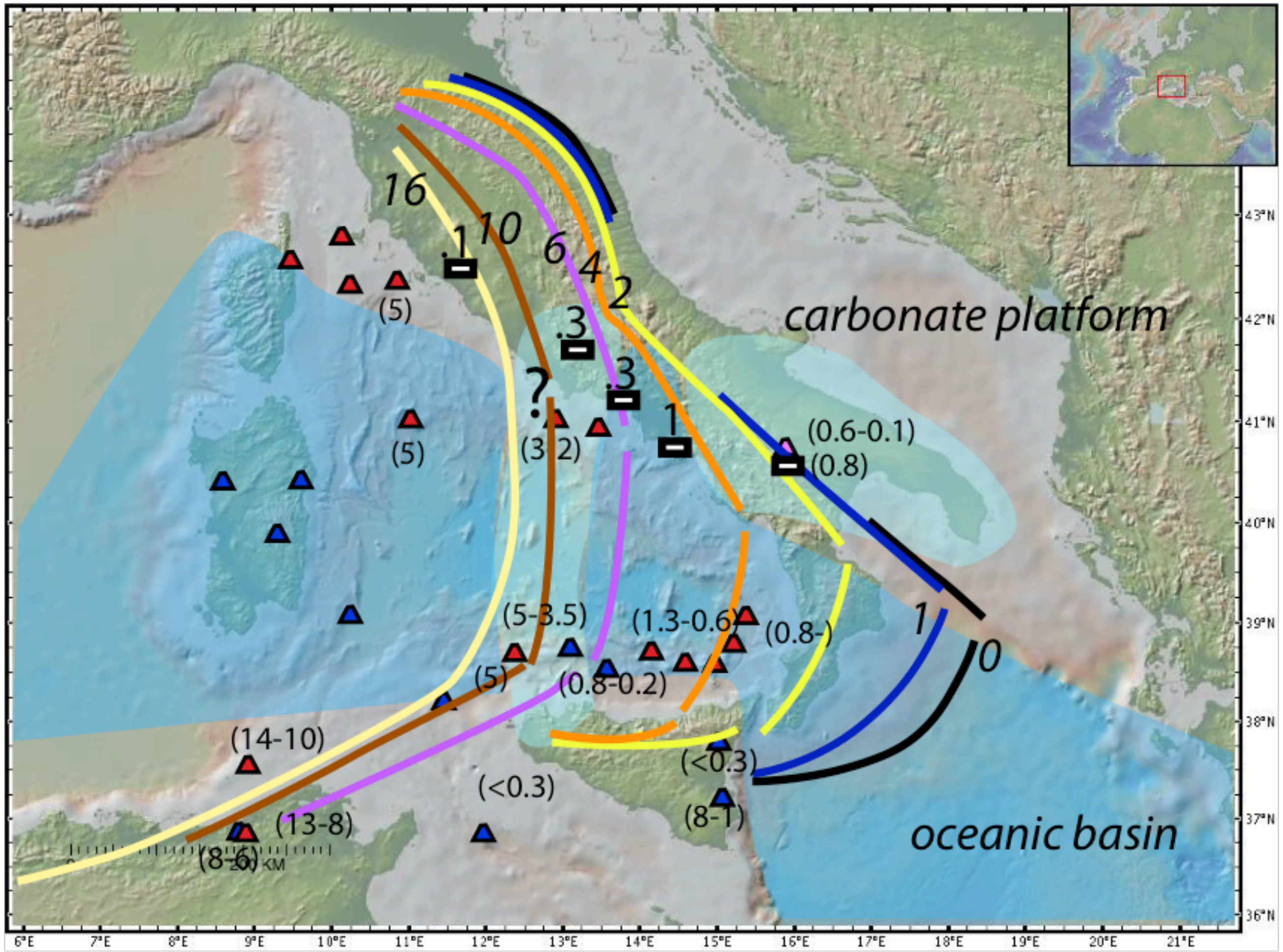

16
10
6
4
2
1
0
.1
.3
.3
1
?
carbonate platform
oceanic basin
(5)
(5)
(3-2)
(0.6-0.1)
(0.8)
(5-3.5)
(1.3-0.6)
(0.8-)
(5)
(0.8-0.2)
(14-10)
(<0.3)
(<0.3)
(8-1)
(13-8)
(8-6)

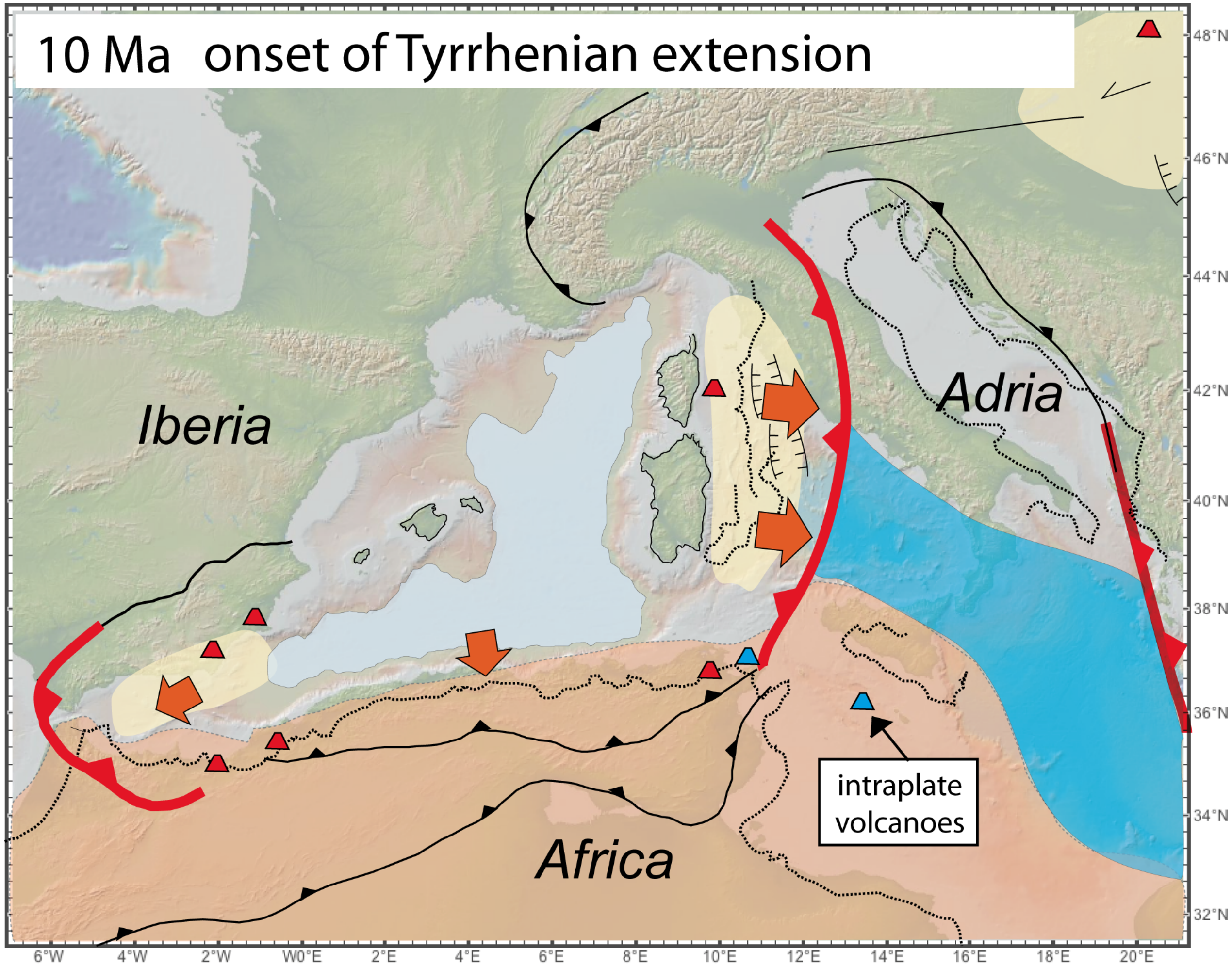
10 Ma onset of Tyrrhenian extension
Iberia
Adria
Africa
intraplate
volcanoes
48°N
46°N
44°N
42°N
40°N
38°N
36°N
34°N
32°N
6°W
4°W
2°W
W0°E
2°E
4°E
6°E
8°E
10°E
12°E
14°E
16°E
18°E
20°E

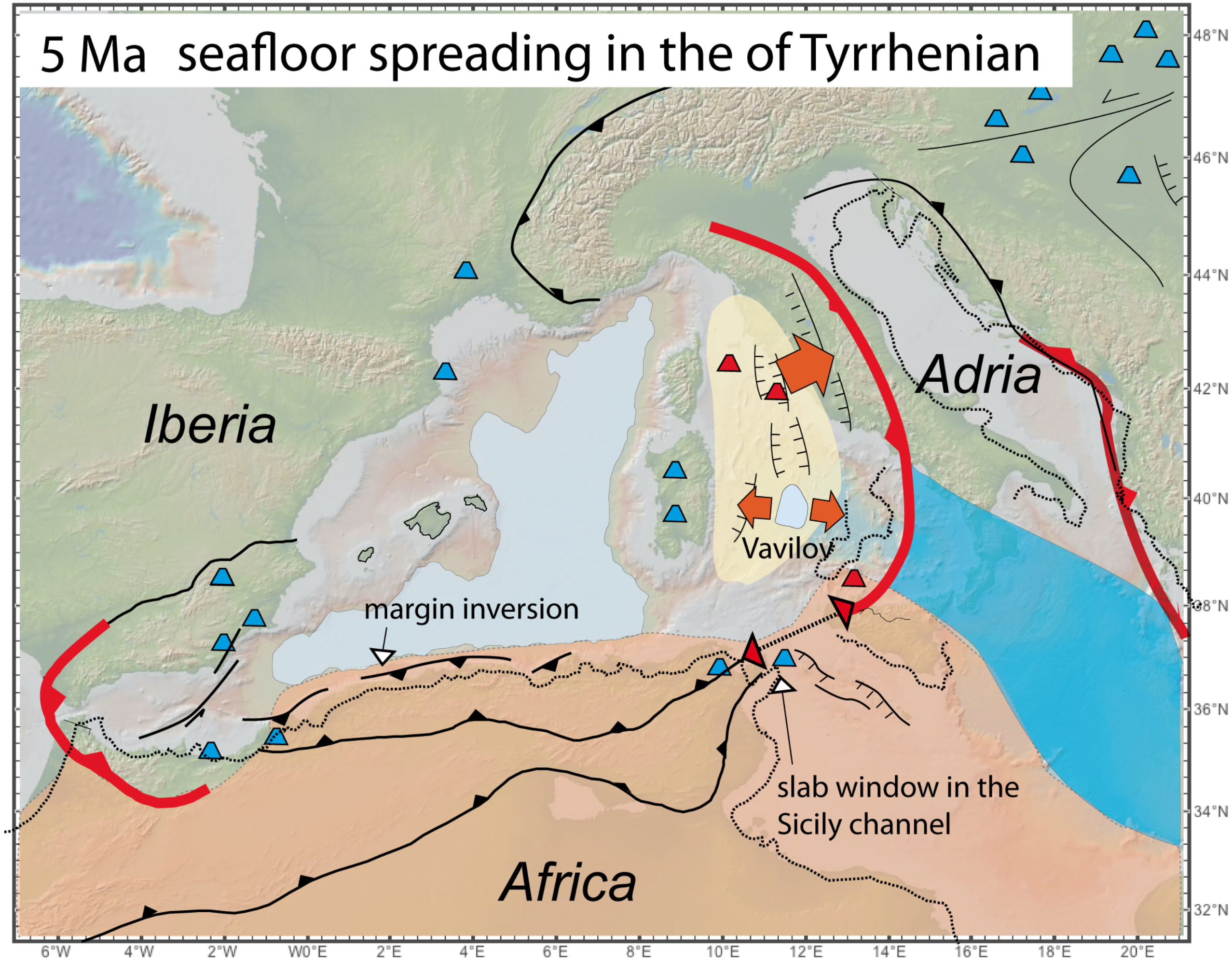
5 Ma seafloor spreading in the of Tyrrhenian
Iberia
Adria
Africa
Vavilov
margin inversion
slab window in the
Sicily channel
48°N
46°N
44°N
42°N
40°N
38°N
36°N
34°N
32°N
6°W
4°W
2°W
W0°E
2°E
4°E
6°E
8°E
10°E
12°E
14°E
16°E
18°E
20°E

2 Ma seafloor spreading in the of Tyrrhenian

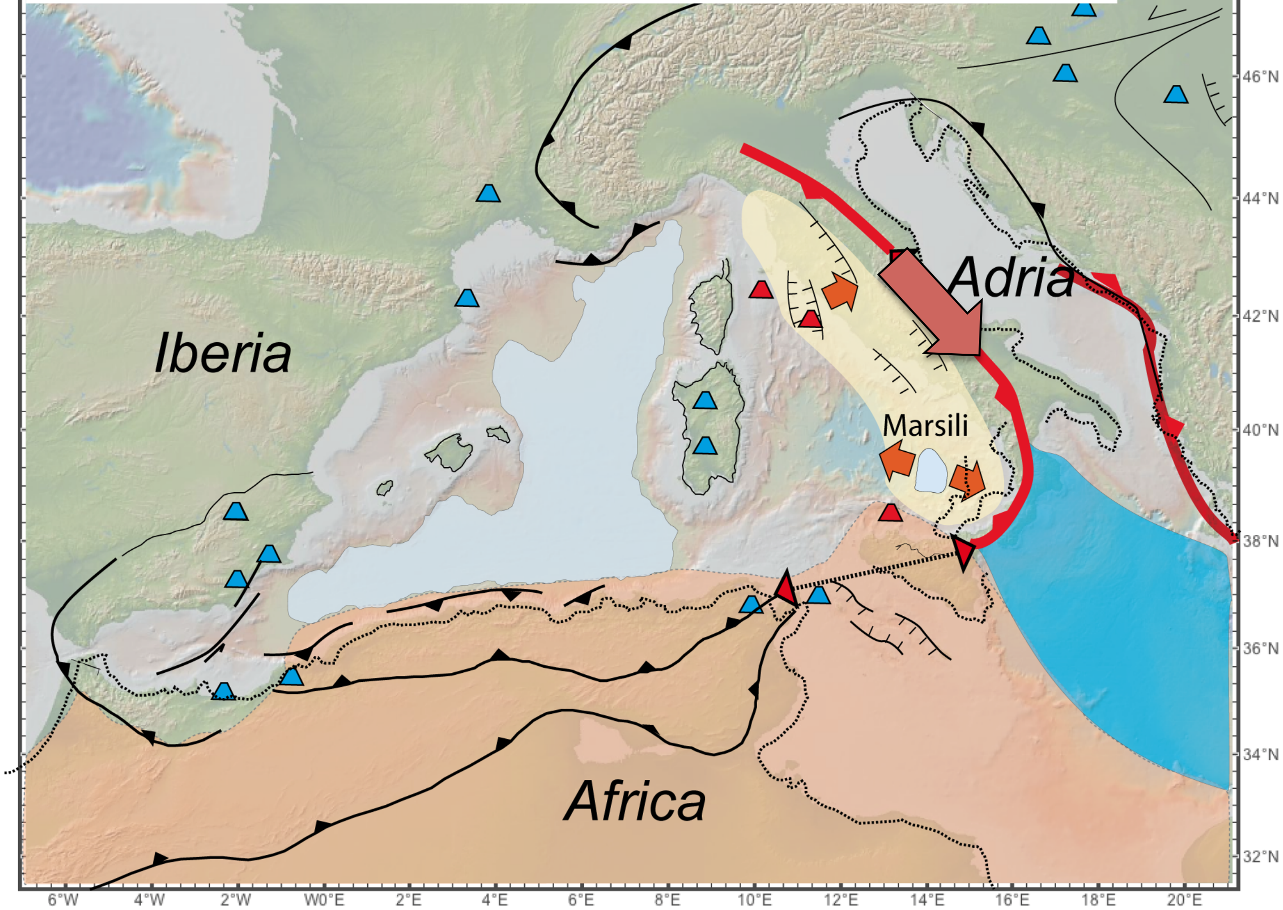

Tear propagation

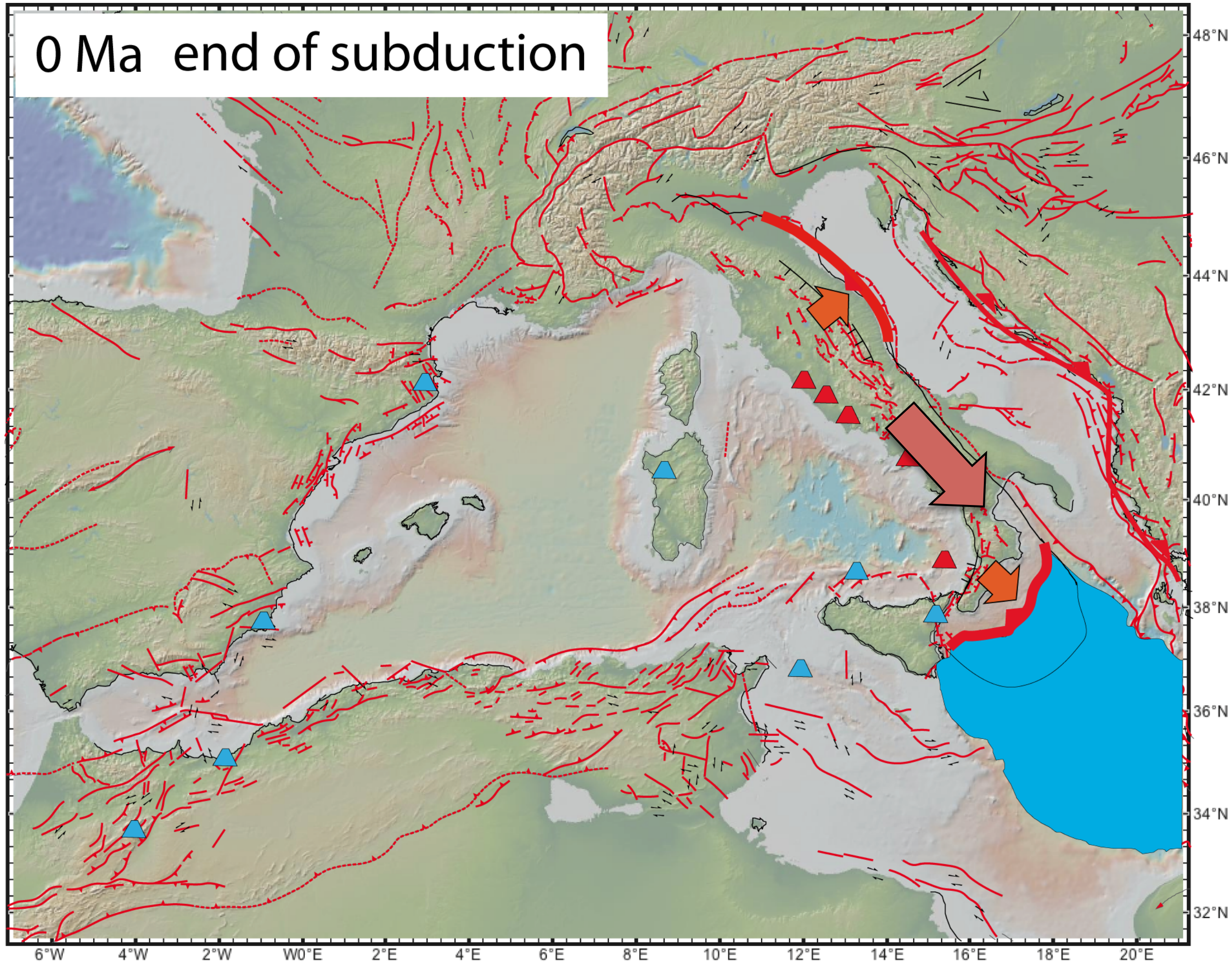
0 Ma end of subduction
48°N
46°N
44°N
42°N
40°N
38°N
36°N
34°N
32°N
6°W
4°W
2°W
W0°E
2°E
4°E
6°E
8°E
10°E
12°E
14°E
16°E
18°E
20°E

Previous 3D models (advancing subduction)

Slab breakoff is necking (boudinage)

Burkett and Billen (2010)

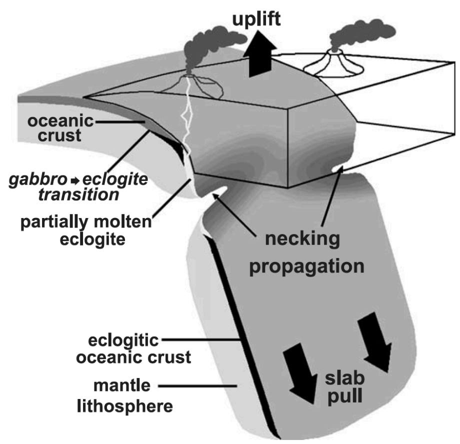

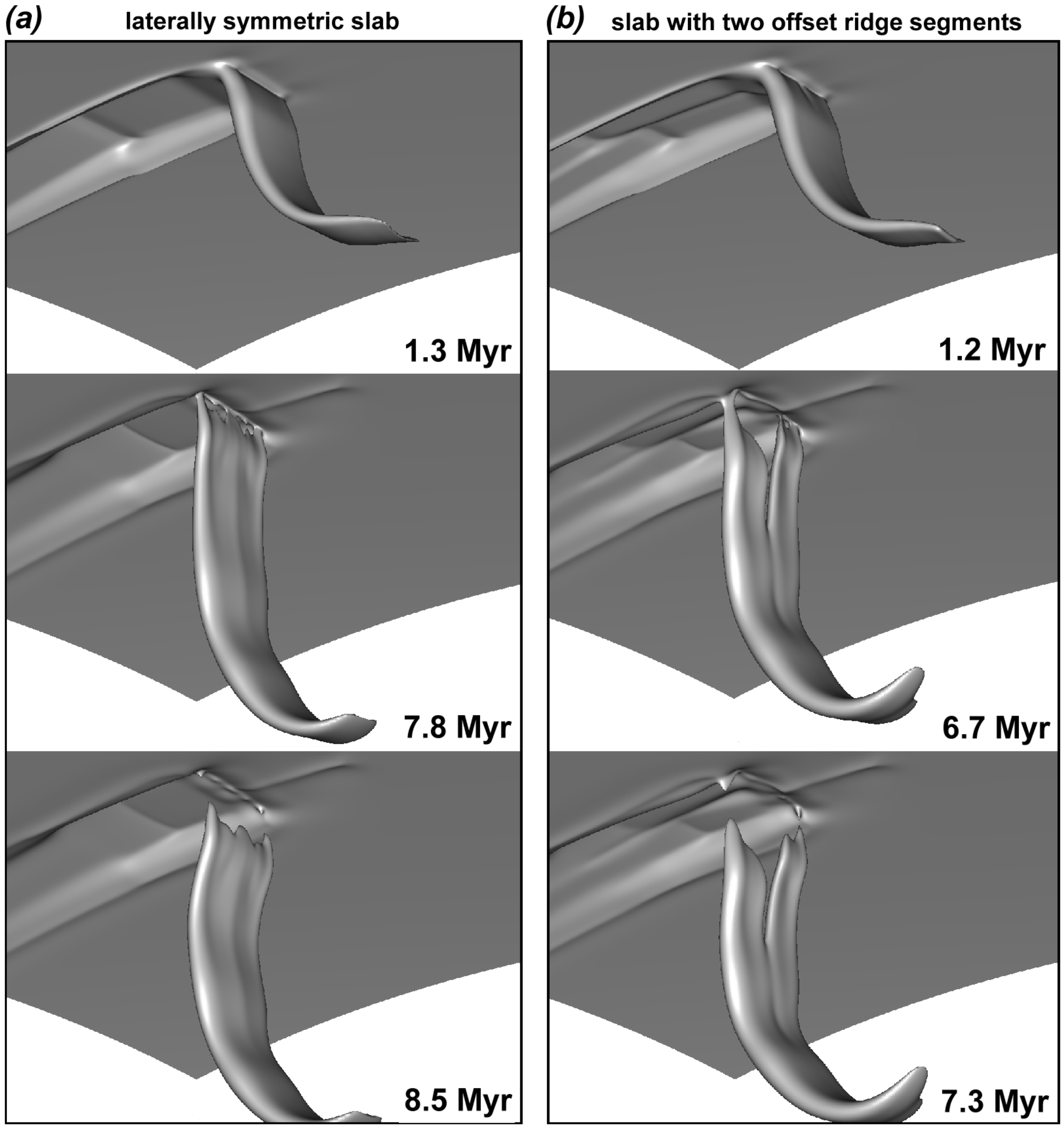

Slab breakoff is necking (boudinage)

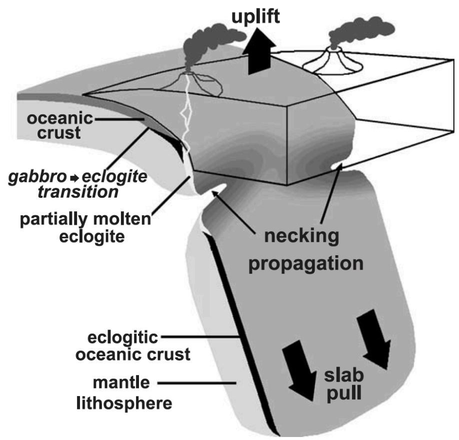

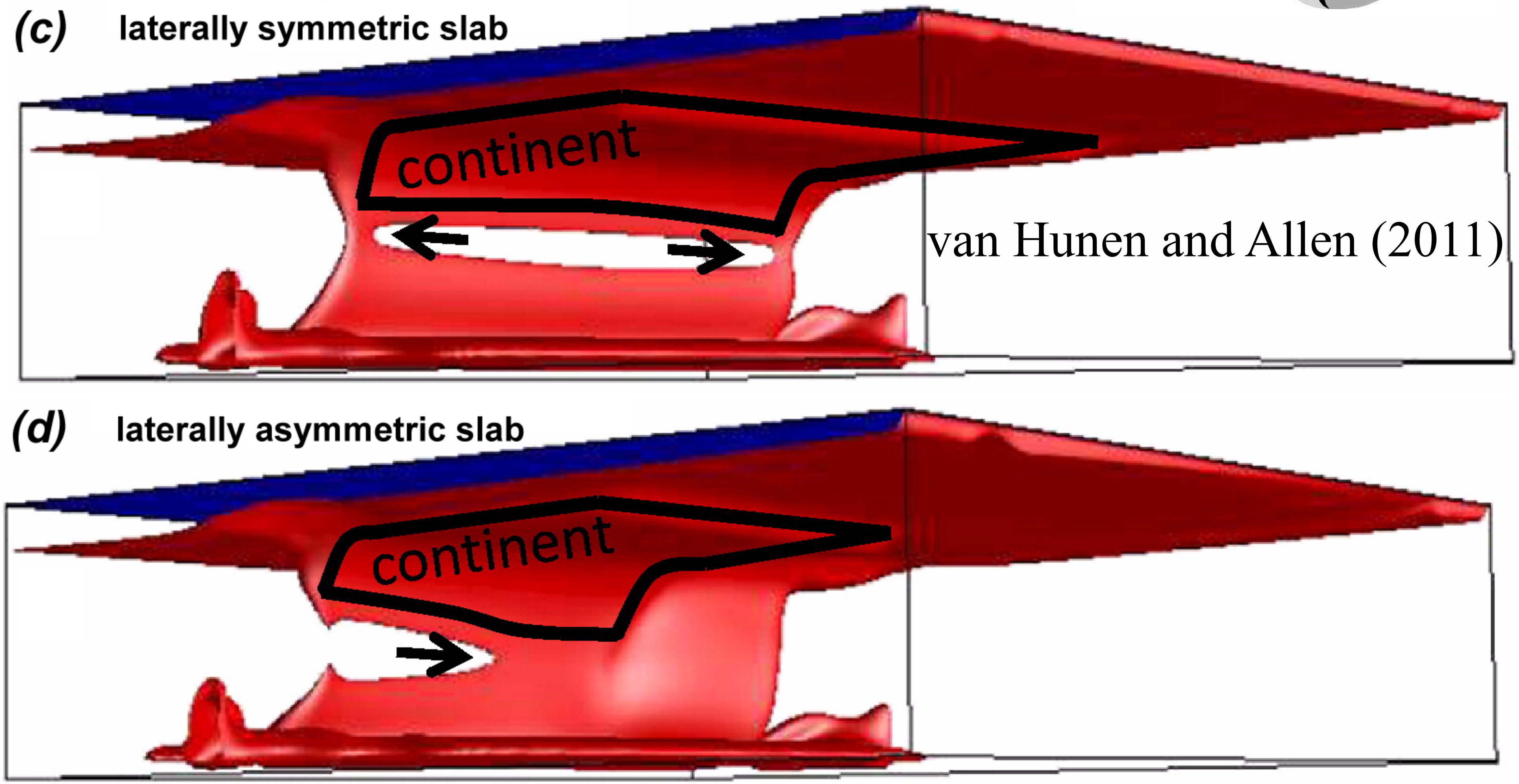

van Hunen and Allen (2011)

Numerical Model (retreating subduction)

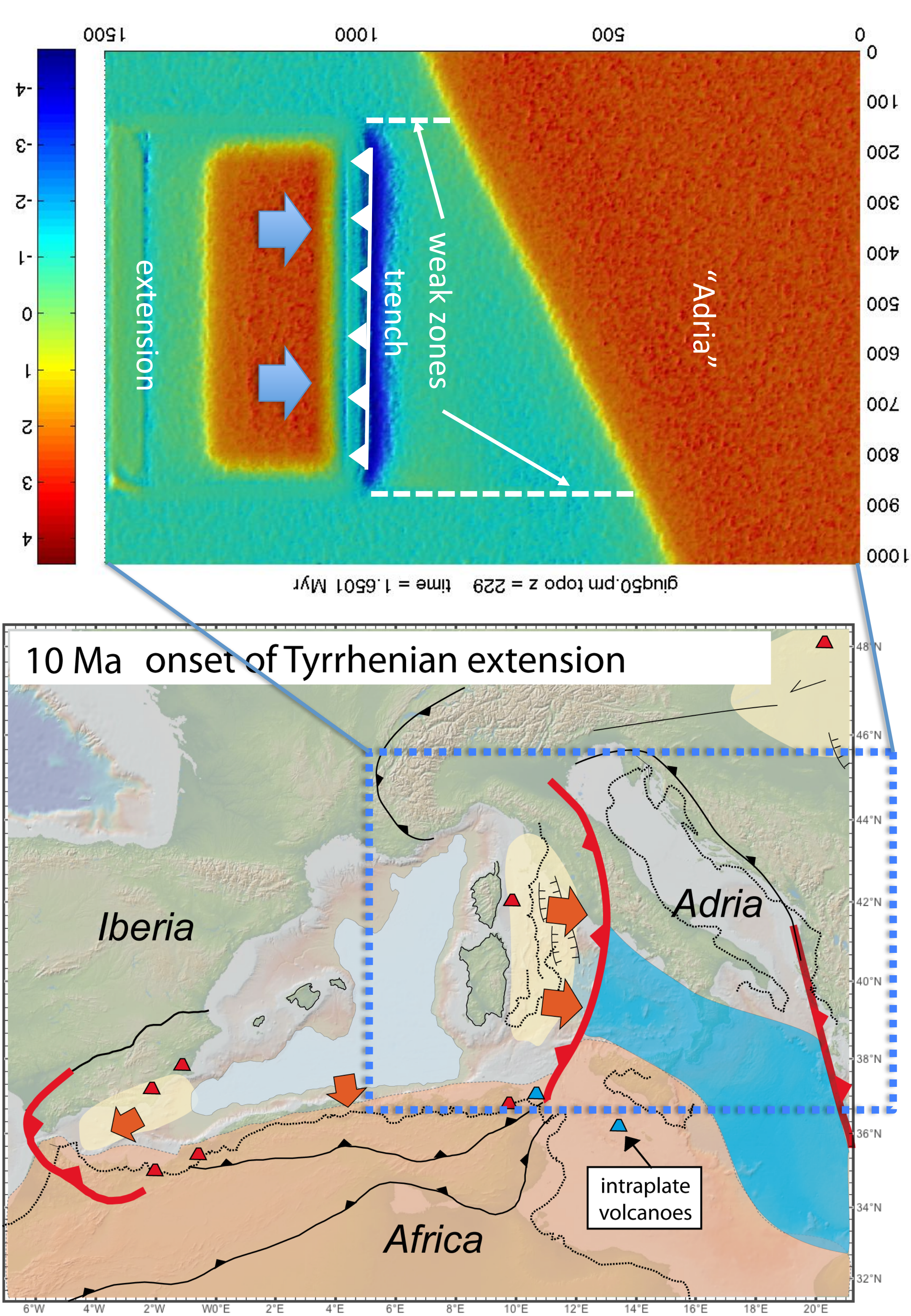

10 Ma onset of Tyrrhenian extension
Iberia
Adria
Africa
intraplate volcanoes
"Adria"
weak zones
trench
extension
giug50.prn topo z = 229 time = 1.6501 Myr

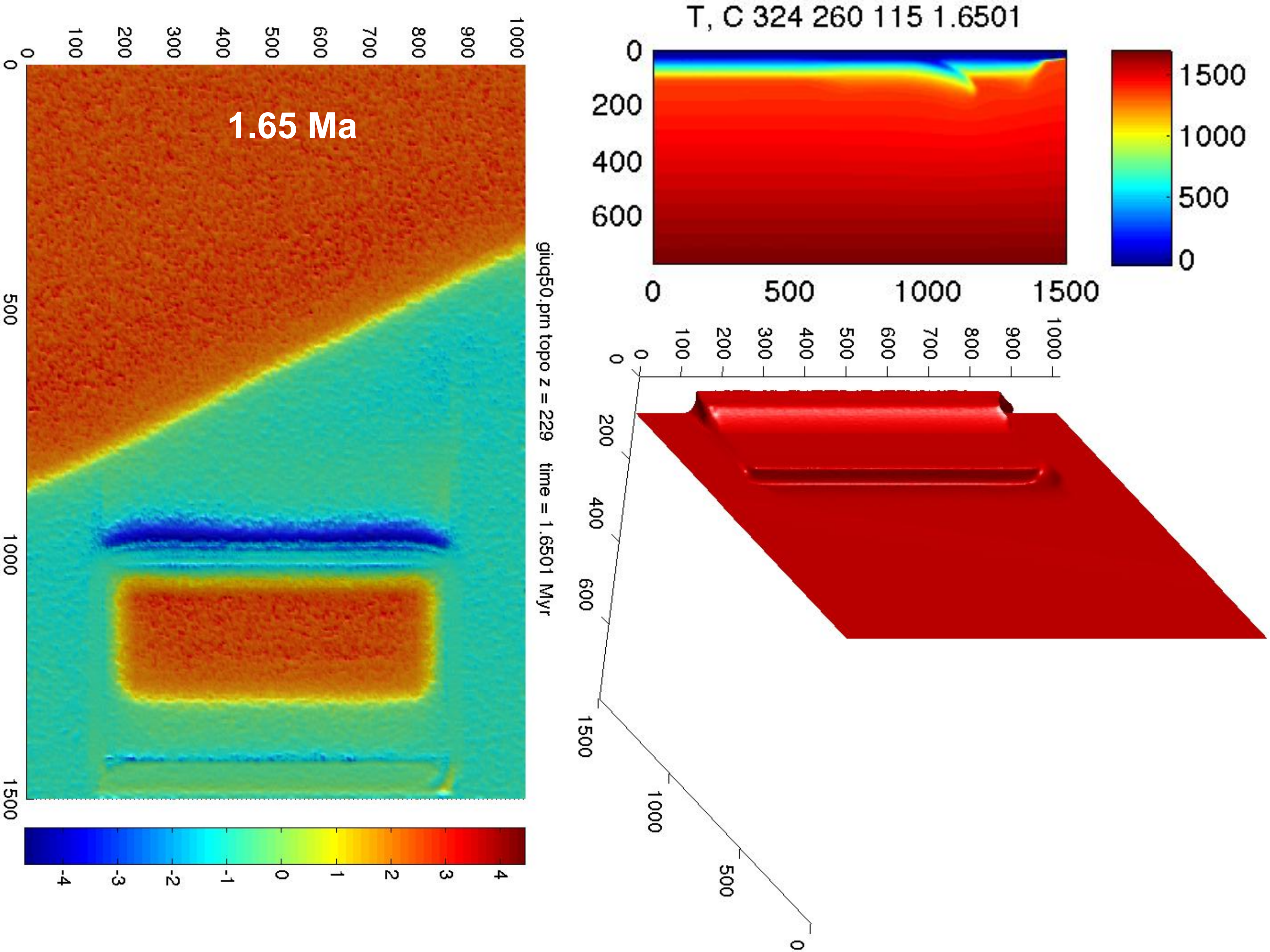
1.65 Ma
giuq50.prn topo z = 229 time = 1.6501 Myr
T, C 324 260 115 1.6501

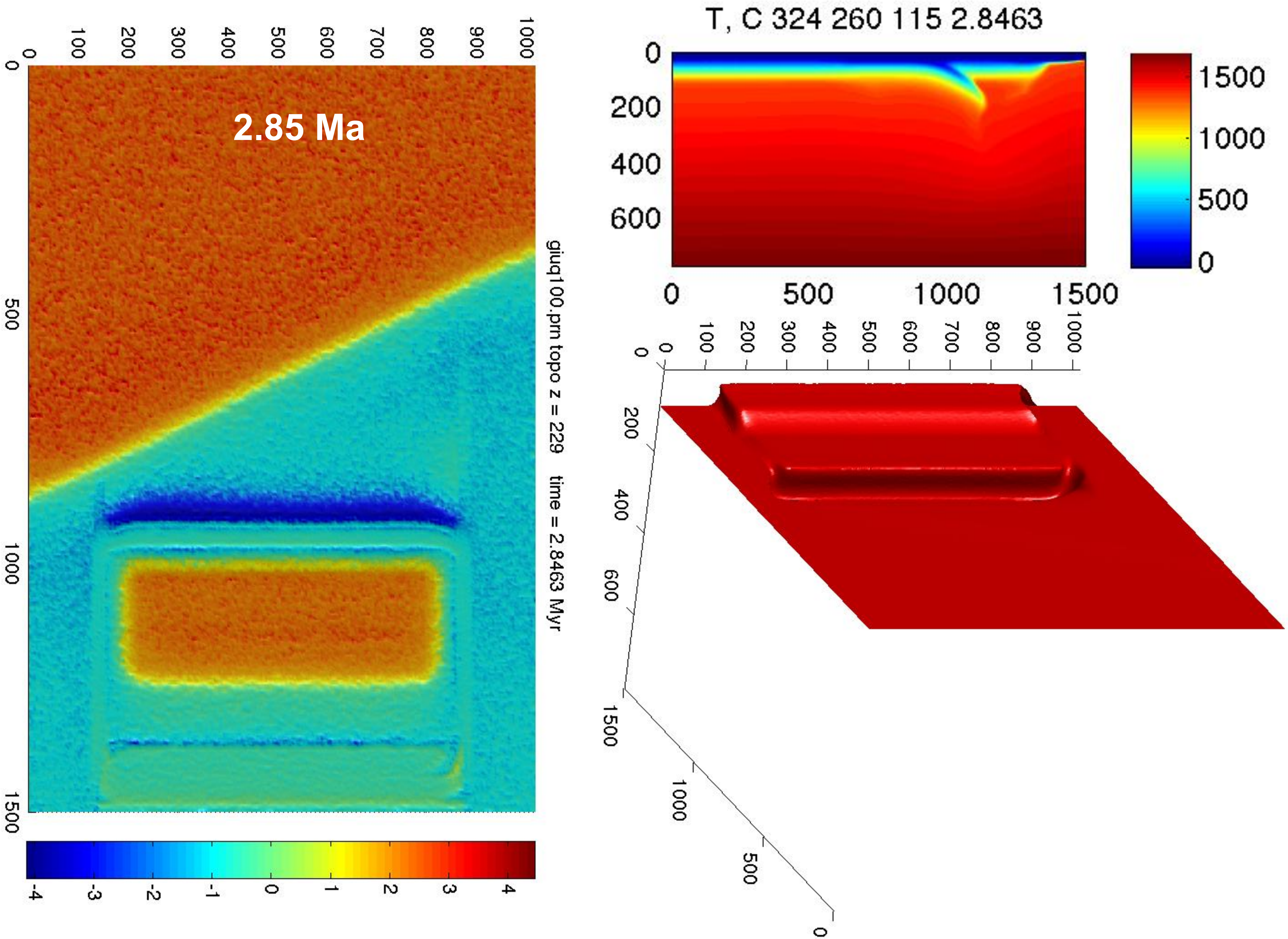

2.85 Ma
giuq100.prn topo z = 229 time = 2.8463 Myr
T, C 324 260 115 2.8463

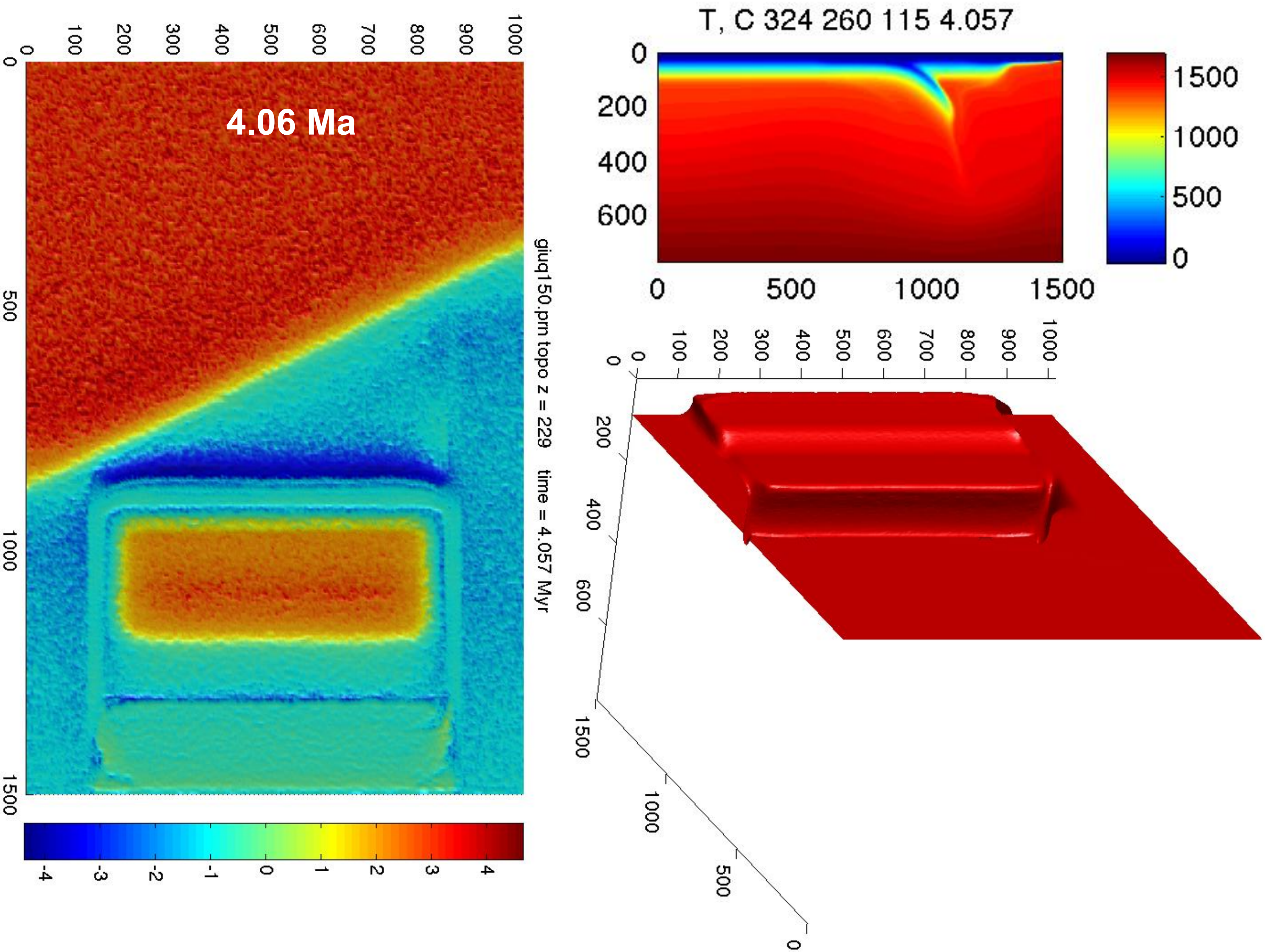
4.06 Ma
giuq150.prn topo z = 229 time = 4.057 Myr
T, C 324 260 115 4.057
0
200
400
600
0
500
1000
1500
1500
1000
500
0

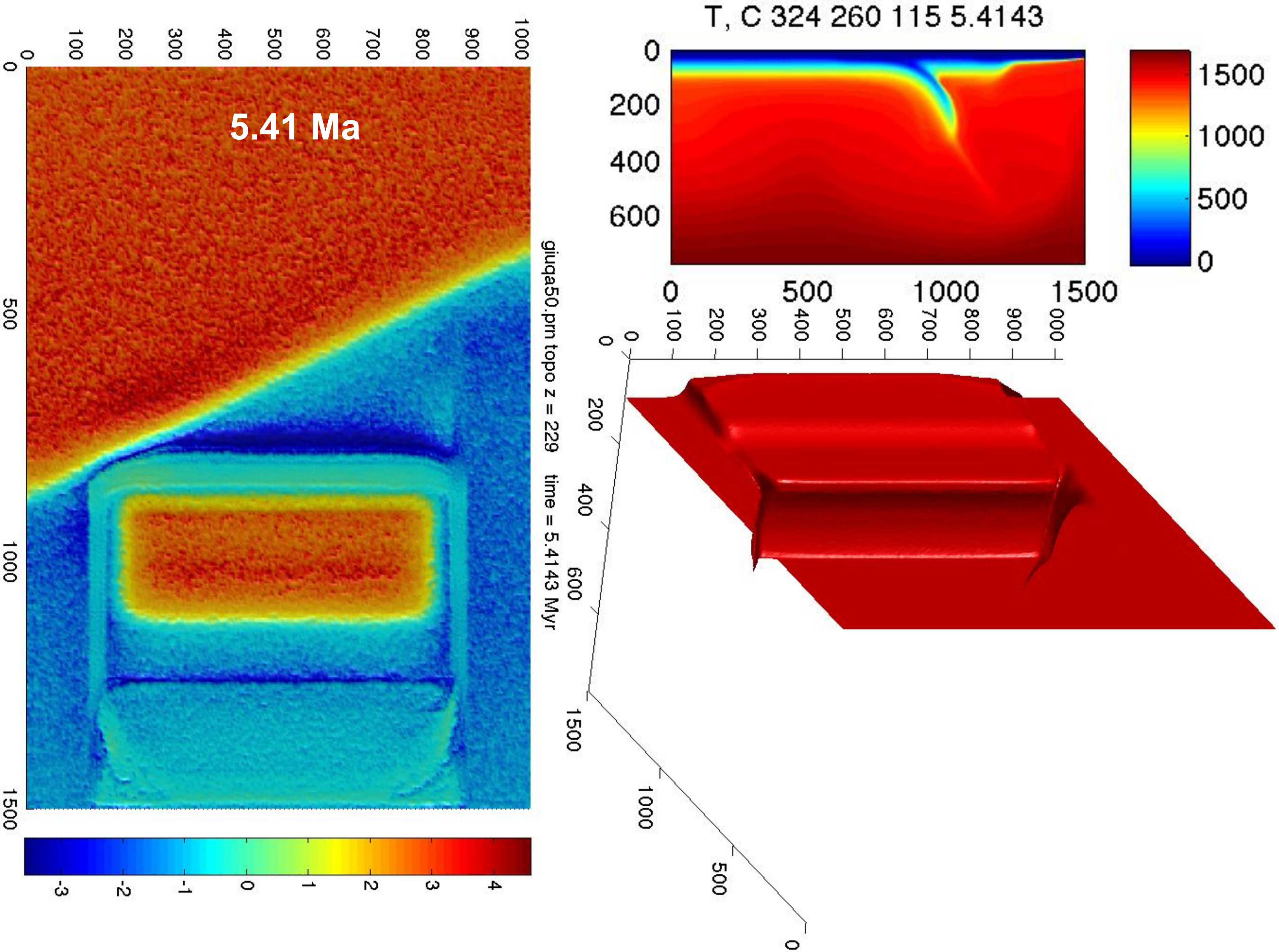

5.41 Ma
giuga50.prn topo z = 229 time = 5.4143 Myr
0 100 200 300 400 500 600 700 800 900 1000
0 500 1000 1500
-3 -2 -1 0 1 2 3 4
T, C 324 260 115 5.4143
0 200 400 600
0 500 1000 1500
1500 1000 500 0

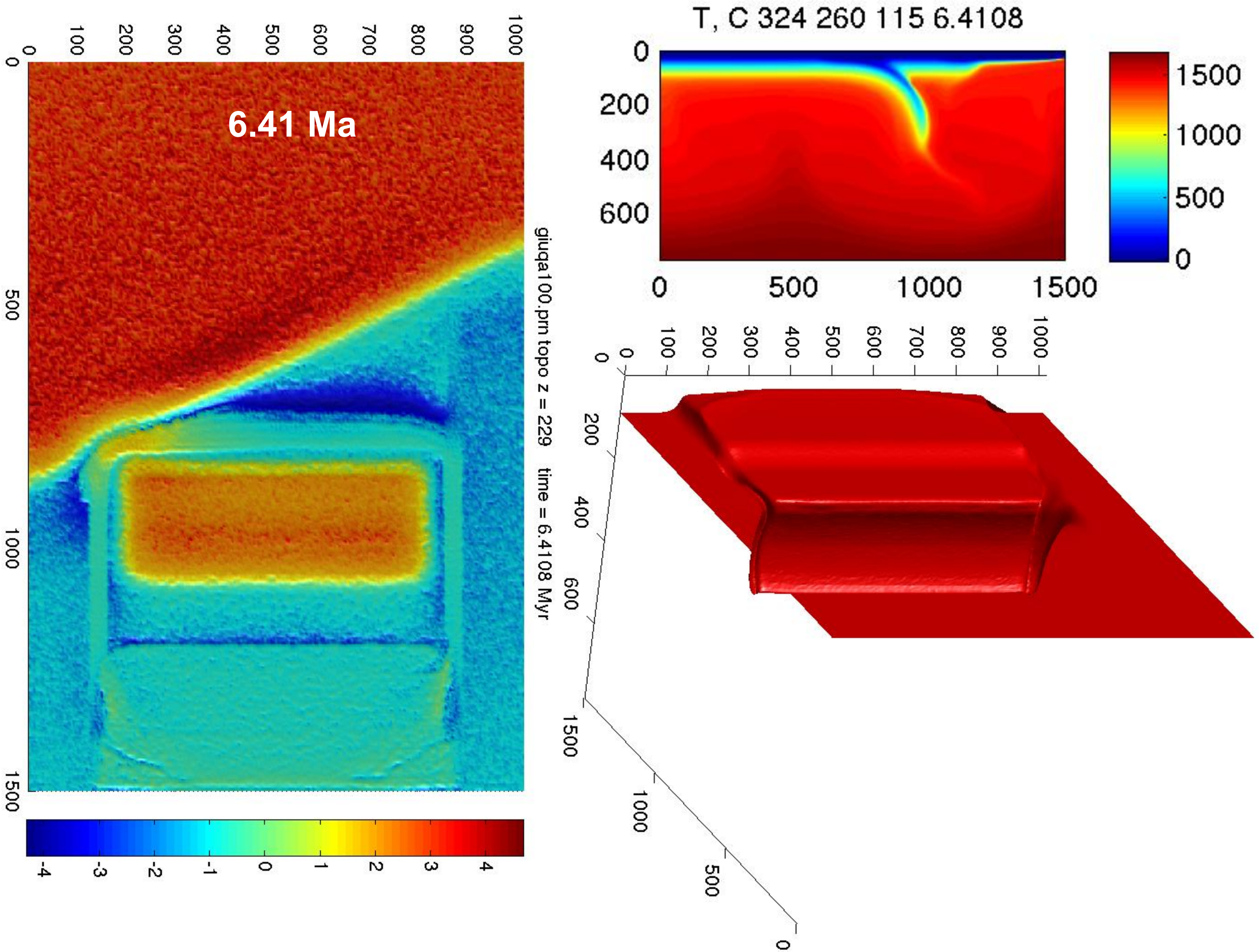

T, C 324 260 115 6.4108
6.41 Ma
giuqa100.prn topo z = 229 time = 6.4108 Myr

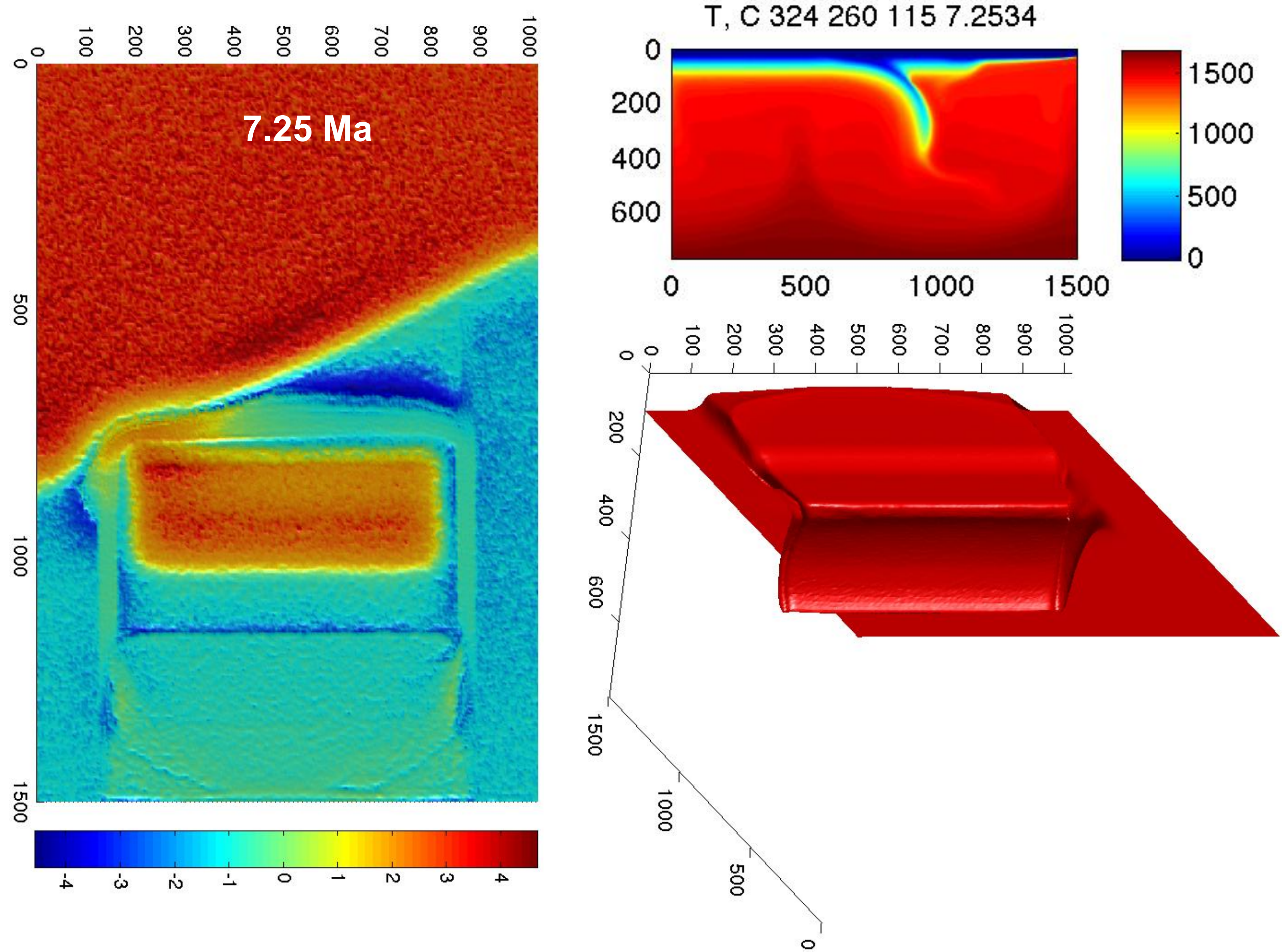
7.25 Ma
T, C 324 260 115 7.2534
0
200
400
600
0
500
1000
1500
1500
1000
500
0

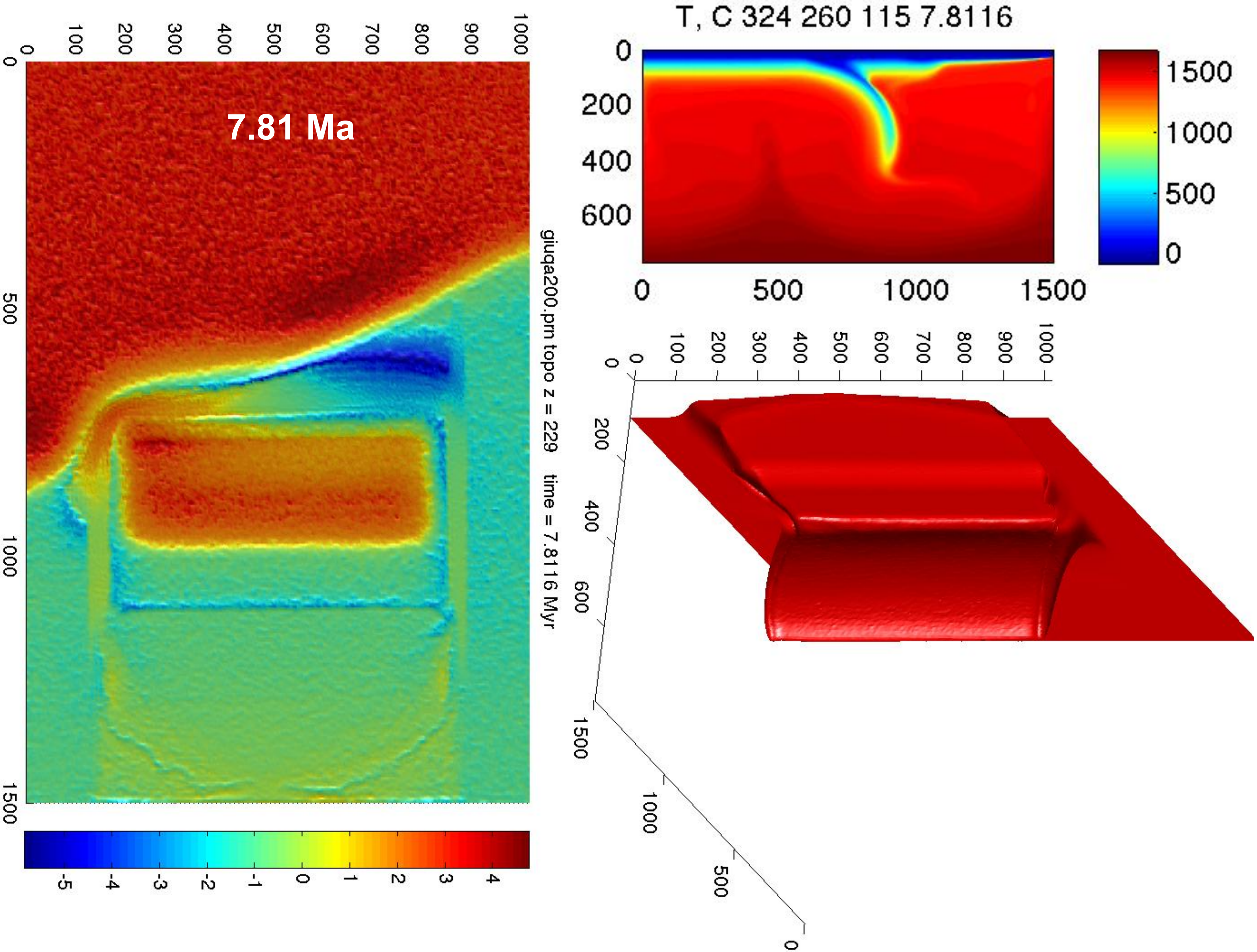
7.81 Ma
giuqa200.prn topo z = 229 time = 7.8116 Myr
T, C 324 260 115 7.8116

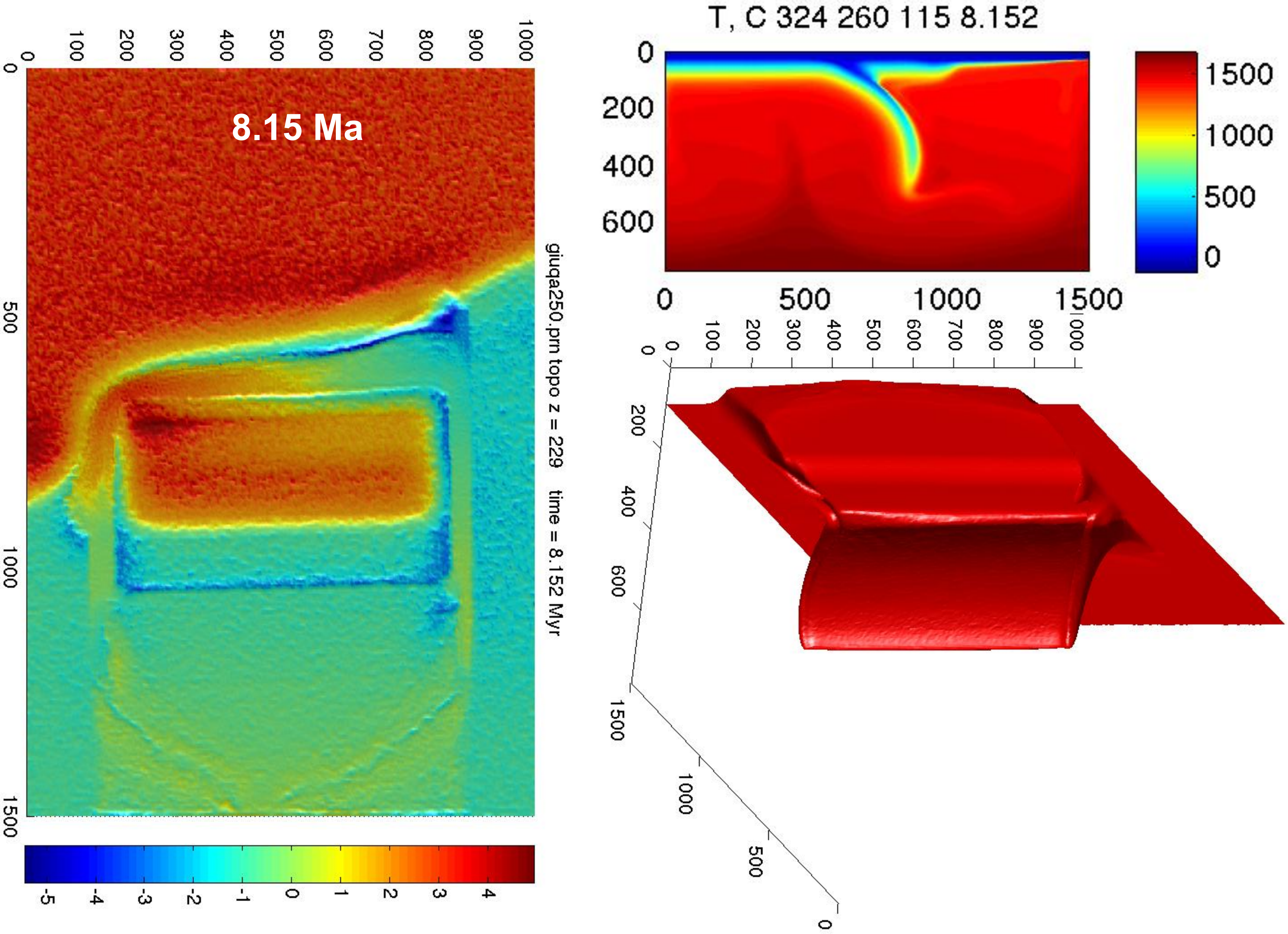

8.15 Ma
giuqa250.prn topo z = 229 time = 8.152 Myr
T, C 324 260 115 8.152

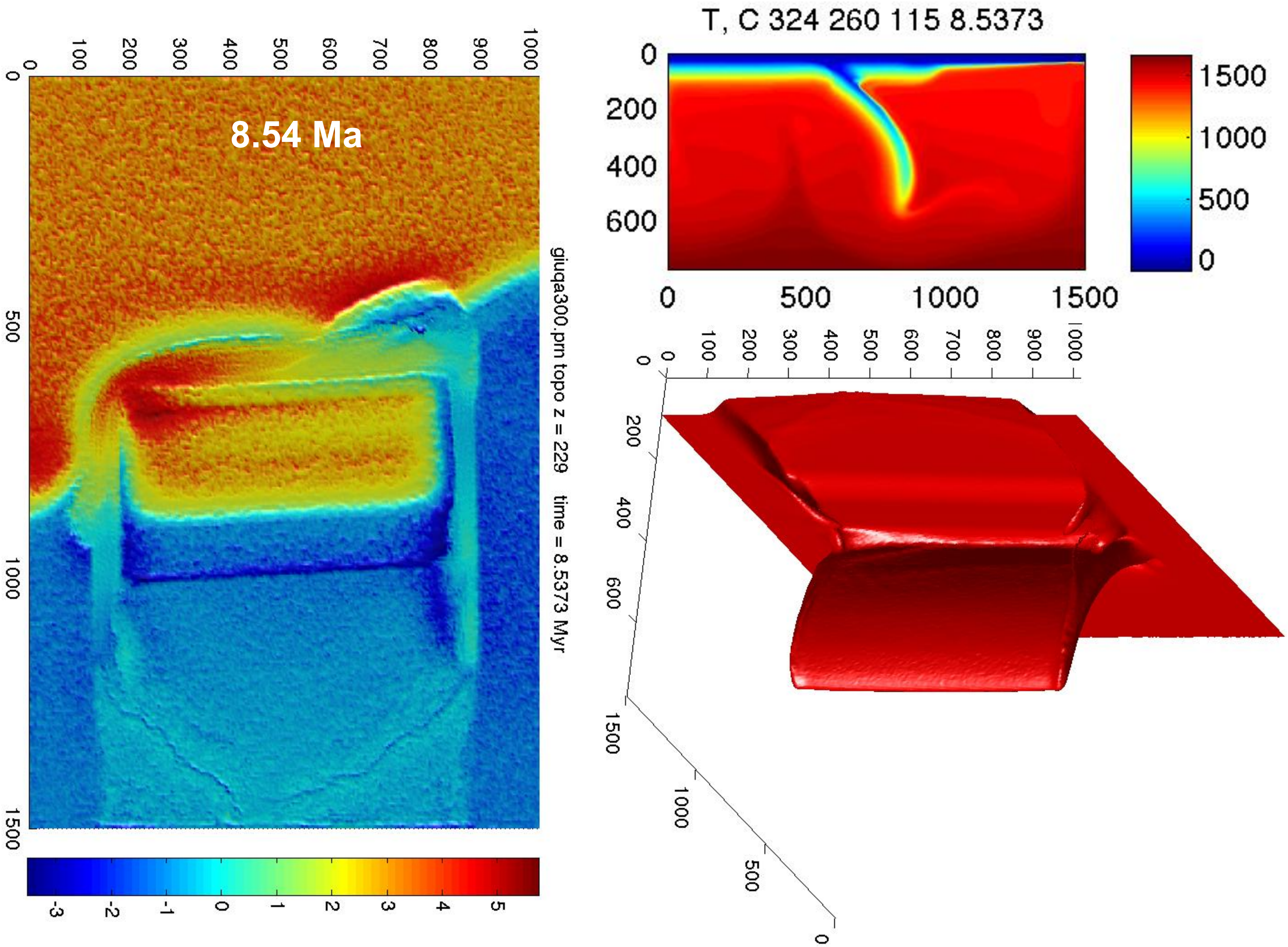

8.54 Ma
giuqa300.prn topo z = 229 time = 8.5373 Myr
T, C 324 260 115 8.5373

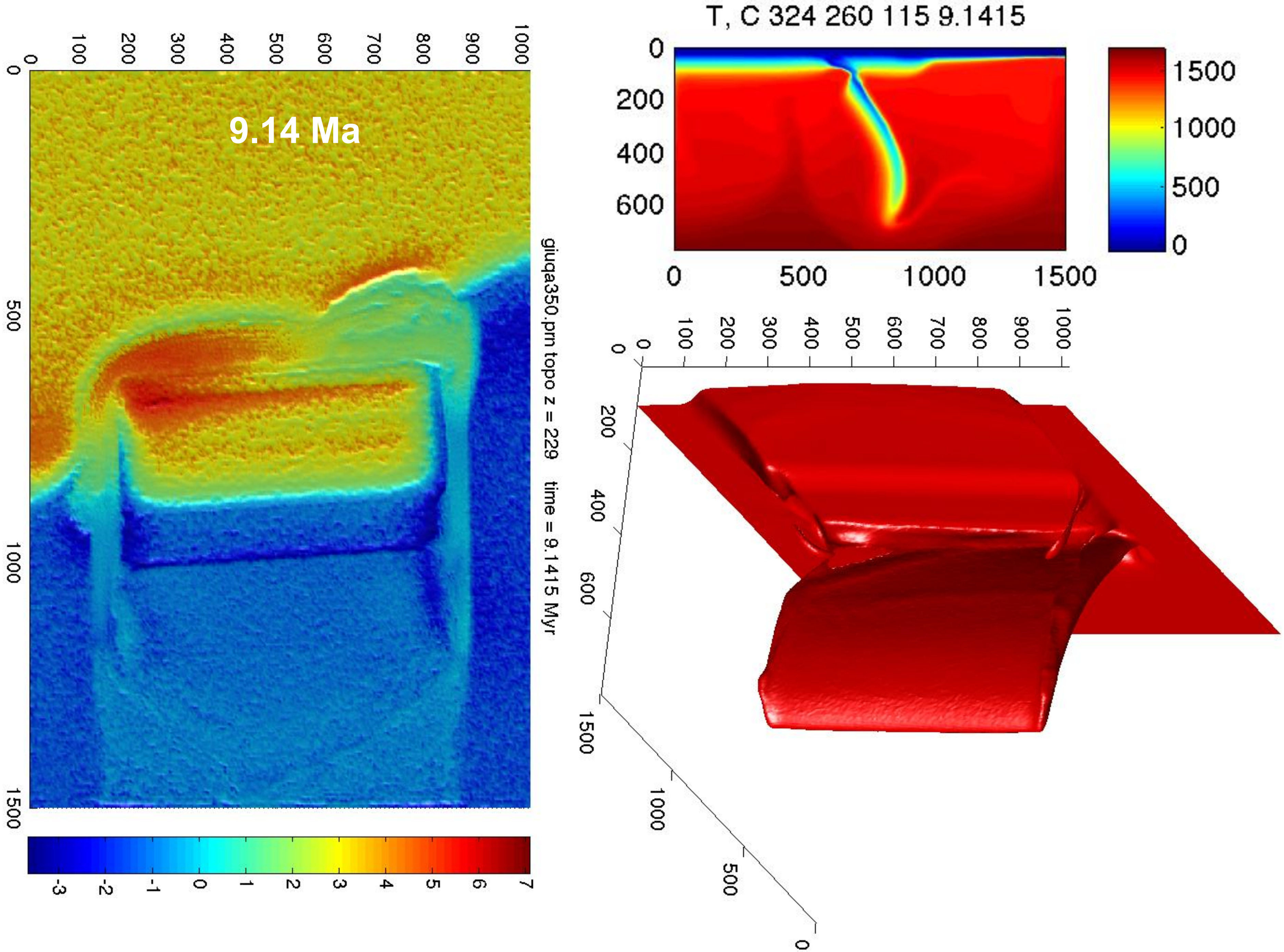
9.14 Ma
giuqa350.pm topo z = 229 time = 9.1415 Myr
T, C 324 260 115 9.1415

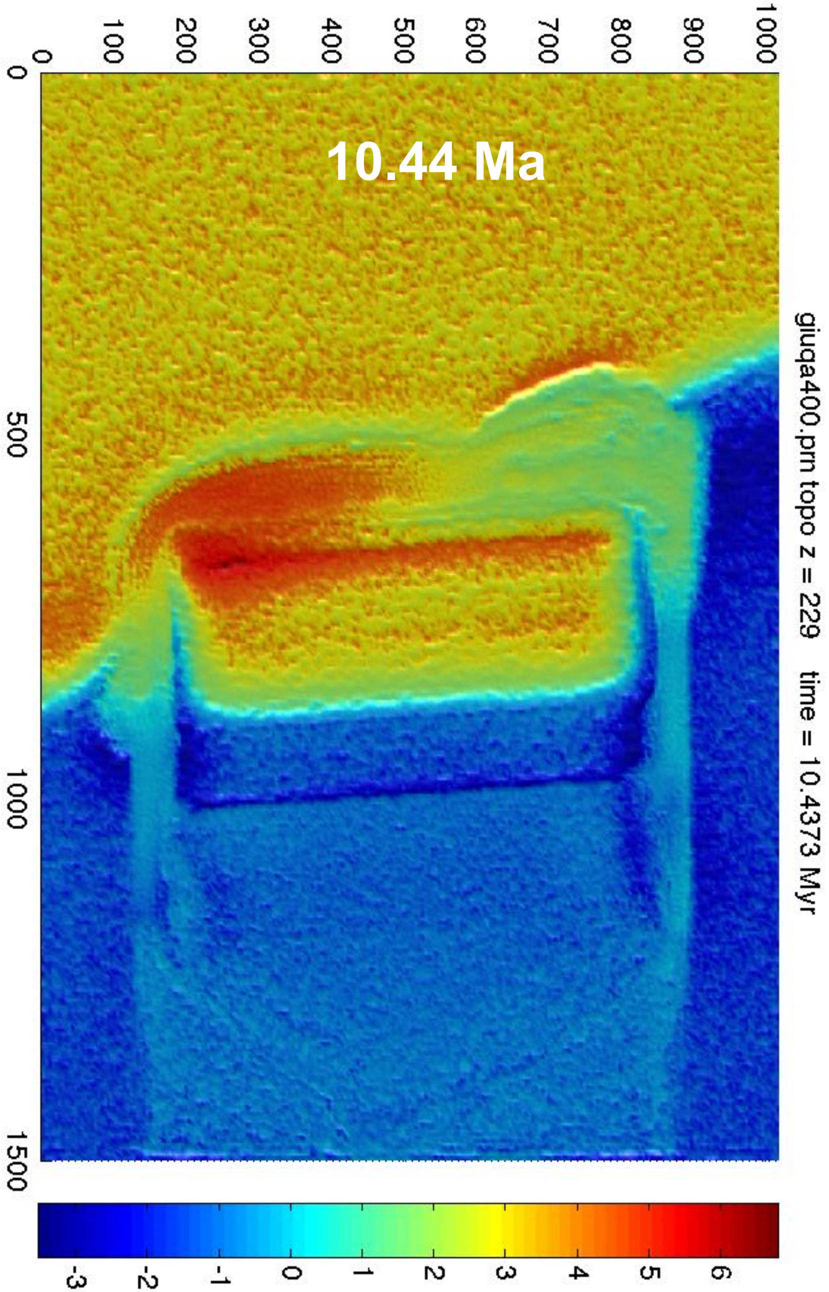
10.44 Ma
giuqa400.prn topo z = 229 time = 10.4373 Myr

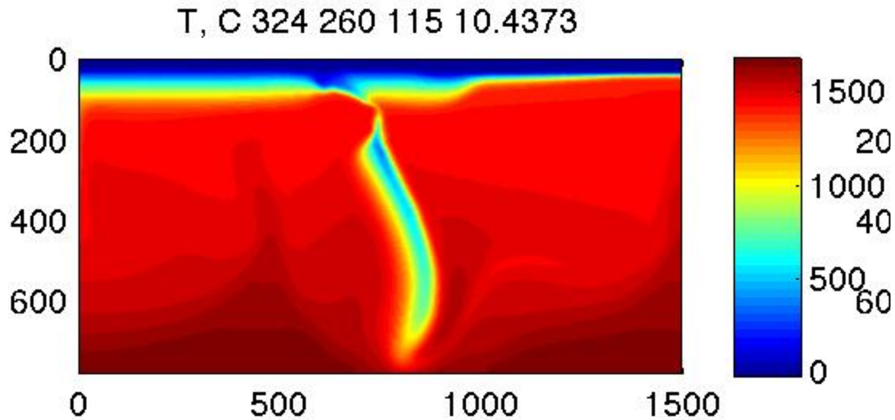
T, C 324 260 115 10.4373

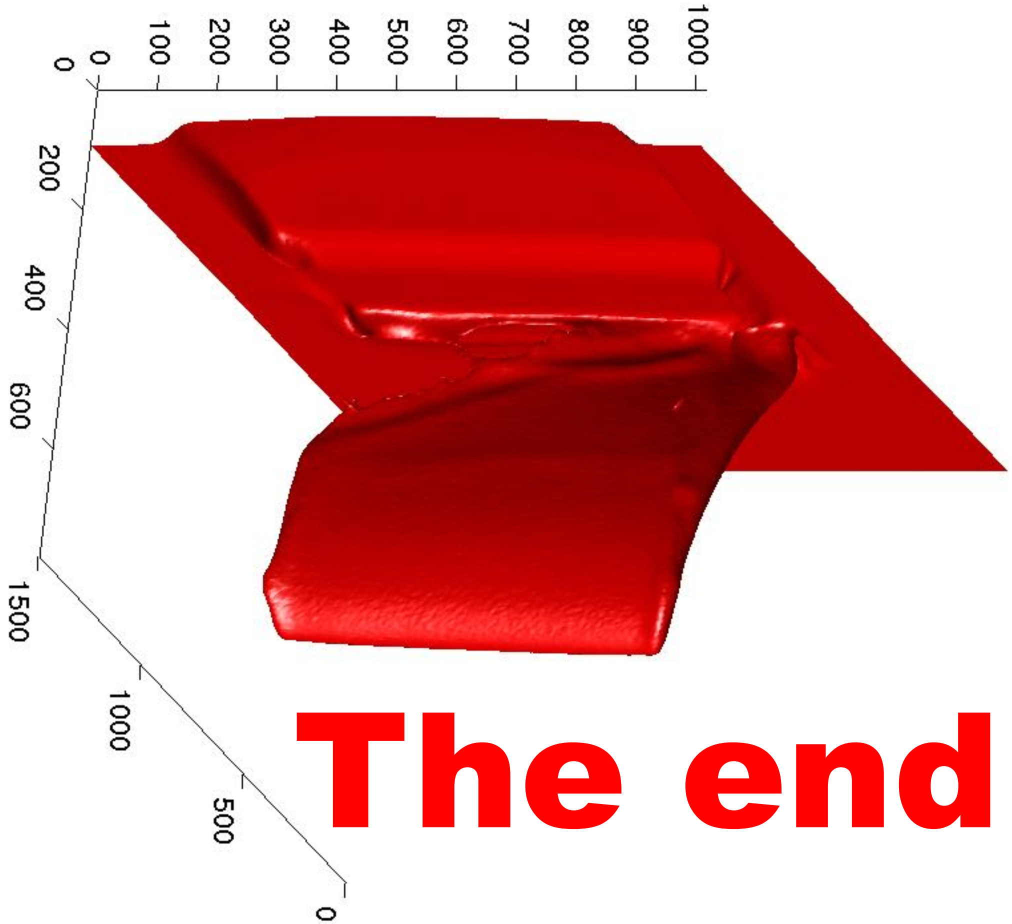

The end

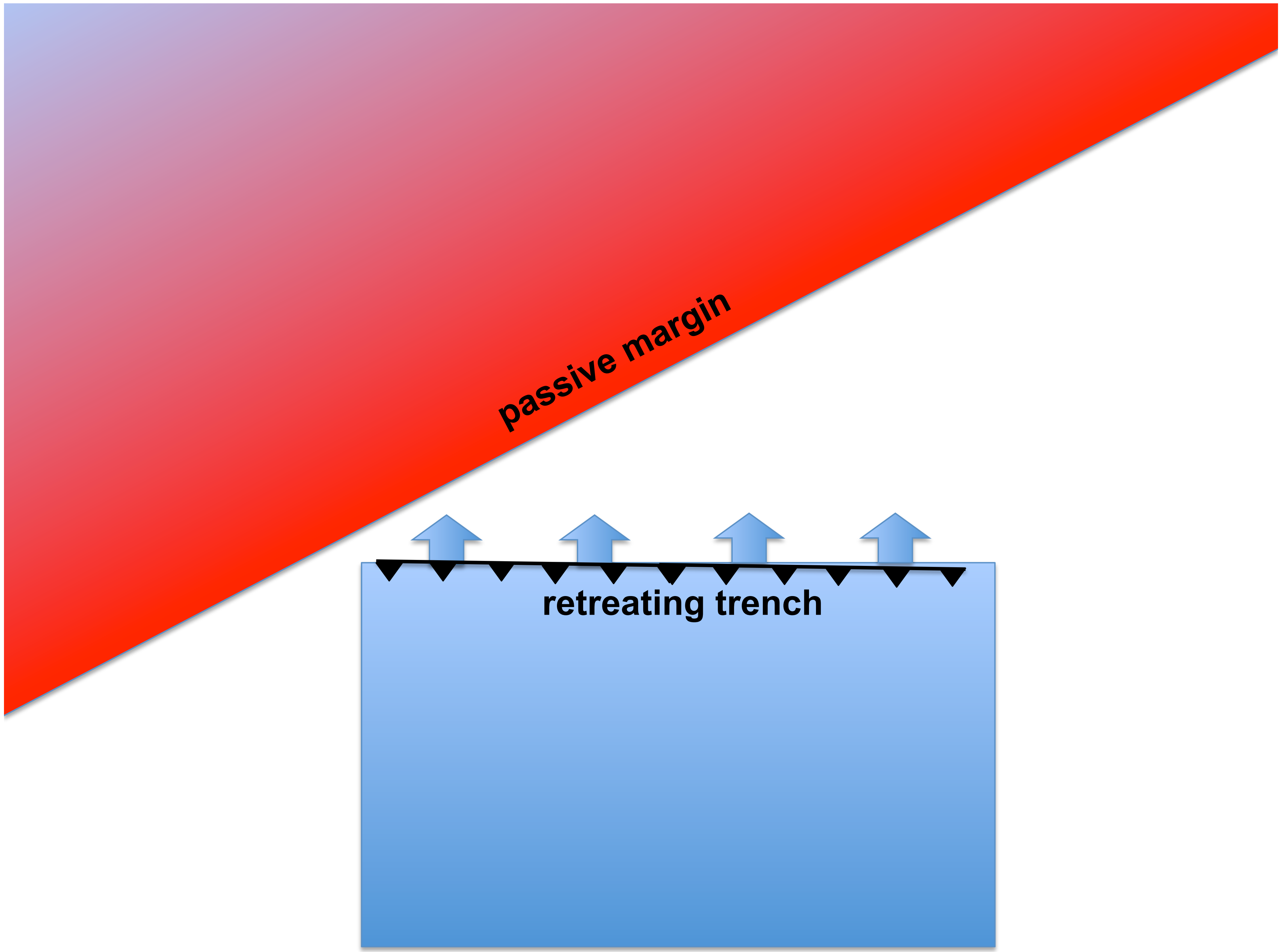
passive margin
retreating trench

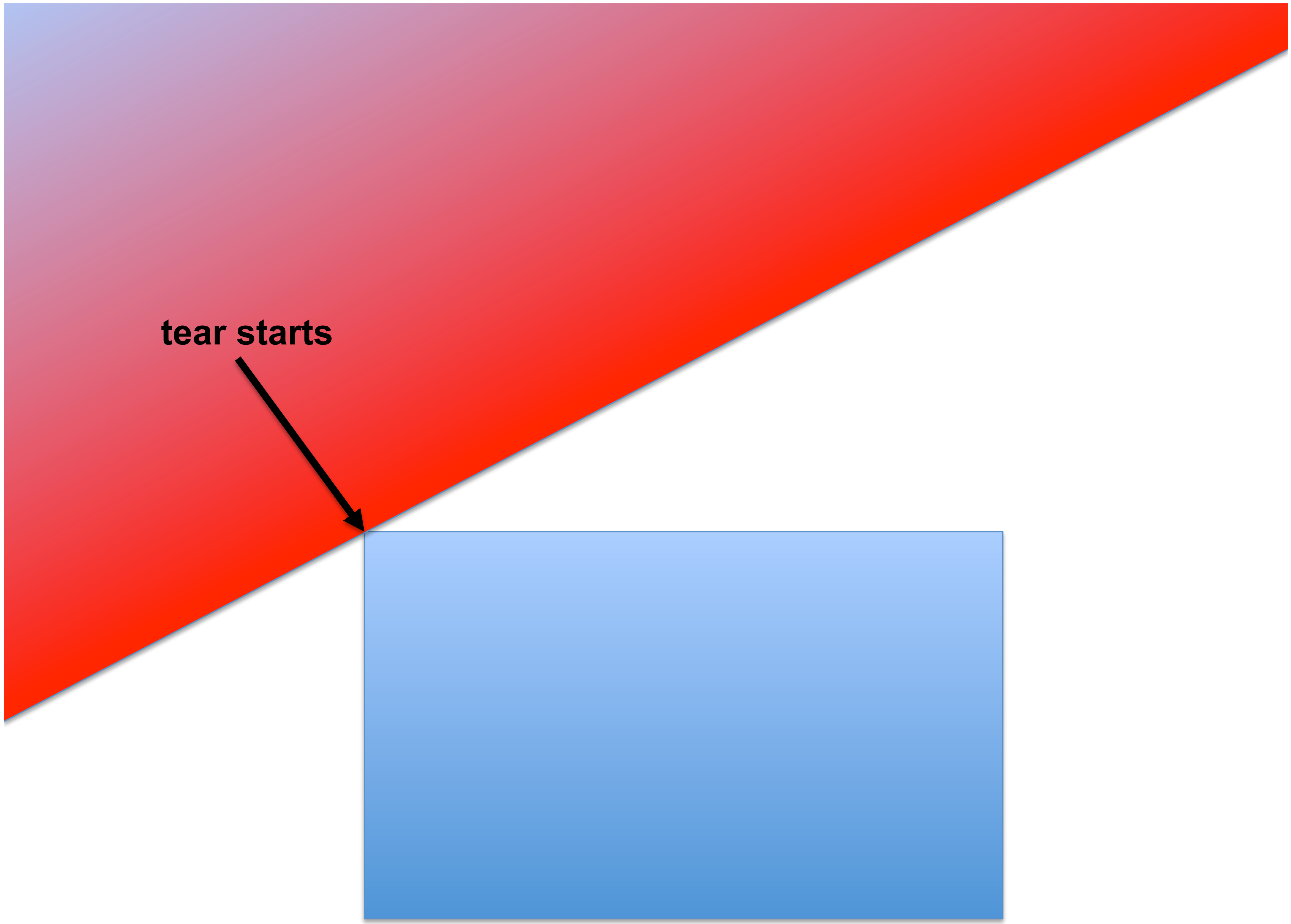
tear starts

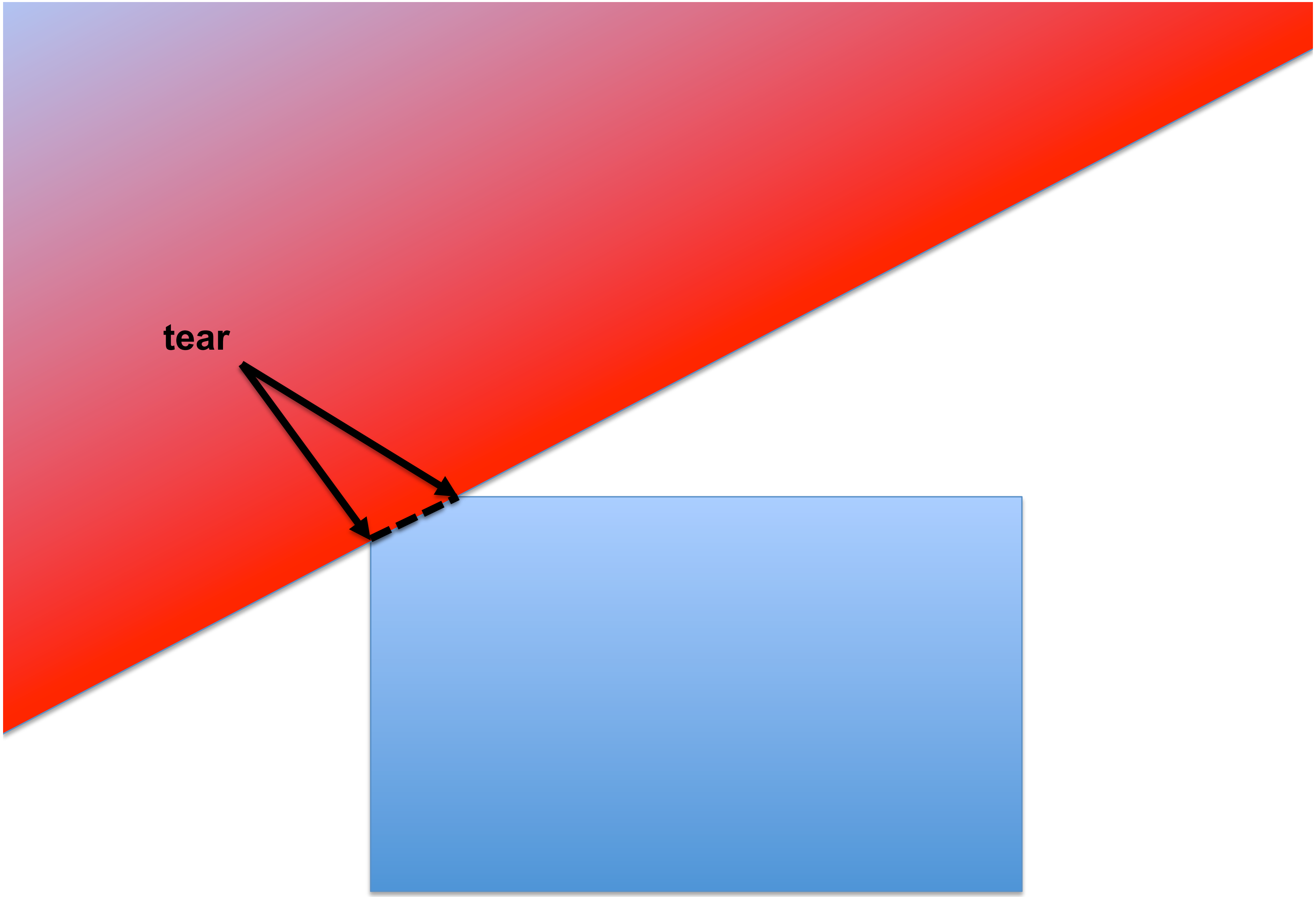
tear

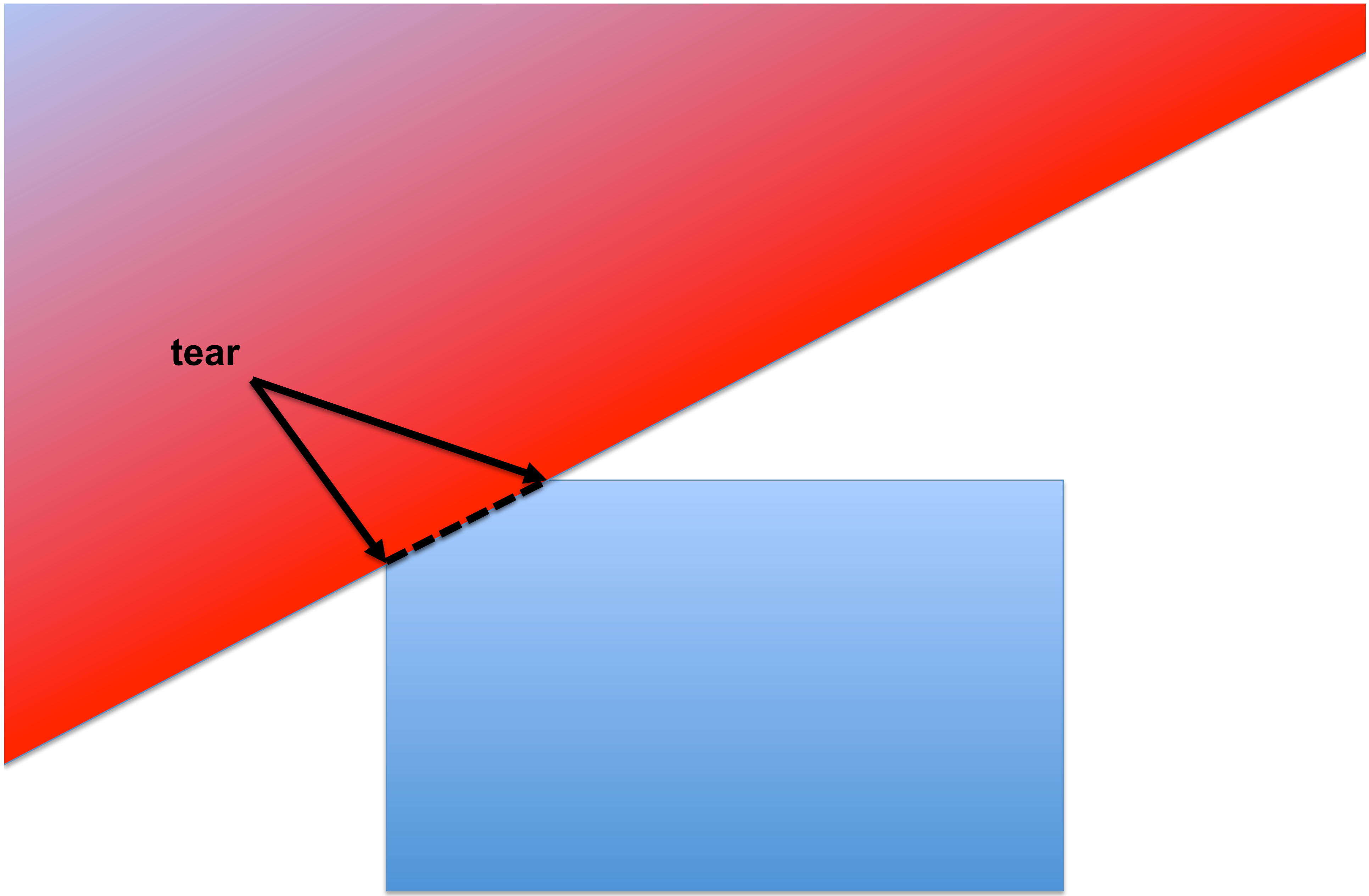
tear

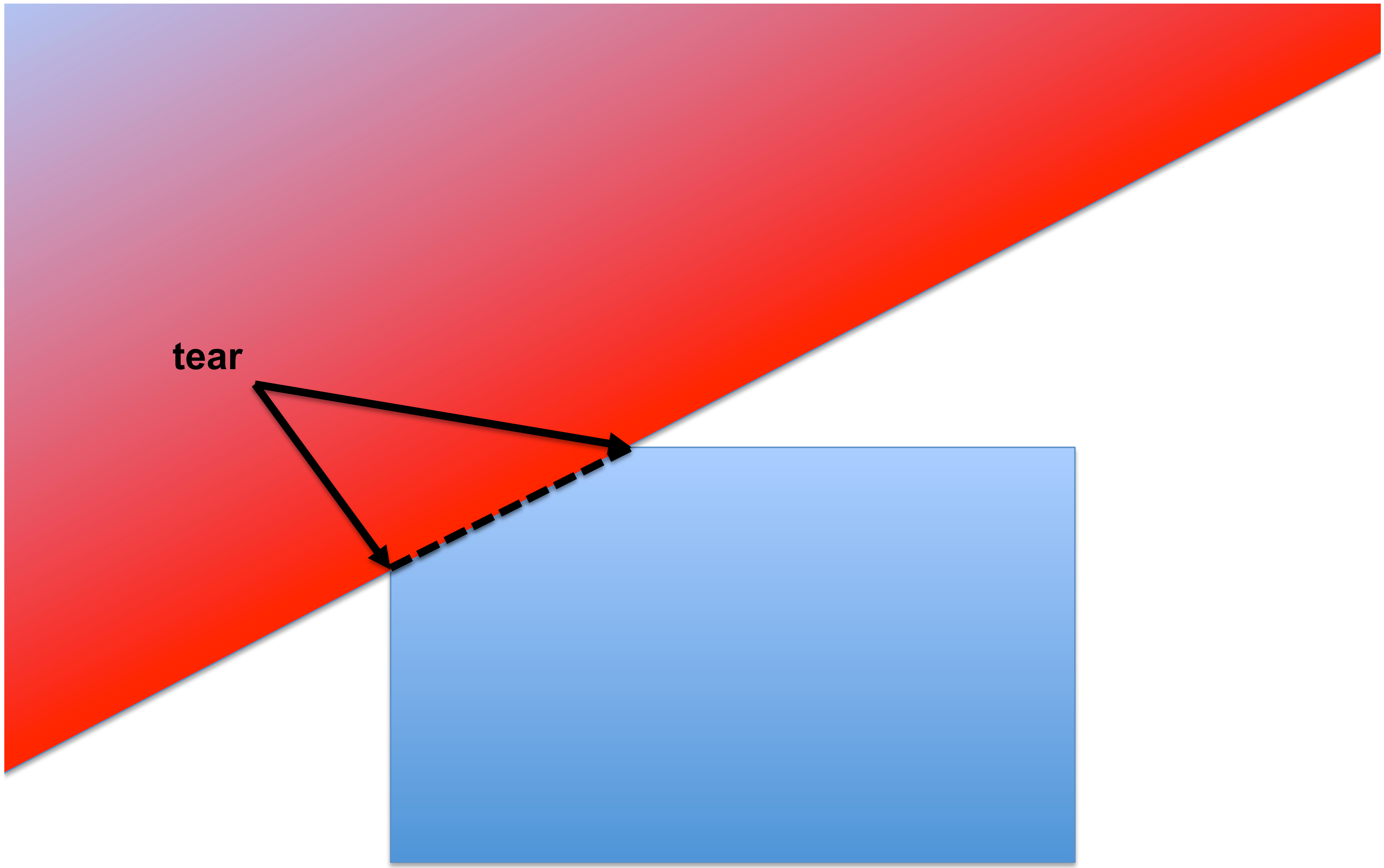
tear

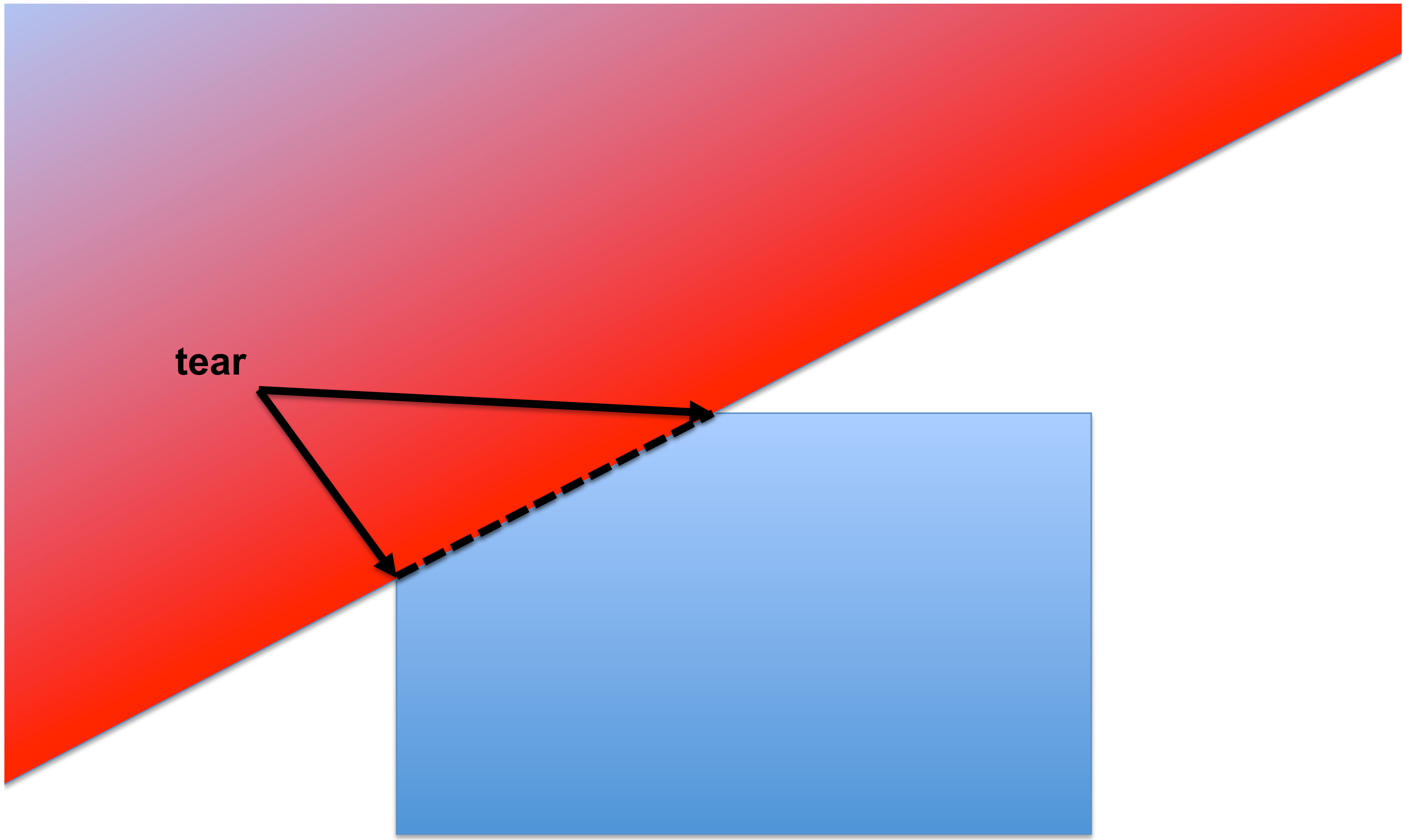
tear

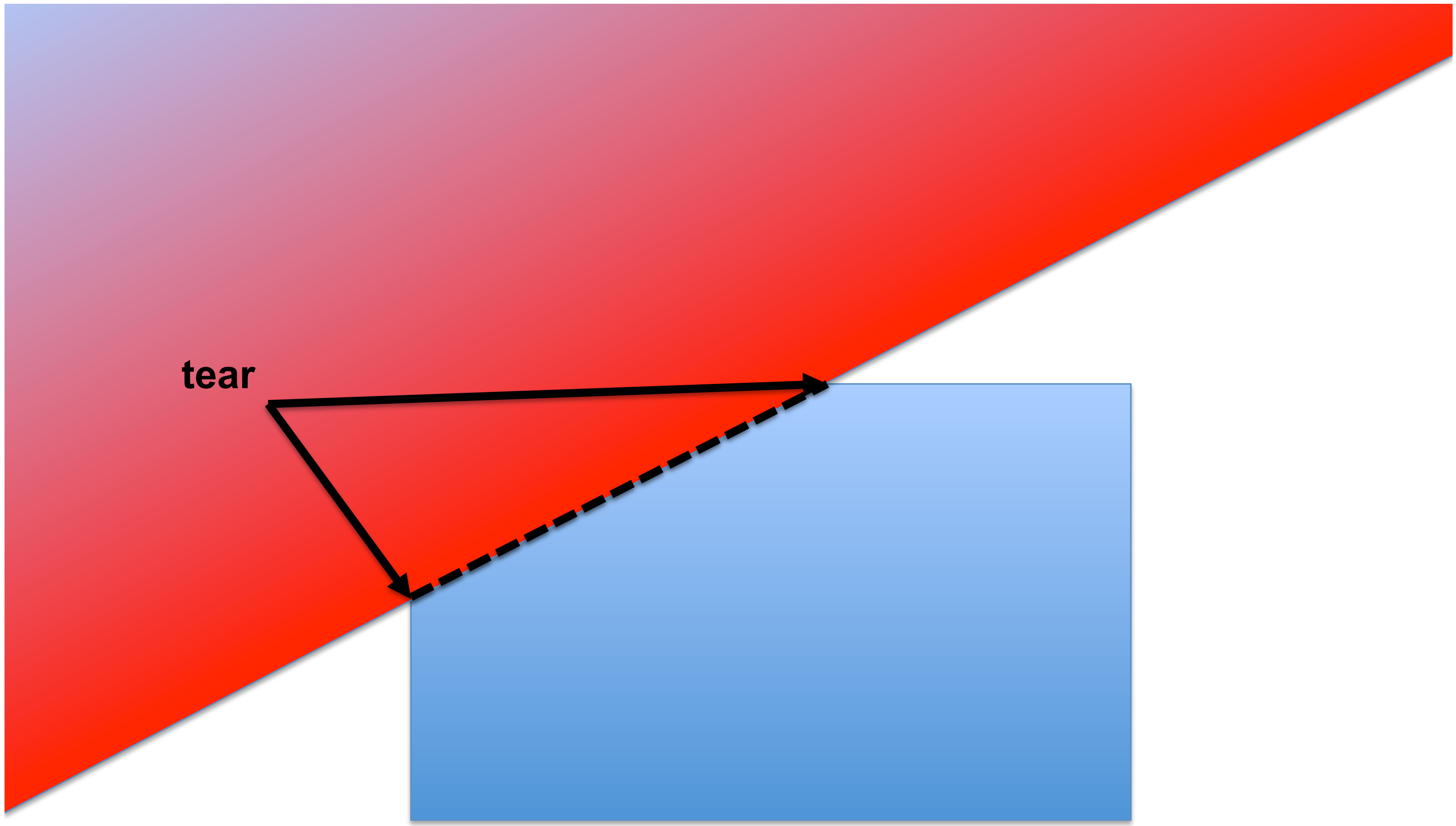
tear

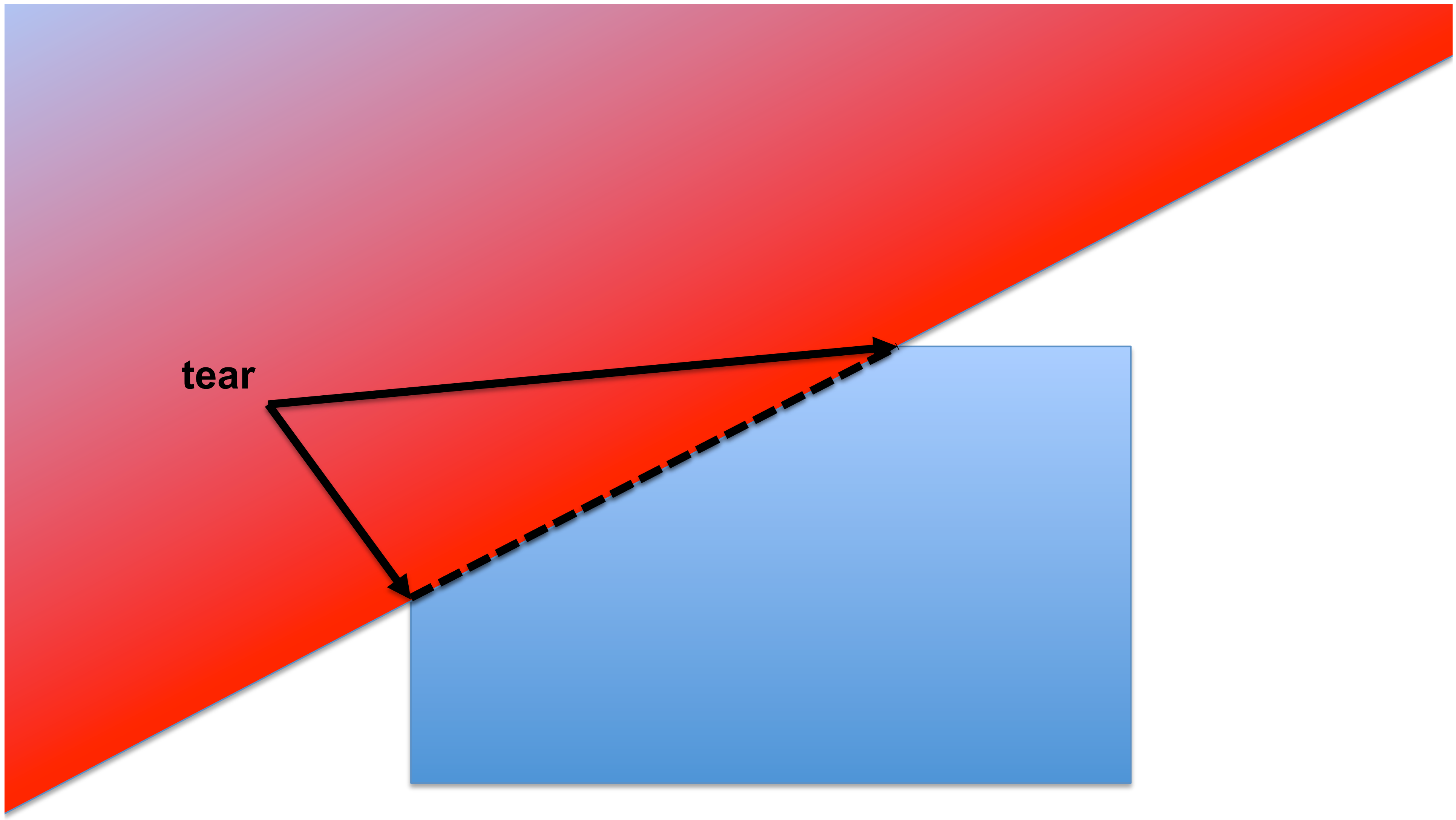
tear

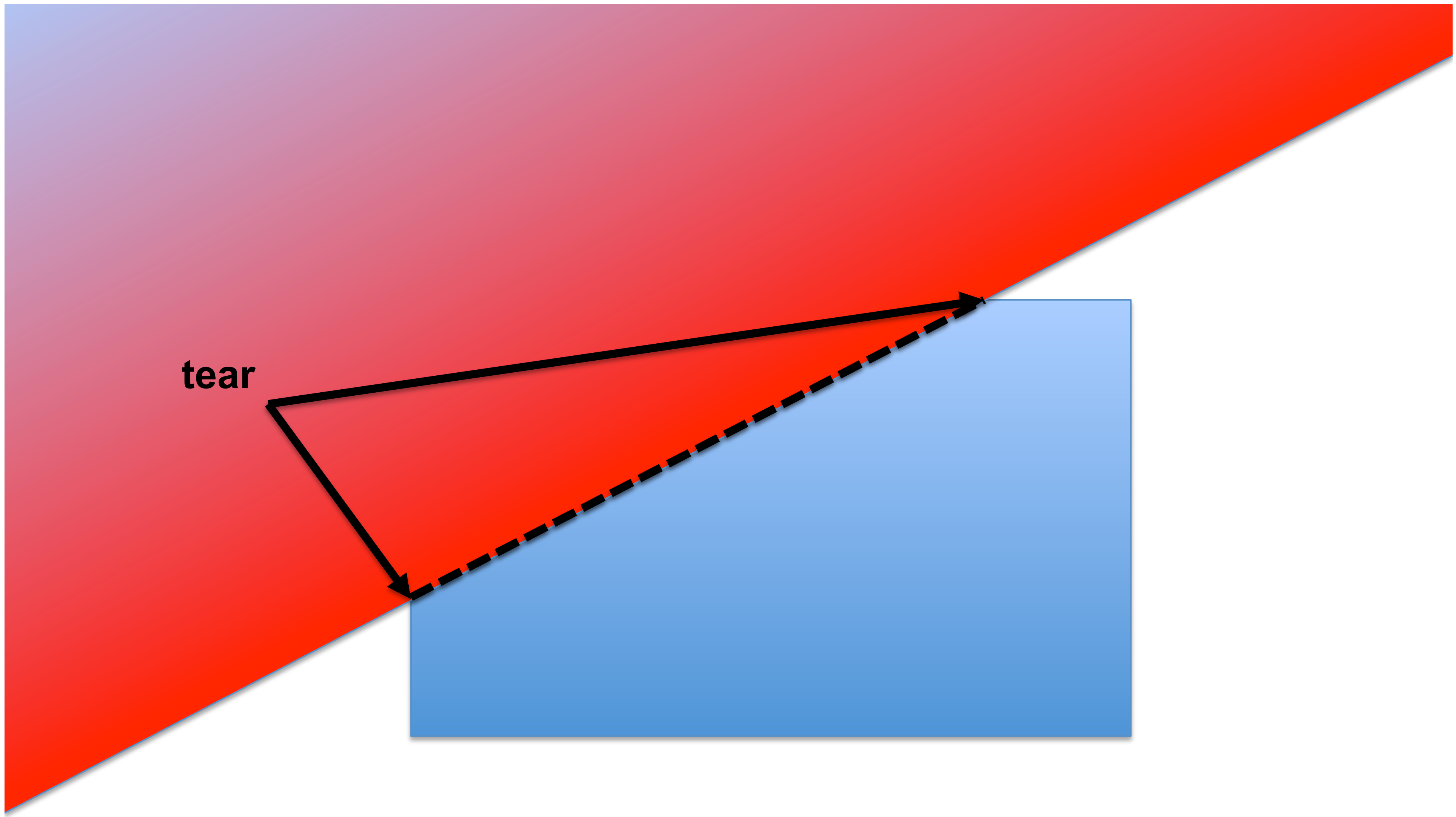
tear

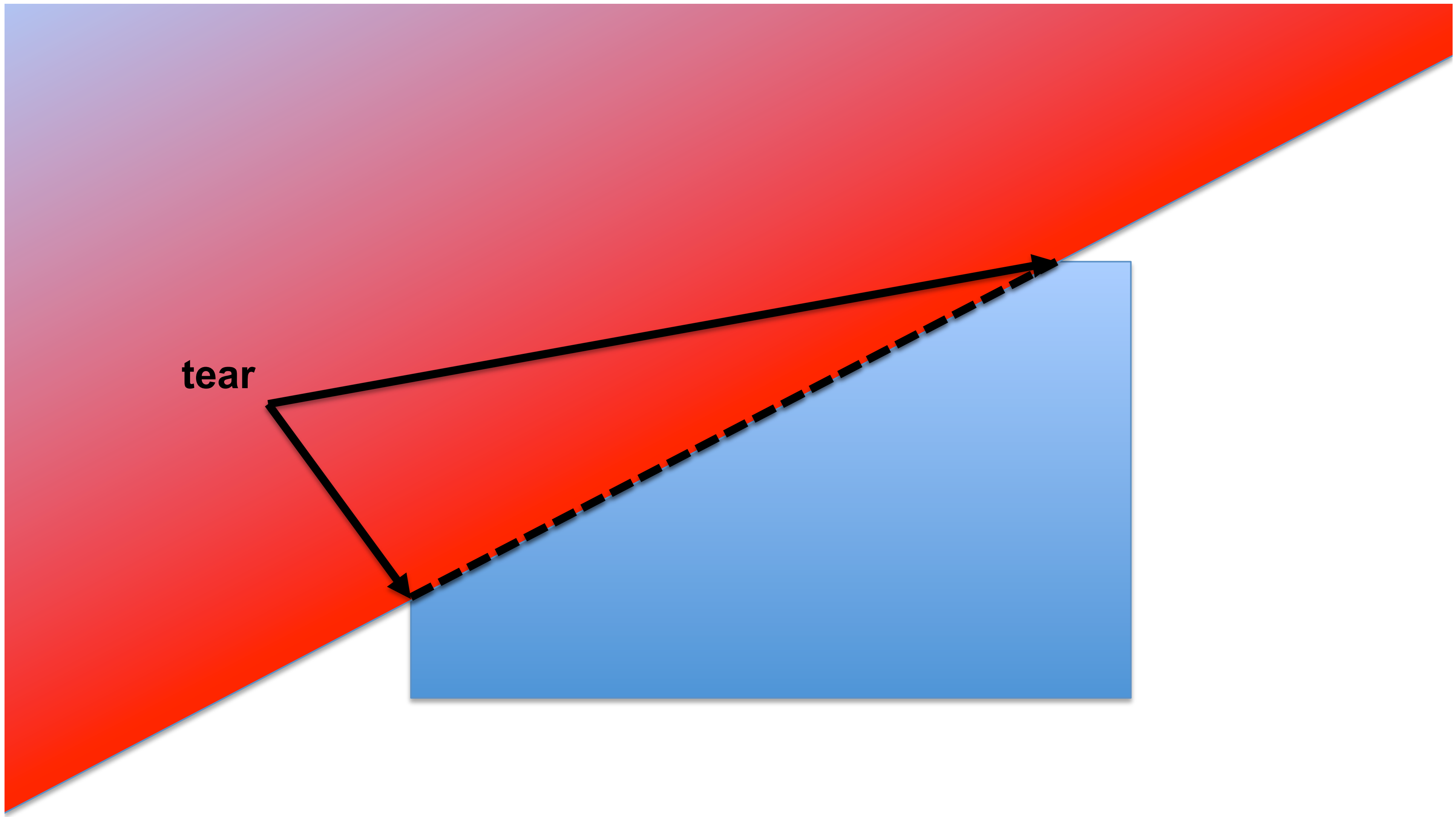
tear

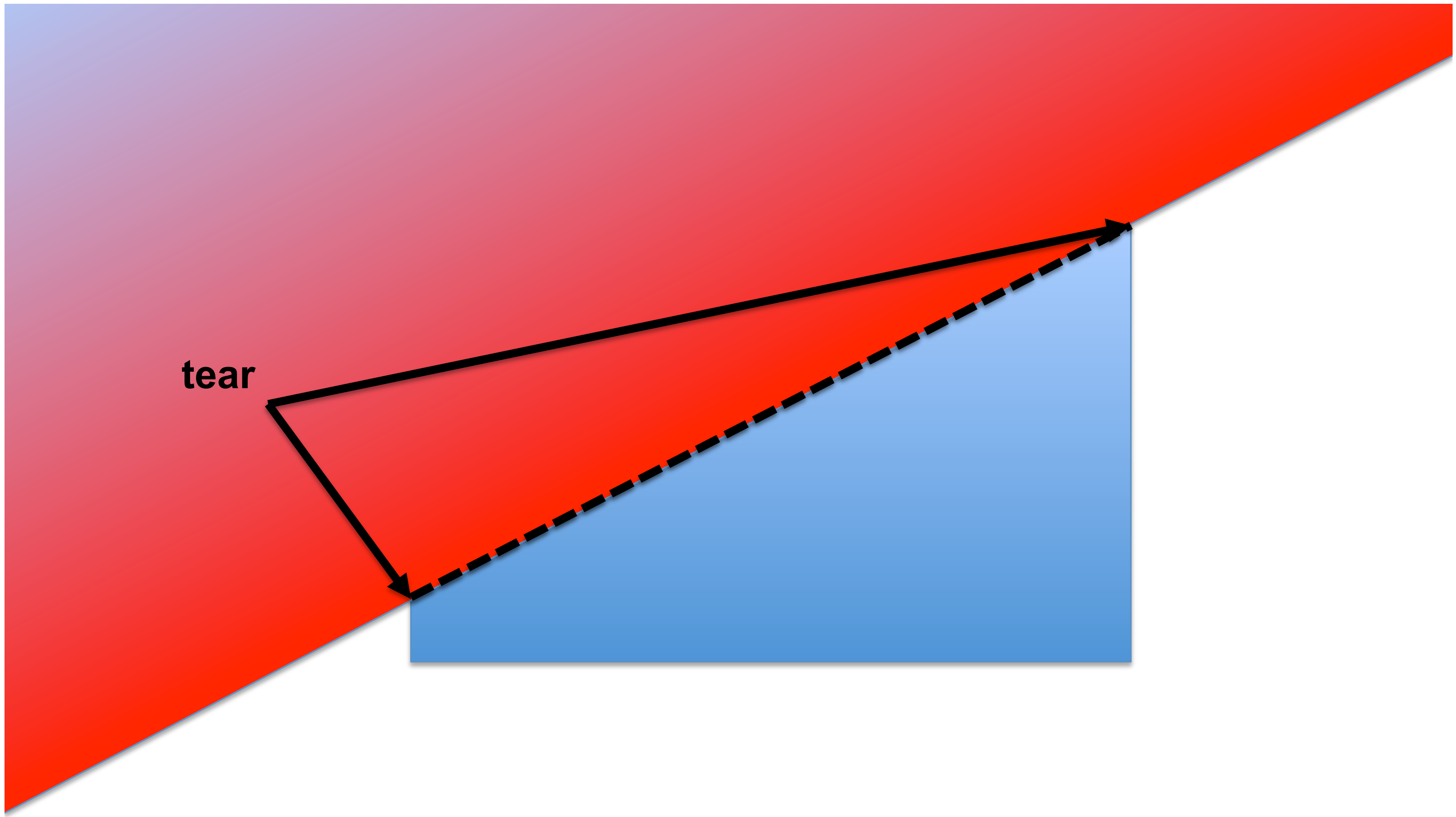
tear

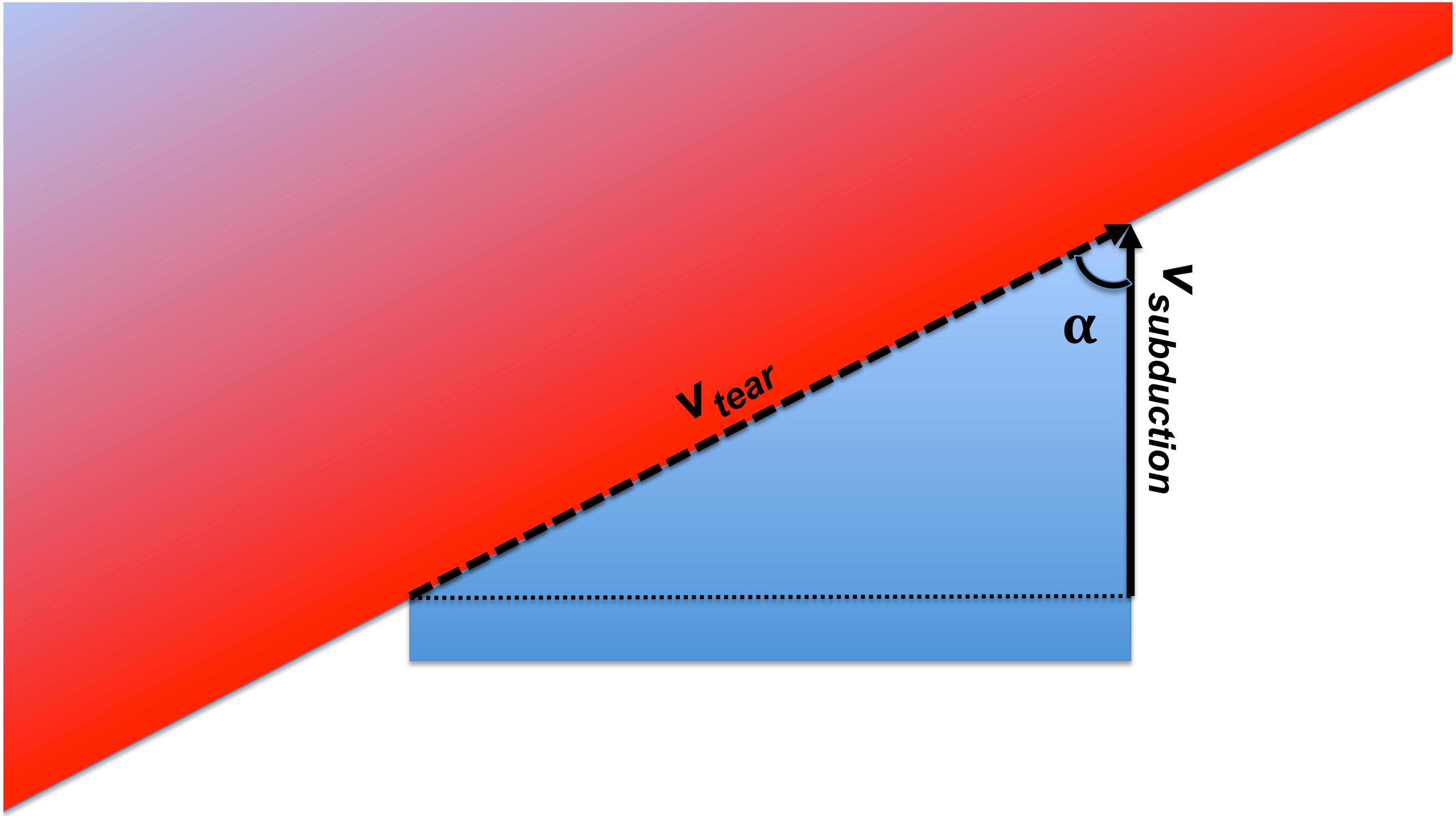

$$v_{tear} = v_{subduction} / \cos(\alpha)$$

$$\text{if } \alpha = 90^{o} \text{ then } v_{tear} = \infty$$

Short initial weak zones

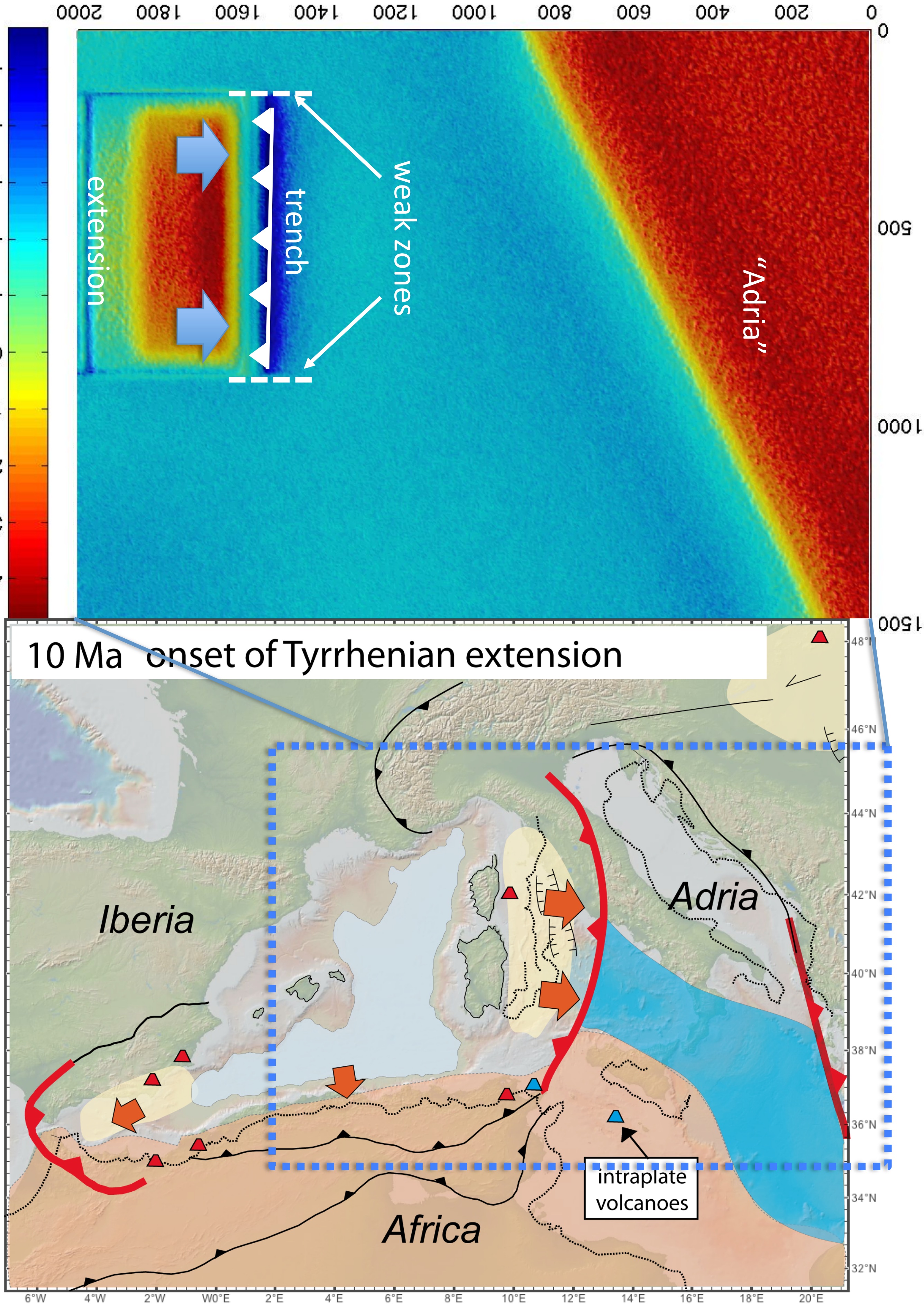

"Adria"
weak zones
trench
extension
10 Ma onset of Tyrrhenian extension
Iberia
Adria
Africa
intraplate volcanoes

STEP faults develop spontaneously

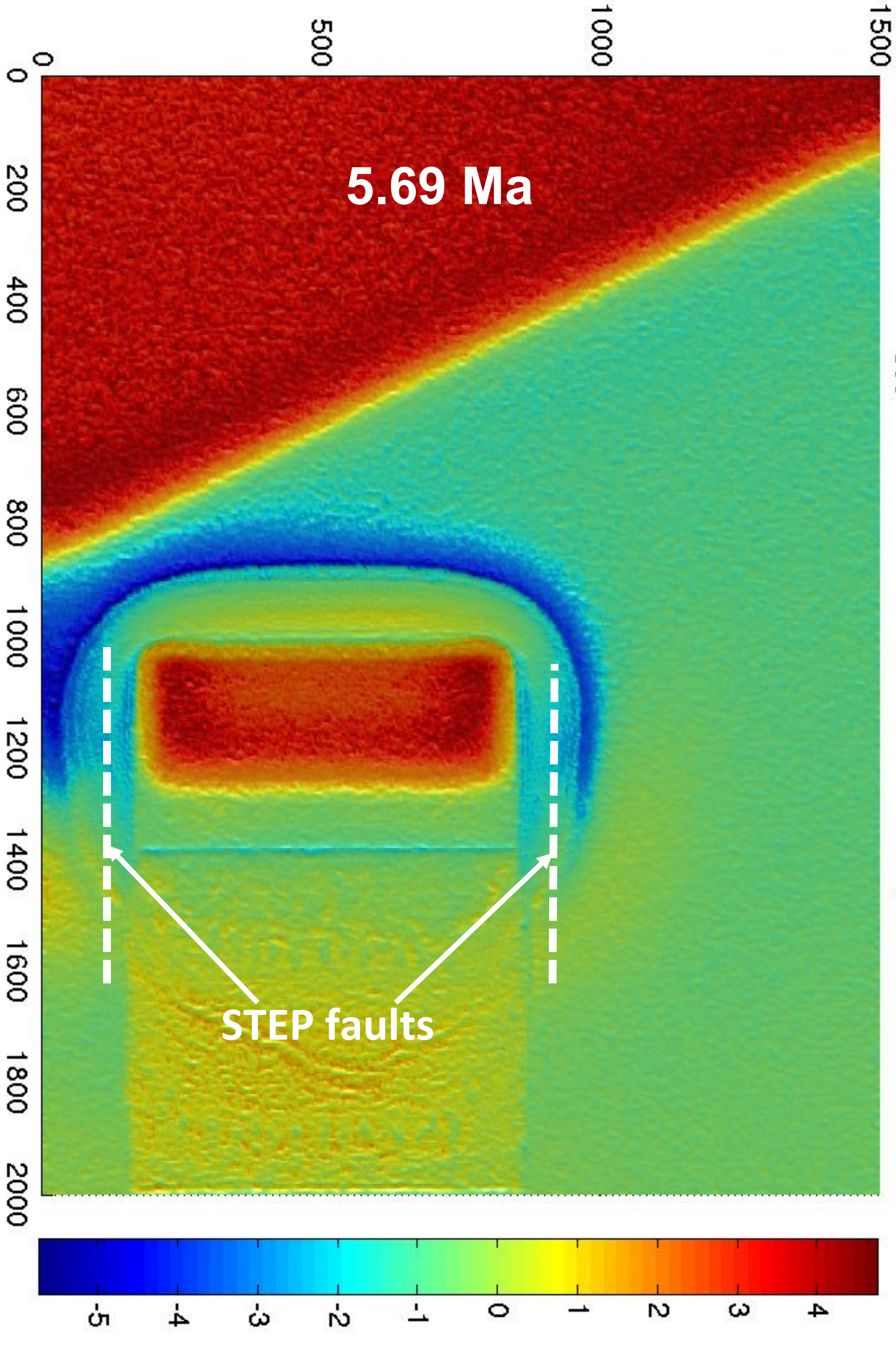

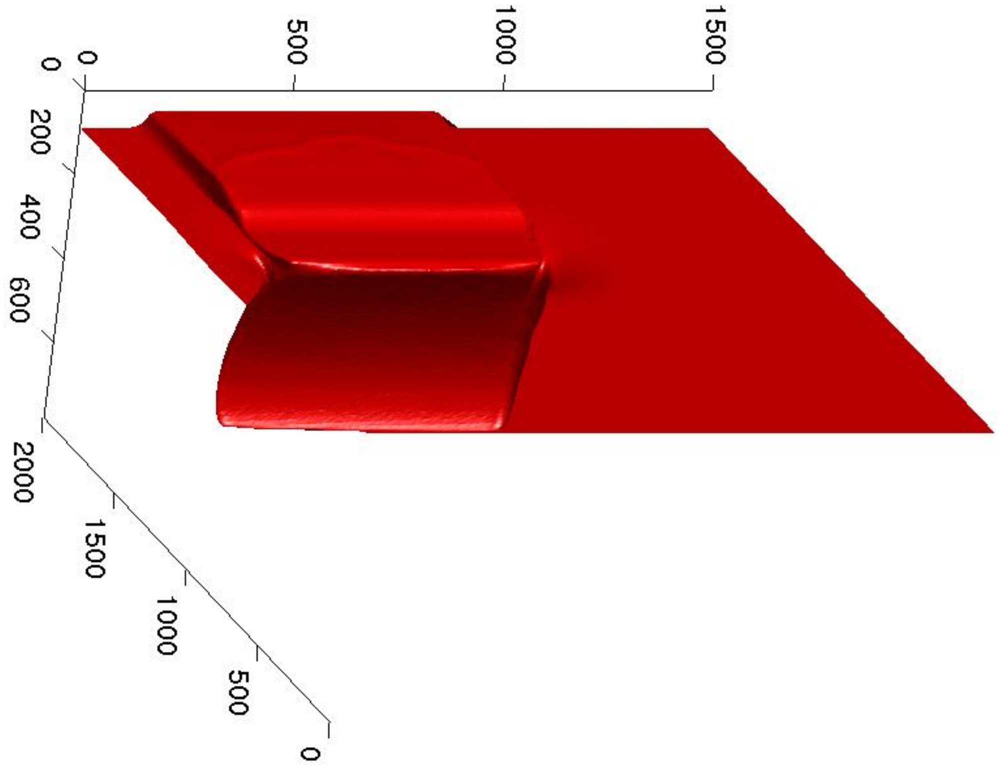

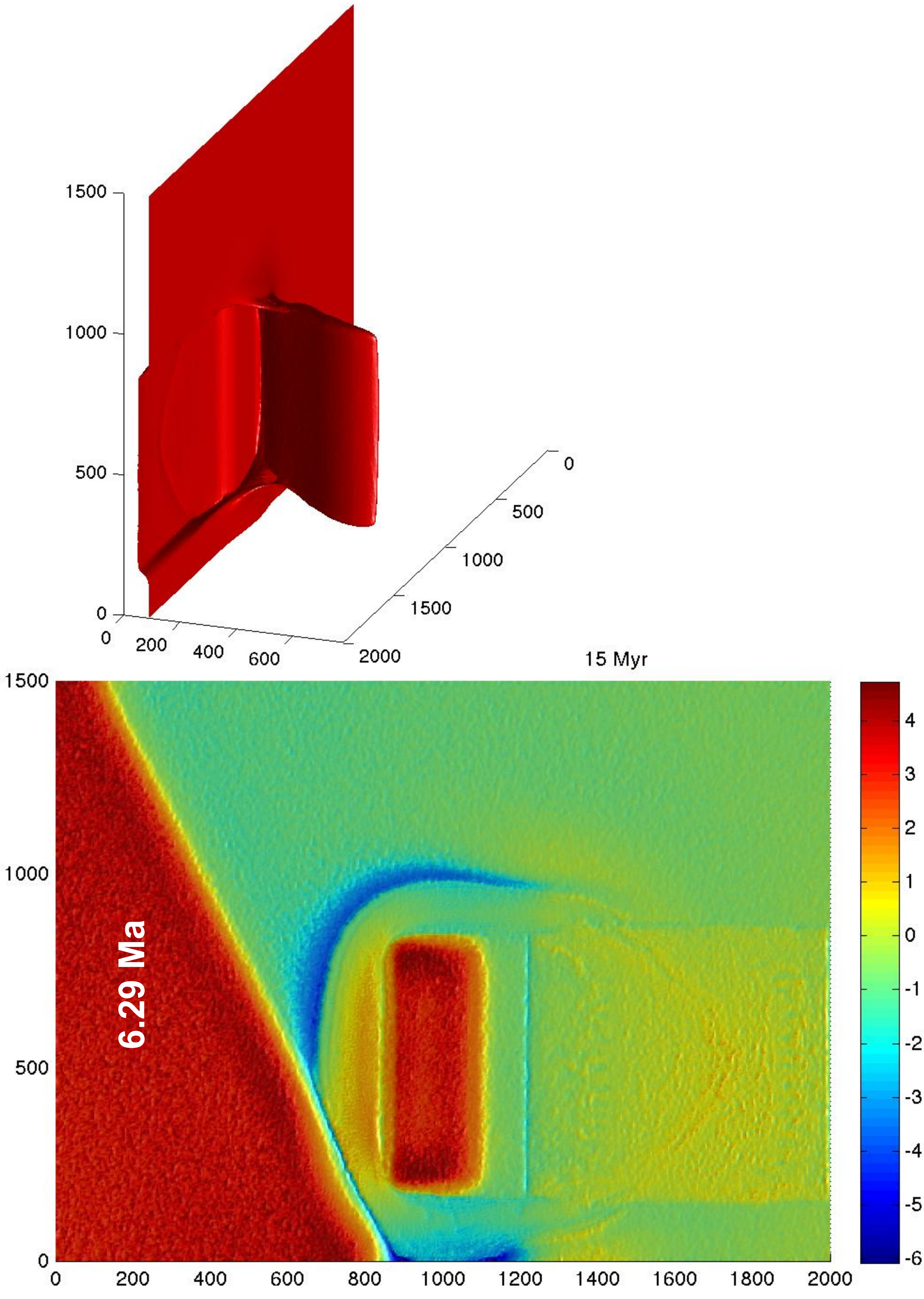

0
500
1000
1500
0
200
400
600
2000
1500
1000
500
0
15 Myr
6.29 Ma
0
500
1000
1500
0
200
400
600
800
1000
1200
1400
1600
1800
2000
4
3
2
1
0
-1
-2
-3
-4
-5
-6

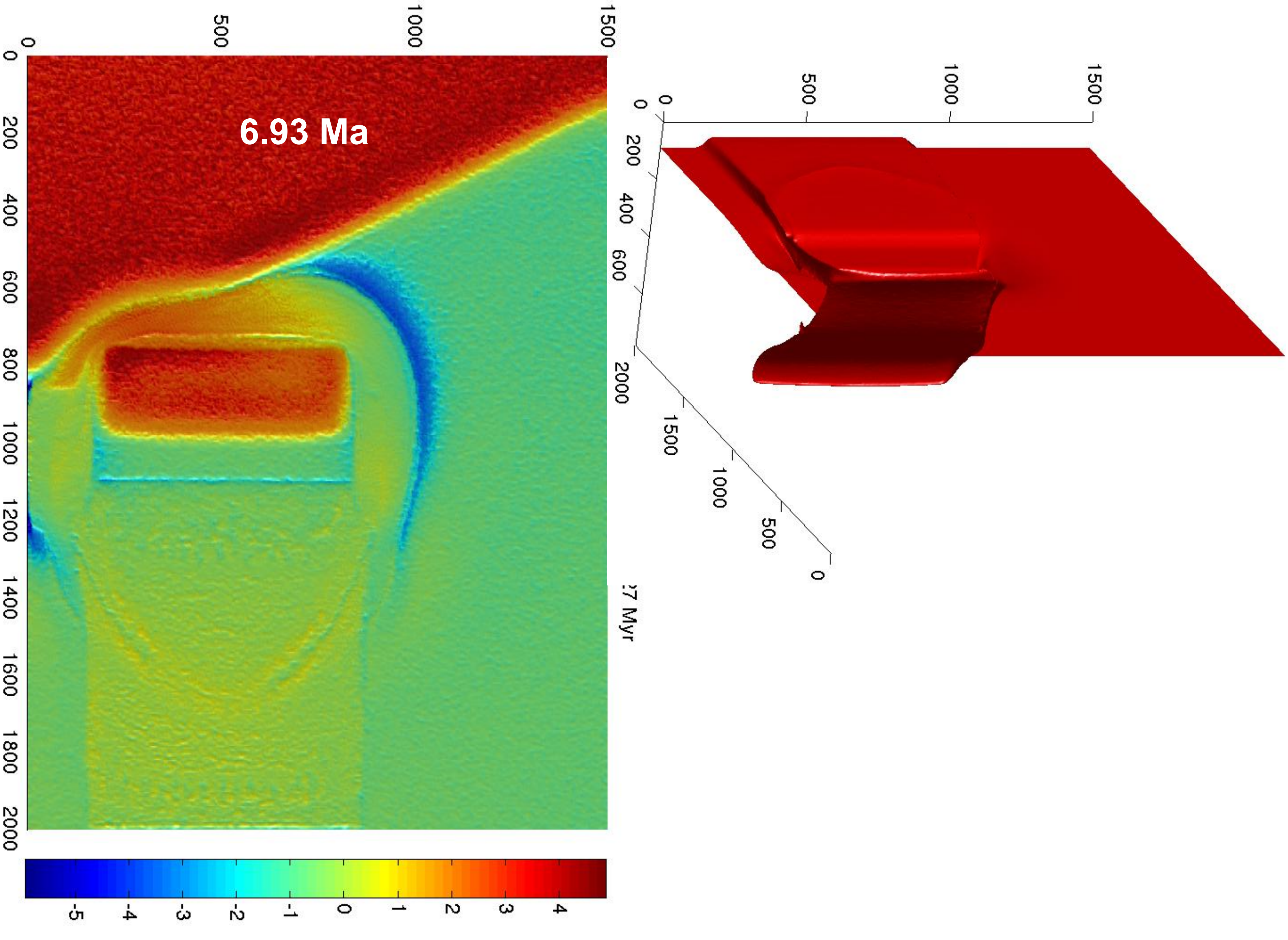
6.93 Ma

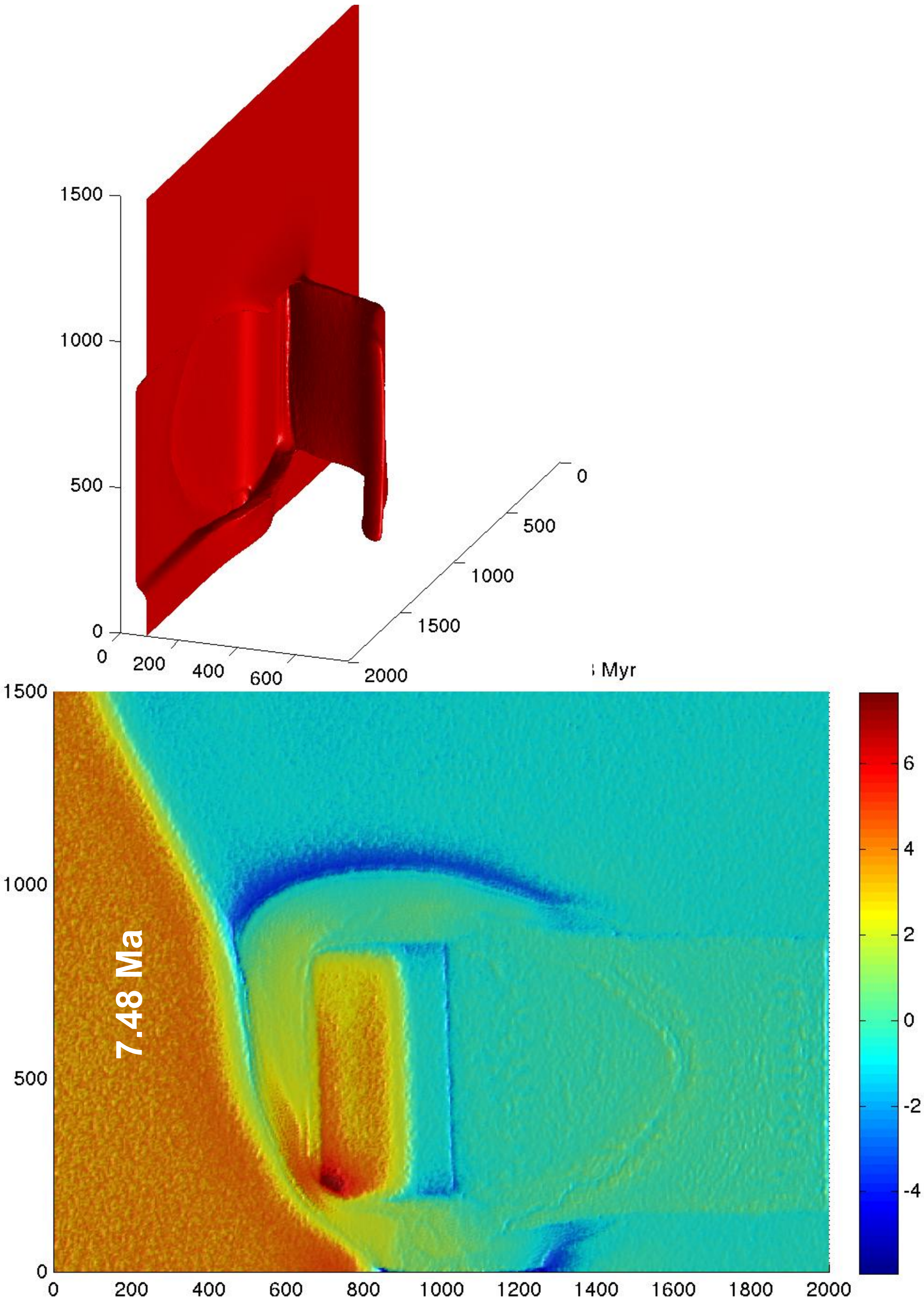

7.48 Ma
Myr

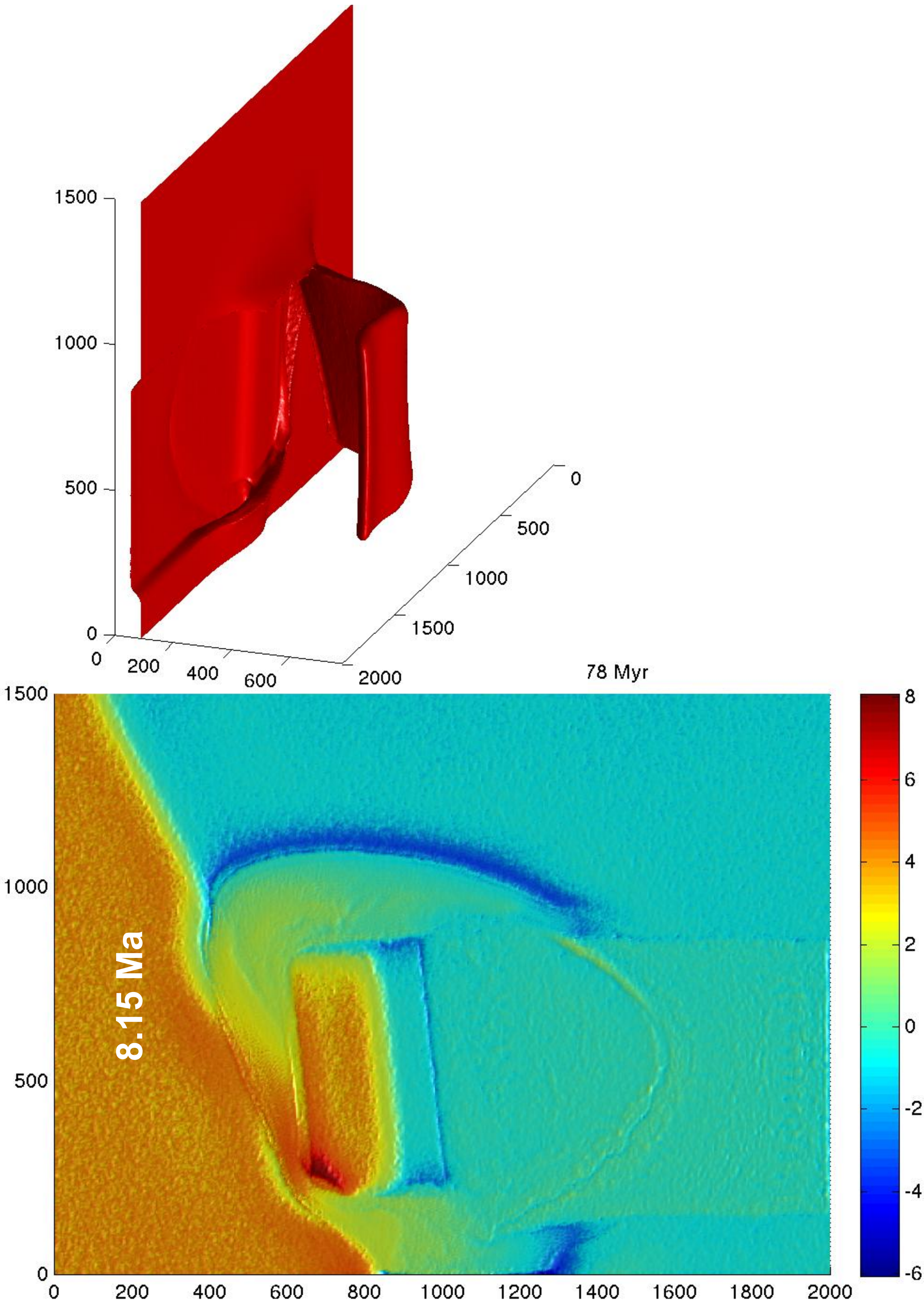

78 Myr
8.15 Ma

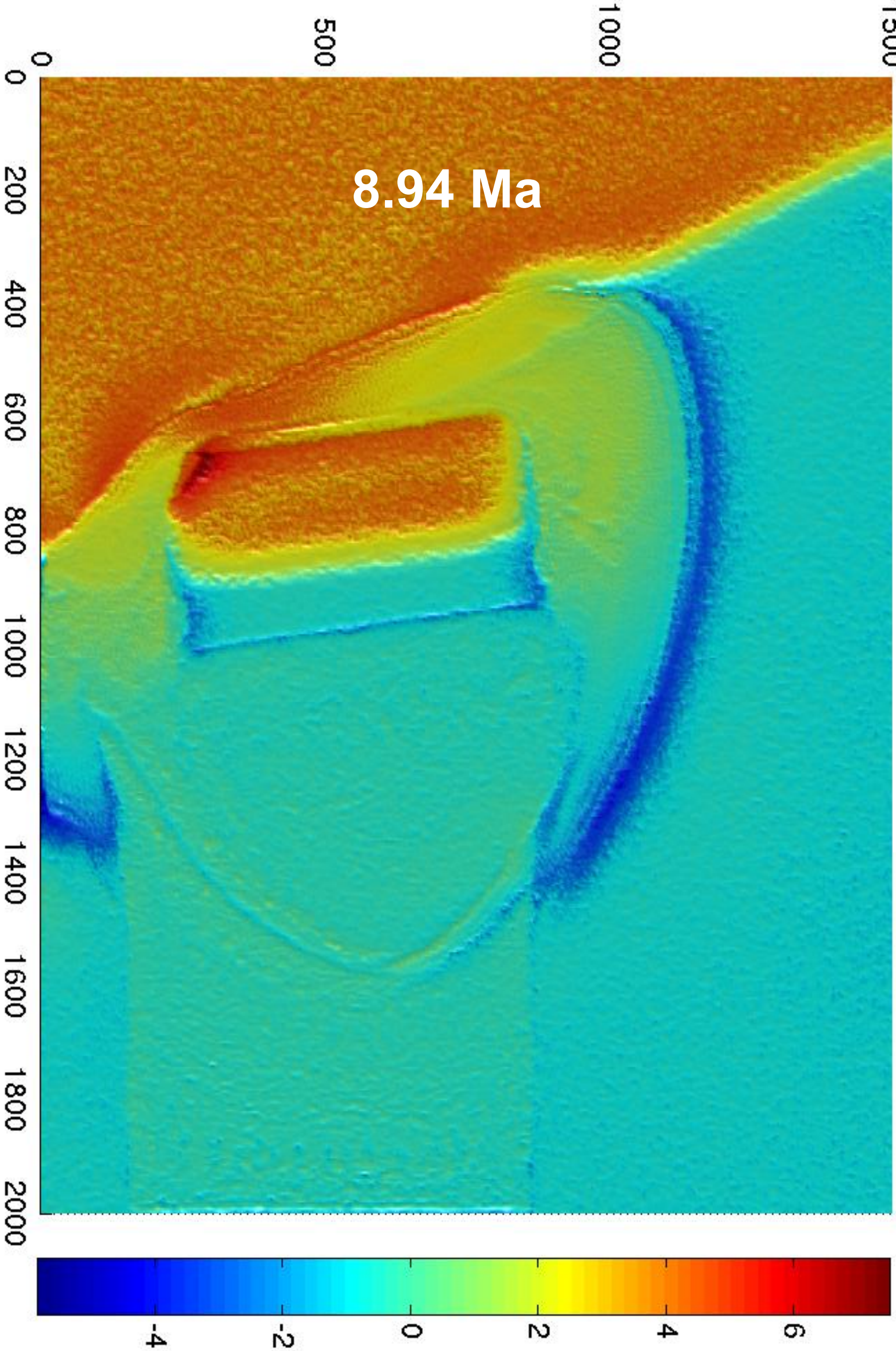
8.94 Ma
0
500
1000
1500
0
200
400
600
800
1000
1200
1400
1600
1800
2000
-4
-2
0
2
4
6

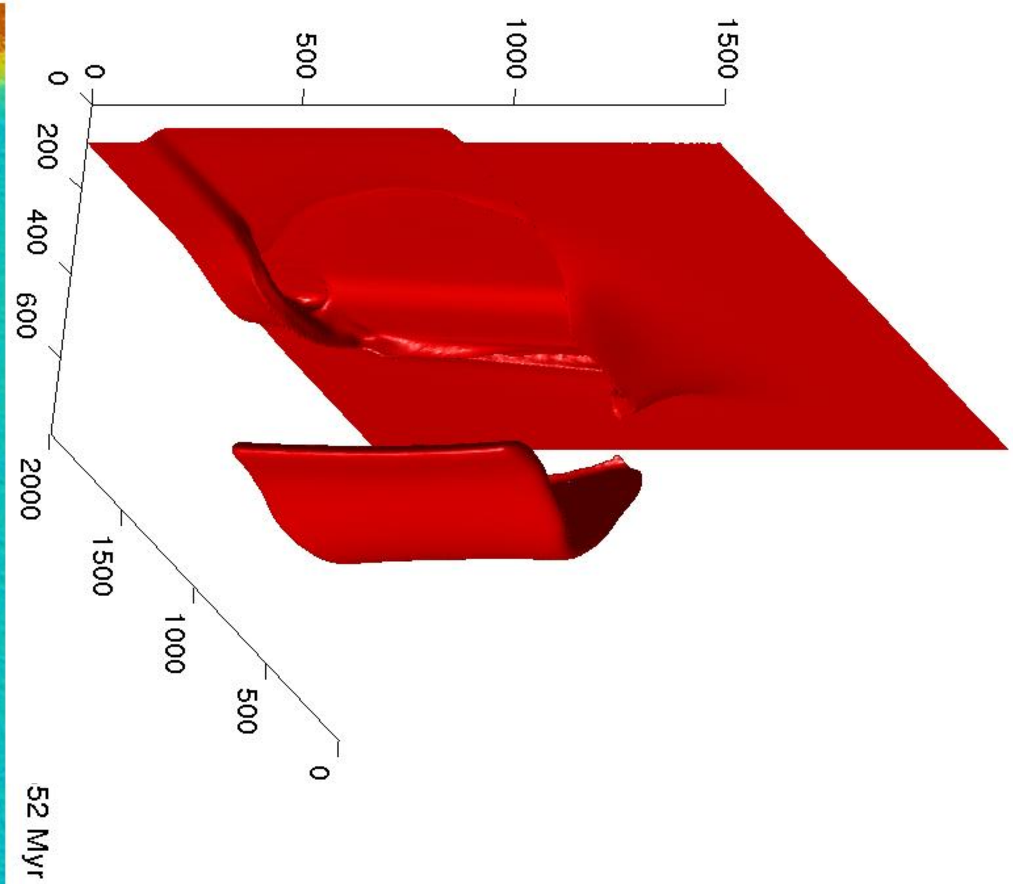
52 Myr
0
500
1000
1500
0
200
400
600
2000
1500
1000
500
0

The end

Subduction changes polarity

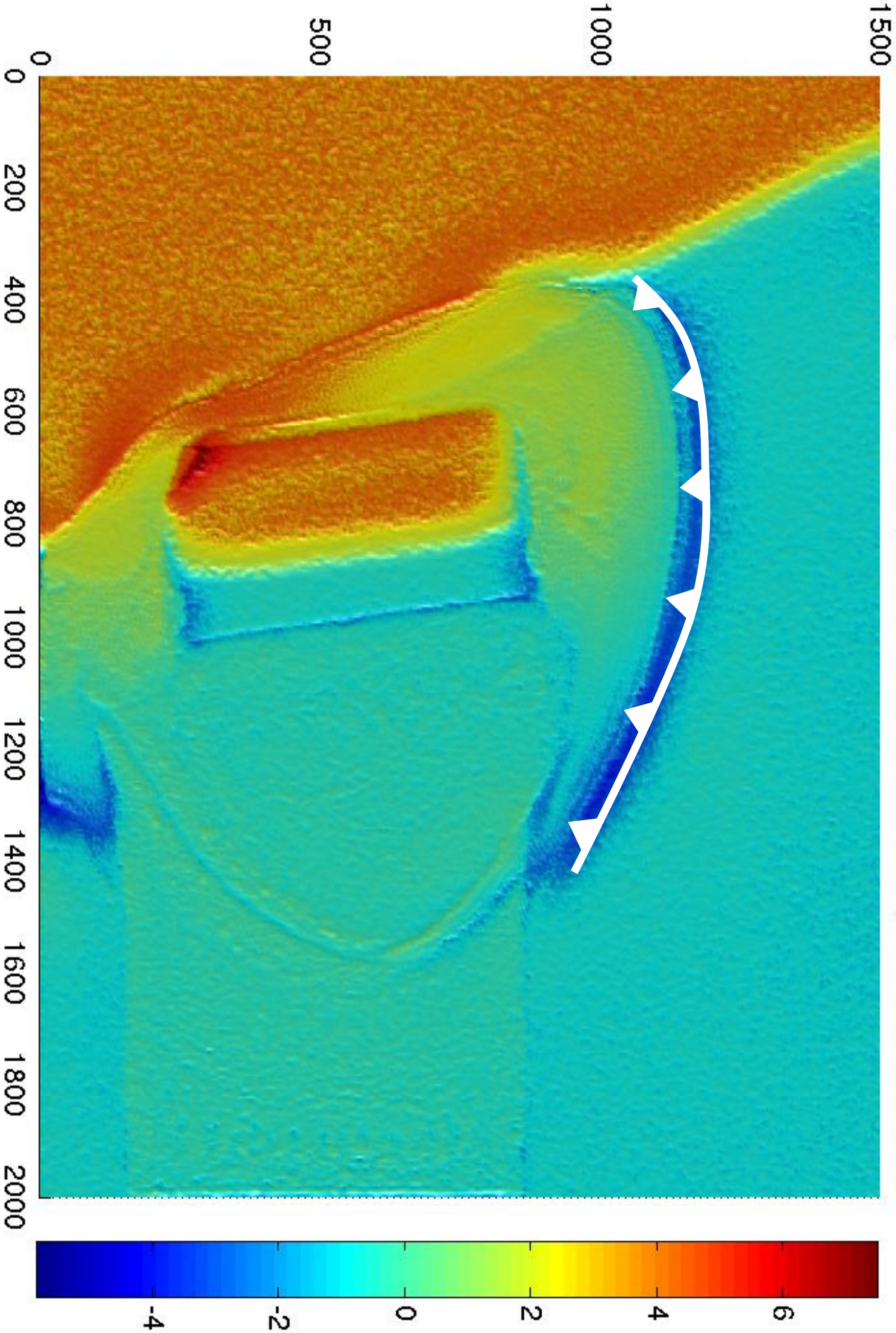

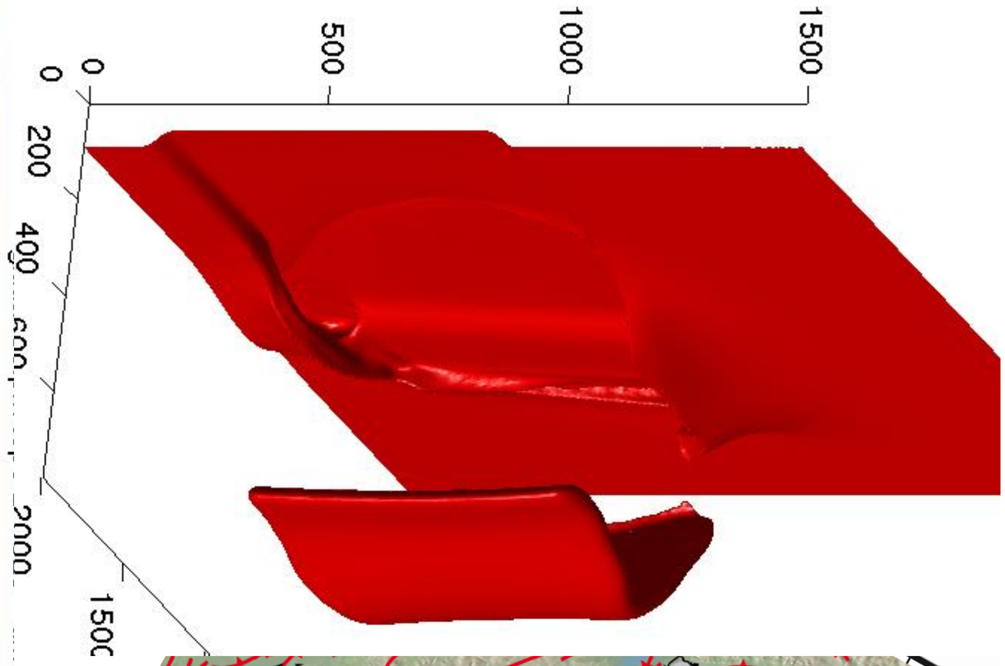

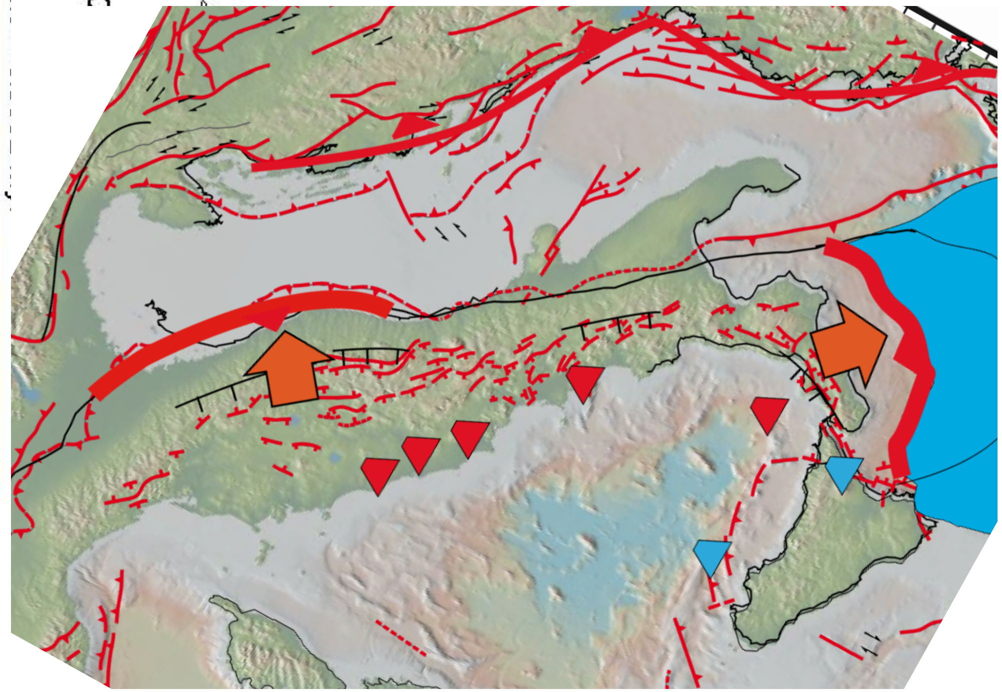

Conclusions

1. Retreating subduction is very efficient in causing slab tearing

2. Lateral tear propagation is controlled by the passive margin obliquity:

$v_{tear} = v_{subduction} / \cos(\alpha)$,

where α is the angle between the margin and subduction direction

3. Subduction may continue with different polarity after tearing